Gert Rudolf Trausinger, Bakk.techn.

Mass spectrometry-based quantitative analysis of intracellular metabolites of yeasts converting xylose to ethanol

MASTER'S THESIS

to achieve the university degree of

Diplom-Ingenieur

Master's degree programme: Biotechnology

submitted to

Graz University of Technology

Supervisor

Dipl.-Ing. Dr.nat.techn. Univ.-Doz., Mario Klimacek

Institute for Biotechnology and Biochemical Engineering

Graz, August 2015

AFFIDAVIT

I declare that I have authored this thesis independently, that I have not used other than the declared sources/resources, and that I have explicitly indicated all material which has been quoted either literally or by content from the sources used. The text document uploaded to TUGRAZonline is identical to the present master‘s thesis dissertation.

Date

Signature

Acknowledgement

This work was made possible by the cooperation of the Institute of Biotechnology and Biochemical Engineering (I.B.B.) at Graz University of Technology and HEALTH – the Institute of Biomedicine and Health Sciences at JOANNEUM RESEARCH Forschungsgesellschaft mbH Graz. Financial support came from the I.B.B. and from the Austrian Ministry for Transport, Innovation and Technology (bmvit) through the project Met2Net carried out at HEALTH.

I would like to thank the following people for their support:

Dipl.-Ing. Dr. Univ.-Doz. Mario Klimacek for providing this topic and the excellent supervision during my time at I.B.B. and the writing process of this master thesis.

Univ.-Prof. Dipl.-Ing. Dr. Bernd Nidetzky who enabled this work.

Mag. Dr. Christoph Magnes for the constructive mentoring in LC/MS analytics at HEALTH.

Elmar Zügner for the countless hours together in the laboratory and his friendship.

Karin Longus and Margaretha Schiller for the helpful laboratory assistance at I.B.B.

All the members of the I.B.B. and the Bioanalytics and Metabolomics group at HEALTH for providing a pleasant and stimulating work environment.

My special thanks go to my family for all their great assistance.

I would like to express my eternal gratitude to my lovely wife Lisa, to my son Elias and to my daughter Lorena for their strength and tolerance. Thanks a million for the numerous shortcomings you accepted without a word of protest.

This work is dedicated to my children Elias and Lorena.

List of Abbreviations

μ	Specific growth rate
6PG(DH)	6-phospogluconate (dehydrogenase)
ADH	Alcohol dehydrogenase
ARC	Anabolic reduction charge
(B)EF	(Baffled) Erlenmeyer flask
BE	Boiling ethanol
BL	Blank
BSA	Bovine serum albumin
CCM	Central carbon metabolism
CDW	Cell dry weight
CE	Capillary electrophoresis
CM	Cold methanol
CRC	Catabolic reduction charge
CS	Calibration standard
Ct	*Candida tenuis*
EC	Energy charge / enzyme class
ES	Extraction solvent
F	Fermentation
G	Glucose fermentation
G6P(DH)	Glucose 6-phosphate (dehydrogenase)
GC	Gas chromatography
(H)ESI	(Heated) electrospray ionization
(HP)LC/MS	(High performance) liquid chromatography coupled with mass spectrometry
(HP)LC/RI	(High performance) liquid chromatography coupled with refractive index detection
HRMS	High resolution mass spectrometry
I.B.B.	Institute for Biotechnology and Biochemical Engineering - Graz University of Technology
ISTD	Isotope-labeled internal standard
LDH	Lactate dehydrogenase
m/z	Mass-to-charge ratio
MAR	Mass action ratio
MM	Mineral medium
n.a.	Not available
n.d.	Not determined / not determinable
n.m.	Not measured
n.s.	Not separable
(o)PPP	(Oxidative) pentose phosphate pathway
OD_{600}	Optical density at 600 nm wavelength
[P]	Product concentration
PC	Preculture
P_i	Phosphate
PK	Pyruvate kinase
PPB	Potassium phosphate buffer
ppm	Parts per million
QC	Quality control sample / quality criteria

QqQ-MS	Triple quadrupole mass spectrometry
QS	Quenching solution
R	Resolution
R^2	Correlation coefficient
rpm	Rounds per minute
RT	Room temperature
S.D.	Standard deviation
S/N	Signal-to-noise ratio
[S]	Substrate concentration
SC	Sample class
S_i	Sulphate
SV	Sample volume
TCA	Tricarboxylic acid cycle
WB	Water bath
XDH	Xylitol dehydrogenase
XK	Xylulose kinase
XR	Xylose reductase
Y	Yield
YPD	Yeast peptone dextrose

Metabolites

6PG	6-Phosphogluconic acid
AcLYS	Acetyllysine
AcCoA	Acetyl Coenzyme A
ADP	Adenosine 5´-diphosphate
ALA	Alanine
AMP	Adenosine 5´-monophosphate
ARG	Arginine
ASN	Asparagine
ASP	Aspartic acid
ATP	Adenosine 5´-triphosphate
BPG	X,3-Diphosphoglyceric acid
CDP	Cytidine 5´-diphosphate
CitrA	Citric acid
CMP	Cytidine 5´-monophosphate
CTP	Cytidine 5´-triphosphate
CYS	Cysteine
dAMP	dAMP
DHAP	Dihydroxyacetone phosphate
dTDP	dTDP
dTTP	dTTP
F1P	Fructose 1-phosphate
F6P	Fructose 6-phosphate
FAD	Flavin adenine dinucleotide
FBP	Fructose X,6-bisphosphate
FMN	Flavin mononucleotide
FumA	Fumaric acid
G1P	Glucose 1-phosphate
G3P	Glycerol 3-phosphate

G6P	Glucose 6-phosphate
GABA	γ-Aminobutyric acid
Gal1P	Galactose 1-phosphate
GAP	Glyceraldehyde 3-phosphate
GDP	Guanosine 5´-diphosphate
GlcA	Gluconic acid
Glcs6P	Glucosamine 6-phosphate
GLN	Glutamine
GLU	Glutamic acid
GLY	Glycine
GlycA	Glyceric acid
GlyoxA	Glyoxylic acid
GMP	Guanosine 5´-monophosphate
GTP	Guanosine 5´-triphosphate
HIS	Histidine
hPRO	Hydroxyproline
HXP	Hexose X-phosphates
IcitrA	Isocitric acid
ILE	Isoleucine
IMP	Inosine monophosphate
LacA	Lactic acid
LEU	Leucine
LYS	Lysine
M1P	Mannose 1-phosphate
M6P	Mannose 6-phosphate
MalA	Malic acid
MET	Methionine
NAcALA	N-Acetyl -alanine
NAcGLN	N-Acetyl-glutamine
NAcGLU	N-Acetyl-glutamic acid
NAcORN	N-Acetyl -ornithine
$NAD(P)^+$	β-Nicotinamide adenine dinucleotide (phosphate) - oxidized form
NAD(P)H	β-Nicotinamide adenine dinucleotide (phosphate) - reduced form
NCarbASP	N-Carbamoylaspartic acid
ORN	Ornithine
OxalA	Oxaloacetic acid
PEP	Phosphoenolpyruvic acid
PHE	Phenylalanine
PRO	Proline
PRPP	Phosphoribosylpyrophosphate
PSER	Phosphoserine
PYR	Pyruvic acid
PyrGLU	Pyroglutamic acid
R5P	Ribose 5-phosphate
Ru5P	Ribulose 5-phosphate
S7P	Sedoheptulose 7-phosphate
SBP	Sedoheptulose 1,7-bisphosphate
SER	Serine
SuccA	Succinic acid

T6P	Trehalose 6-phosphate
THR	Threonine
Treha	Trehalose
TRP	Tryptophan
TYR	Tyrosine
UDP	Uridine 5`-diphosphate
UDPGlc	UDP-Glucose
UDPNAcGlcs	UDP N-Acetyl-glucosamine
UMP	Uridine 5`-monophosphate
UTP	Uridine 5`-triphosphate
VAL	Valine
X5P	Xylulose 5-phosphate
XPG	X-Phosphoglyceric acid
αKG	α-Ketoglutaric acid

Table of Contents

1 Summary

1.1 Background

Intracellular metabolite levels are a direct reflection of a certain cellular phenotype. Consequently determination of metabolite profiles is a powerful tool to investigate microbial cell factories to identify metabolic bottlenecks that preclude efficient production of a desired product. In this work natural and recombinant xylose-utilizing yeast strains were analysed by semi-quantitative and quantitative metabolome analysis. Strains investigated differed either in their ability to produce ethanol from xylose although expressing the same xylose reductase and a similar xylose assimilation pathway or to grow on xylose under anaerobic conditions. However unbiased quantitative metabolome analysis requires a sample work-up routine that combines rapid quenching of the metabolism with complete isolation of intracellular metabolites and that is compatible with the subsequent metabolite analysis. Because known sample work-up protocols were not applicable to the analytical platform (ion-pairing reversed phase liquid chromatography (LC) coupled to an Exactive^{TM} orbitrap mass spectrometer (MS)) used here an improved protocol had to be developed before the scientific question could be addressed.

1.2 Results

Reduction of phosphate and sulphate ions by a factor of 58 and 20, respectively, in the fermentation medium, altering of the volume ratio of sample and quenching solution from 1:4 to 1:10, altering sample handling during metabolite extraction by boiling ethanol and addition of a ^{13}C-labeled metabolite extract as internal standard were identified as the most important factors affecting quality of subsequent quantitative metabolite analysis by LC/MS.

Quantitative and semi-quantitative metabolome analyses addressing metabolites (127 in total) of the central carbon, the redox and the energy metabolism as well as amino acids revealed distinct metabolite profiles for each phenotype studied in this work. Thirty-two metabolites could be quantified and more than 100 were targeted semi-quantitatively. Using thermodynamic analysis resultant levels of metabolites of the central carbon metabolism could be verified. Key metabolites representative for each phenotype investigated could be identified. Differences in metabolite profiles were discussed in the context of ethanol productivity and the ability to grow on xylose.

1.3 Conclusion

A LC/MS-based targeted metabolomics approach was established in this work with which a broad range of chemically diverse intermediates of the yeast's central carbon metabolism, the redox and energy metabolism but also a number of amino acids and precursors thereof can be determined semi-quantitatively and quantitatively. The suitability of the improved sample work-up procedure was demonstrated and applied to scientific relevant questions. Metabolomics investigations of different yeast phenotypes clearly lead to targets responsible for (i) efficient xylose-to-ethanol conversion and (ii) anaerobic growth on xylose. The now available metabolomic data represent a valuable fundament for subsequent studies.

2 Introduction to metabolomics

Metabolites are small molecules permanently transformed in metabolic pathways. They provide a "functional readout of cellular state" and serve as "direct signature of biochemical activity" [1]. Contrary to genes, proteins and lipids, metabolite levels have a fast response on environmental impacts. This is specified by endogenous enzyme properties and activity levels, various concentrations of reactants and thermodynamics. All metabolites (and reactions) within a biological system are summarized as metabolome [2], [3].

The investigation of the metabolome is the matter of metabolomics, the latest of the "omics" research fields. Metabolomics complements genomic, transcriptomic, proteomic as well as fluoric data and thus lead to a more comprehensive view of cell biology. As the metabolite profile quickly reflects distinct phenotypes, metabolomics gives great opportunities in facilitating metabolic engineering thus represent a valuable tool in systems biology [4]. The potential of metabolomics is emphasized in the design of superior biocatalysts and cell factories for industrial production of high value chemicals. Beside applications in microbial biology metabolomics is also a mighty tool in the health sector. Discovery and identification of "biomarkers" for distinct dietary exposures [5], certain diseases or pharmaceuticals, underline the importance of that technology for today's scientific community.

2.1 Classification of metabolomics

The terminology of metabolomics classification is yet not consistent in literature. According to *Fiehn et al. (2002)* metabolomics as multi-functional discipline can be subdivided into three categories [6]. First, metabolite target analysis, dealing with the quantification of substrate and/or product of a specific reaction of a target protein, second, metabolic profiling, aiming at the quantitative analysis of a set of pre-defined compounds representing a distinct metabolic pathway or a class of metabolites, and third, metabolomics focusing on an unbiased overview of the whole-cell metabolites and networks [7]. Taking "metabolomics" into consideration as a widely accepted scientific keyword instead of an analytical section a classification into two subdivisions is reasonable, targeted analysis and metabolic profiling which comprises metabolic finger- and footprinting [8]. In that approach metabolic profiling deals with the semi-quantitative data of qualified or even unknown intracellular (metabolic fingerprinting) or extracellular (metabolic footprinting) metabolites. More recently, a more appropriate terminology has been introduced. Targeted metabolomics involves focused qualitative and quantitative identification of known compounds, while untargeted

metabolomics deals with mostly unknown unbiased metabolite data. Frequently used terms are summarized in Table 2-1.

Table 2-1: Metabolomics terminology

Metabolome	[2], [3]	Entirety of all metabolites within a biological system
Endo-/Exometabolome	[4]	Entirety of all intra-/extracellular metabolites within a biological system
Metabolomics	[6], [7]	Unbiased overview of the whole-cell metabolites, networks and reactions
Metabolite target analysis	[6], [7]	Quantification of intracellular concentrations of reactants of a specific reaction of a target protein
Metabolite/Metabolic profiling	[6], [7]	Quantitative analysis of a set of pre-defined compounds representing a distinct metabolic pathway or class of intracellular and/or extracellular metabolites
Targeted metabolite analysis/Targeted metabolomics	[1], [9]	Focused qualitative or quantitative determination of known intracellular and/or extracellular metabolites
Metabolic fingerprinting	[9]	Semi-quantitative analysis of qualified or even unknown intracellular metabolites
Metabolic footprinting	[9]	Semi-quantitative analysis of qualified or even unknown extracellular metabolites
Untargeted metabolomics	[1]	Unbiased global metabolite analysis

2.2 Analytical platforms

As metabolites differ a lot in terms of chemical and structural properties there is no “all-in-one” solution in metabolite analysis. To cover this heterogeneity multiple analytical platforms are applied such as enzymatic assays, thin-layer chromatography, gas chromatography (GC), nuclear magnetic resonance (NMR), high performance liquid chromatography (HPLC or LC), direct infusion mass spectrometry (MS) and mass spectrometry coupled to capillary electrophoresis (CE), GC or LC. However, there is a trend to highly selective and sensitive multifunctional methods with a broad range of detectable metabolites and the capability to get by with minimal sample volumes [7]. Among these methods MS coupled to LC or GC has

become the analytical platform of choice for most metabolomics approaches [10]. As LC and GC both have their advantages for separation of different metabolite classes (see Figure 2-1) the combination of these technologies is beneficial for comprehensive metabolomics studies.

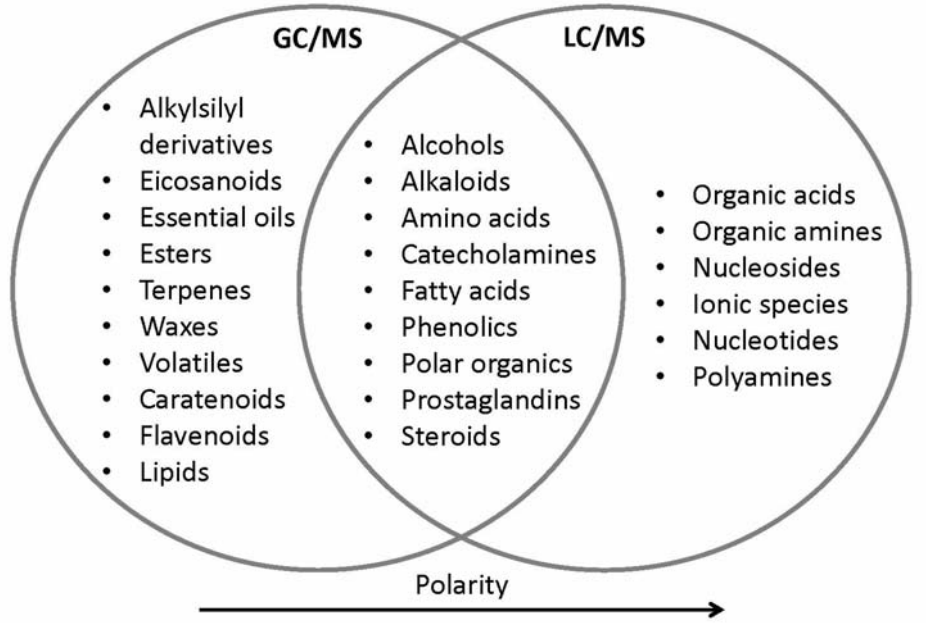

Figure 2-1: Overlap of GC/MS and LC/MS applicability. This is a reproduction of Figure 1 of the online article "Mass Spectrometry for Metabolomics" from *D.L. Haviland 2007* **[11]**.

For the subsequent analyte detection several MS systems are available on the market, each of them with their pros and cons. For almost every metabolomics question adequate MS types exist. Triple quadrupole MS (QqQ-MS) for example shows excellent results in focused analysis of distinct compounds in targeted approaches [12]–[14]. That targeted approaches are widely applied in pharmacy, driven by specific biochemical questions or hypothesis concerning particular pathways. Targeted analysis therefore acts as an effective tool in pharmacokinetic studies or influence measurements of therapeutics and genetic modifications of enzymes [1].

Developments towards advanced high resolution mass spectrometry (HRMS) expand the field of LC/MS applications. HRMS coupled to LC allows routine detection of hundreds of metabolites in biological samples. Thus they are most appropriate for metabolic finger- and footprinting and generate valuable data for "biomarker" identification [10]. HRMS technology is capable to detect all metabolites of a predefined mass range simultaneously in one scan event. In contrast to QqQ-MS no masses are excluded prior to the detection. Metabolites of interest can be considered retrospectively. Therefore it is a mighty tool for combining targeted and untargeted approaches in order to accomplish a more comprehensive

metabolomics analysis. The higher resolution settings offer important benefits for more accurate metabolite identification. Opposed to QqQ-MS no specific fragmentation scan, called single reaction monitoring (SRM), for metabolites of interest is required to obtain an adequate analyte specificity [15]. Additional structural information for all metabolites can be obtained via in-house fragmentation and MS detection of these fragments (MS/MS or MS^2).

2.2.1 High resolution MS coupled to ion-pair reversed phase HPLC

Among the standard separation techniques (LC, GC, CE) prior to MS detection LC was concluded as most suitable for quantitative metabolomics approaches, mainly ascribed to the broad metabolite coverage and the analytical robustness [16]. Several LC techniques are available focusing on different metabolite classes. As conventional reversed phase LC (RPLC) is restricted to non-polar and neutral species, often hydrophobic interaction LC (HILIC) is used to complement for polar analytes. Alternatively the application of ion-pair RPLC (IP-RPLC) additionally covers a broad range of (highly) polar compounds of the central carbon metabolism (CCM) and therefore represents a valuable compromise in metabolite analysis. In that technique an ion-pair reagent, a molecule with non-polar chains such as tributylamine, is part of the mobile phase. The reagent interacts with charged analytes, decreases their polarity and therefore leads to an enhanced separation of even very polar metabolites. Currently many LC/MS methods are based on that technique [13], [15], [17]. But, as a drawback these methods are restricted to negative ionization modes as positive ionization leads to severe and persistent contamination of the MS instrument with the ion-pair reagent. Consequently only compounds displaying negative ionization can be addressed.

Today electrospray ionization (ESI) and heated ESI (HESI) are well-established ionization sources for metabolomics approaches. ESI is a mild ionization technique with very low fragmentation of the analytes, e.g. when compared to atmospheric pressure chemical ionization (APCI). In contrast to other mild ionization techniques, as matrix-assisted laser desorption ionization (MALDI), ESI can be coupled directly to LC systems. The advantage of HESI is that it is possible to apply high LC flow rates and highly aqueous eluents. Beside that ESI/HESI has some drawbacks. Most prominently ESI is very prone to so-called matrix effects, indicated by weak ionization performance and deficient MS signals [18], [19] which makes an internal standardization absolutely necessary for quantitative approaches (see Section 2.4.4).

The subsequent detection with HRMS allows the simultaneous recording of all co-eluting metabolites with excellent mass precision. This enables applicability for targeted and untargeted approaches in parallel. The storage of all MS signals gives access to information for comprehensive post-analytical analysis. Contrary to QqQ-MS no information about metabolites and theirs masses is required prior to the analysis.

2.3 Mass spectrometry-based quantitative metabolomics

The quantification of intracellular metabolites is a prerequisite for interpretation of cellular properties at molecular and kinetic levels and therefore of remarkable importance in biotechnological process development [7], [20]. But to obtain quantitative metabolite data as close as possible to *in vivo* conditions many hurdles need to be resolved. Biological variability, type of cultivation and conditions used for cultivation, sampling, sample work-up, chromatography and MS detection can contort the quantification output [21]. These factors can be summarized (i) in the issue of the representative biological sample, which means conserving predefined physiological states through all subsequent sample work-up steps, and (ii) in the issue of the LC/MS analysis [20].

Of these the biggest impact hindering correct, comparable and reproducible metabolite level determination is the biological variance. Particle size, cell viability and slightly different physiological states represent a big source of variability which can exceed by far the variability of modern analytical methods such as current LC/MS setups [21].

To record *in vivo* conditions fast sampling and instantaneous stopping (quenching) of all enzymatic activity in a sub-second range is required [22]. Exact withdrawal of a defined sample volume and avoidance of contaminations are crucial. Metabolite leakage in the quenching step can be significant and correction is essential for appropriate quantification [23]. That demands the subsequent metabolite level determination in the quenching supernatant after separation of biomass and of the exometabolites in the culture medium [24]. But in particular the LC/MS-based determination of exometabolites is strongly hindered by matrix effects caused by culture medium components. In succession additional washing steps of the quenched biomass minimize carry-over of extracellular metabolites and medium components in dead volumes, but increase the risk of cell leakage.

Extraction should be as quantitative as possible accompanied by minimal metabolite degradation and complete enzyme inactivation. As the metabolome consists of enormous chemical diversity total metabolite extraction remains theoretical [8]. The extraction method applied is therefore a compromise between extraction efficiency and unwanted physical,

chemical and biochemical reactions and degradation processes influencing the extraction recovery. Further used extraction solvents (ES) should not interfere with the subsequent analysis [21]. In case of LC/MS analysis the evaporation of the ES from the metabolomics samples accompanied by a concentration of the metabolites is often inevitable to reach quantifiable signals [13], [16], [25].

Matrix effects exerted by high levels of either metabolites or salts can affect both separation by LC and ionization by MS. Chromatographic separation efficiency is very sensitive to overloading effects which can contort the elution profile severely. That can lead to a simultaneous elution of multiple analytes. Due to the chemical diversity of metabolites the ionization efficiency varies strongly. Hence the co-elution of matrix compounds often leads to ion suppression of the analyte of interest. In some cases the overloading of the ionization chamber with matrix compounds masks the MS signal for target metabolites completely [26]. Subjected to biological matrices the ionization efficiency of metabolites in samples differs significantly from those of matrix-free calibration standards. This fact requires the application of internal standards to enable the quantification of metabolites and the comparability of samples [21].

Automated spectra evaluation is biased due to different elution profiles and mass deviations, but often not recognized as such. The necessity of manual peak integration is very time consuming, results are operator dependent and thus vary in terms of reproducibility [21].

2.4 Sample preparation for yeast metabolomics

2.4.1 Rapid sampling and cold methanol quenching

In the sampling and quenching process an aliquot of a representative biological sample (cell broth) is transferred rapidly in a precooled quenching solution (QS, < -40°C [27]) which instantaneously stops all enzymatic cell activity and conserves the metabolic state of the cells. For bioreactor cultivations often in-house sampling devices are used to obtain reproducibility in terms of sampling time and volume [22]. As a drawback these devices are not commercially available on the market yet [20].

Enzymatic metabolite turnover rates vary significantly from seconds (central carbon metabolism [28], NADH, ATP [22]) to even minutes (amino acids and some tricarboxylic acid cycle (TCA) intermediates [29], [30]). Therefore the sampling time has to be adapted according to the metabolites to be analysed. The quenched cells are then separated from the supernatant by centrifugation prior to the subsequent extraction.

Among the diverse quenching methods for eukaryotic submerse cultures published in literature the cold methanol/water approach is the most popular. The method was first introduced by *De Koning and Van Dam (1992)* who used as QS 60 % methanol precooled to -40°C and a sample volume (SV)/QS ratio of 1 to 5 [31]. Based on that protocol several studies have dealt with variable methanol/water ratios, different quenching temperatures and SV/QS ratios [27], [32]. Especially the issue of metabolite leakage effect was addressed numerous times in yeast with contradictory outcomes [8], [27]. It is nearby that these inconsistencies concerning the occurrence of leakage effects were not only caused by different quenching conditions. Rather different cultivation methods, resultant cellular states and sensitivity of analytical methods can be a reasonable explanation. Considerable results concerning cell leakage in *Saccharomyces cerevisiae* were presented by *Canelas et al. (2008)* who adapted the original protocol in a comprehensive sample work-up study [27]. They pointed out that metabolite leakage could be completely prevented by quenching in pure methanol and temperature lower than –40°C. The originally recommended SV/QS ratio (1:5) was approved. Further they presented evidence for significant metabolite losses by applying QS with 80 % methanol or less and temperatures above -40°C. As it turned out that the exposure time of cells to the QS played another important role in terms of leakage additional washing steps with QS should be omitted if possible [27].

2.4.2 Boiling ethanol extraction

The completeness of the extraction of the target metabolites is strongly affected by the polarity of the target compounds and the cell integrity. Additionally metabolite stability differs a lot with pH and temperature. Therefore extraction protocols should be adapted to distinct target classes [33], [34].

Canelas et al. (2009) evaluated a number of established extraction methods in *S. cerevisiae* [34]. They opposed hot water [29], boiling ethanol (BE) [35], chloroform/methanol (CM) [8], [31], freezing-thawing in methanol [36] and acidic acetonitrile/methanol [37]. They focused on metabolites of the central carbon metabolism (glycolysis, TCA and pentose phosphate pathway (PPP)), energy metabolism and amino acids. Metabolite degradation was monitored via addition of isotope-labeled internal standard and used for correction. Among all tested methods BE and CM were considered as most appropriate for metabolite extraction in *S. cerevisiae*. Both methods showed excellent recoveries and good reproducibility.

2.4.3 Removing of the extraction solvent and concentration by evaporation

As the ES often interfere with the subsequent analysis method and dilute the concentration of target metabolites the total elimination of ES is a prerequisite for unbiased results. In case of BE vacuum is most commonly applied (frequently at low temperatures) to evaporate the organic fraction or even to complete dryness, followed by dissolving in water [14], [34], [38]. Another approach to evaporate and concentrate cell extracts is the careful blowing out of ES with inert gas such as nitrogen [15].

2.4.4 Internal standardization of biological samples

As already mentioned the LC/MS-based quantification of intracellular metabolites in yeast has to cope with a number of notable issues such as metabolite-specific instabilities, matrix effects and ion suppression. Also day-to-day variations in the analysis have to be considered. In order to correct for these causes of variation internal standardization represents an elegant approach. For this purpose ^{13}C-labeled compounds are ideally suited as they have the identical retention pattern to the various ^{12}C metabolites, but can be detected individually due to different mass signals. Though the availability of isotope-labeled species is limited and the costs are high. As an alternative stable isotope-labeled metabolite extracts can be applied. First introduced by *Mashego et al. (2004)* uniformly ^{13}C-labeled yeast extract was used for internal standardization of ^{12}C metabolites [33], [39]. When adding ^{13}C-labeled internal standards (ISTD) to the sample prior to the metabolite extraction metabolite degradation or losses as well as matrix effects along the work-up sequence from extraction to LC and MS analysis can be compensated [12], [16], [33], [34], [39]. Given that the metabolite of interest or the ^{13}C-labeled isotope is not totally lost, the ratio ^{12}C metabolite/^{13}C metabolite remains stable. As it can be assumed that ion suppression effects in “overloaded” concentration ranges are similar for isotope-labeled and unlabeled species, the ratios should neither be influenced [33]. Therefore even high concentrated species (> 10 µM [26]) can be calibrated what extends the linearity ranges for quantification compared to external calibrations [33], [39]. Despite the advantages of ISTD application it has to be mentioned that the addition of ISTD to biological samples also increases the amount of matrix compounds, particularly when metabolite extracts are used. For instance salt components of the cultivation medium as phosphate (P_i) or sulphate (S_i) can have a huge negative impact on LC/MS analysis [15]. Furthermore ^{12}C impurities in the ISTD can contort the analysis as well.

2.5 Bioethanol production in yeast

Bioethanol has an outstanding relevance in global biogenic fuel supply. Today sugar and starch rich crops are used as feedstock for microbial alcohol fermentation at industrial scale. The resulting competition with the alimentary market, limitations in cultivable land and imbalanced CO_2 cycles initiate sustainable developments in bioethanol production. As the biggest renewable feedstock resource lignocellulose materials represent the most sustainable alternative [40], [41]. One of the main obstacles in economically relevant production of this often called 2nd generation bioethanol is the utilization of all principal sugar components. Beside the glucose polymers of cellulose the hemicellulose fraction of hard woods and agricultural raw materials (straw) is rich in pentose sugars. Xylose represents the main pentose component [41], [42].

The yeast *S. cerevisiae*, although well established for alcoholic fermentation over thousands of years, is not able to use xylose as a substrate [42]–[44]. In the first step of its assimilation xylose is isomerized to xylulose. This is accomplished in case of bacteria and some fungi in one step catalyzed by an isomerase [45], [46] or in two steps by xylose reductase (XR) and xylitol dehydrogenase (XDH) typically seen for xylose-fermenting yeasts [47], [48]. Xylulose is converted to xylulose 5-phosphate (X5P) by an ATP-dependent xylulose kinase (XK). X5P is further metabolized to ethanol through enzymes from the pentose phosphate pathway (PPP), glycolysis and ethanol formation. Xylose assimilation is shown in Figure 2-2. In the following section the focus is laid on the yeast type xylose assimilation pathway as all strains used in this work contain this pathway.

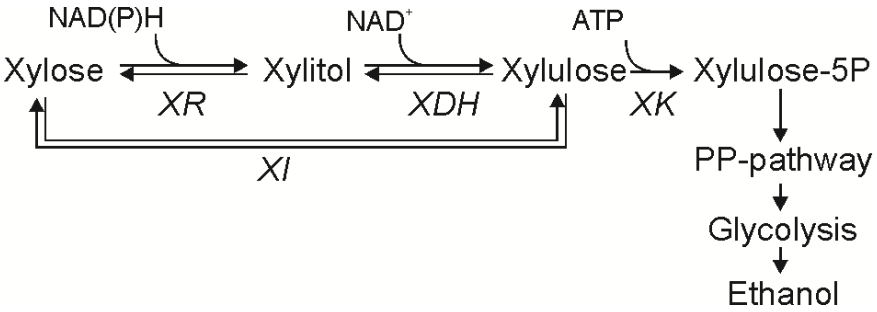

Figure 2-2: Xylose assimilation in recombinant yeast expressing yeast-type or bacterial-type xylose assimilation pathway. XR, xylose reductase; XDH, xylitol dehydrogenase; XK, xylulose kinase; XI, xylose isomerase; PP, pentose phosphate. Figure adopted from *Klimacek et al. 2014* [49].

In the two-step oxidoreductive pathway for xylose assimilation the NADPH-dependent XR catalyses the reduction of xylose to xylitol. The NAD^+-dependent XDH supports the oxidation of xylitol to xylulose (see Figure 2-2). The coenzyme specificities of XR and XDH cause a coenzyme imbalance within the cell which results in slow and inefficient metabolization of xylose by recombinant *S. cerevisiae* strains expressing wild-type forms of XR, XDH and XK. A substantial part of xylose is converted to the undesired by-product xylitol ($Y_{xylitol}$ ~40 % (g g^{-1})) [50]. Stoichiometric and enzymatic considerations show that the amount of NADPH used by XR relates to the amount of formed xylitol [51], [52]. However, natural xylose fermenting yeast strains as *Scheffersomyces stipitis* or *Candida tenuis*, show, despite of the same xylose metabolism, high ethanol yields ($Y_{ethanol}$ ~40 % (g g^{-1})) accompanied by low by-product formation [53], [54]. Reasons for that phenotype differentiation are not known yet, but it denotes an alternative and oxygen independent cofactor regeneration [54].
Recombinant *S. cerevisiae* strains which have integrated the two-step oxidoreductive xylose assimilation route are not able to grow anaerobically on xylose [43], [44], [51]. Nevertheless growth is an essential characteristic, beside sufficient ethanol yields, to reach high productivity and is therefore indispensable for bioethanol process integration and related economic efficiency. Recently, the stepwise metabolic adaption of *S. cerevisiae* strains over multiple generations led from pure metabolization to balanced growth on xylose under anaerobic conditions [49], [55], [56].

2.5.1 Yeast strains used in this work

In this work four yeast strains were used as platform for metabolic analysis. *S. cerevisiae* strain BP000 resulted from strain CEN.PK 113-7D via homologous integration of the *C. tenuis* wildtype form of XR (*Ct*XR) and the XDH from *Galactocandida mastodermitis*. Strain BP10001, resulting from BP000, expresses a double mutated form of *Ct*XR which prefers NADH over NADPH. A copy of endogenous XK was expressed homogenously in both recombinant strains [14], [43], [50], [57], [58]. Strain IBB10B05 was developed out of BP10001 by stepwise metabolic adaption [49], [55], [56]. As natural xylose fermenting model *C. tenuis* strain CBS4435 was chosen. Physiological parameters of yeasts investigated in this study under xylose fermenting conditions are displayed in Table 2-2.

Table 2-2: Yeast phenotypes investigated in this study

	S. cerevisiae				*C. tenuis*
	BP000[a]	BP10001[a]	IBB10B05[b]		CBS 4435[c,h]
Parameter			Phase I	Phase II	
q_{xylose} (g g^{-1}_{CDW} h^{-1})	0.06	0.08[f]	0.80		0.13
$Y_{biomass}$ (g g^{-1})	n.d.[d]	n.d.[d]	0.07[g]		n.d.[d]
$Y_{ethanol}$ (g g^{-1})	0.24	0.34	0.35		0.40
$Y_{xylitol}$ (g g^{-1})	0.39	0.19	0.03[f]	0.20	0.06
$Y_{glycerol}$ (g g^{-1})	0.048	0.021	0.11[g]	0.018	0.04
$Y_{acetate}$ (g g^{-1})	0.019	0.020	0.04[f]	0.03[f]	n.a.[d]
$Y_{ribitol}$ (g g^{-1})	n.m.[d]	n.m.[d]	n.d.[d]	0.011[g]	n.m.[d]
Y_{CO2} (g g^{-1})	0.24[e]	0.34[e]	0.37	0.36	n.a.[d]

Data were obtained from Ref. [43][a] for BP000 and BP10001, Ref. [49][b] for IBB10B05 and Ref. [54][c] for *C. tenuis*. Relative S.D. were < 5 %[a] and < 6 %[b]. [d] n.d.: Not determinable, n.m.: Not measured, n.a.: Not available in the data set. [e] Values were caluculated from the data set presented. [f] Rel. S.D. ~30 %. [g] Rel. S.D. ≤ 20 %. [h] No rel. S.D. available.

3 Aim of work

The aims of this work were

- to establish a sample work-up routine for yeast cells (*C. tenuis* and *S. cerevisiae*) based on available protocols,
- to establish an analytical platform with which intracellular metabolites can be quantitatively addressed,
- to apply targeted metabolomics to xylose-utilizing recombinant *S. cerevisiae* strains and *C. tenuis* to identify factors responsible for (i) efficient xylose-to-ethanol conversion and (ii) anaerobic growth on xylose.

4 Materials

4.1 Instruments

Centrifugation

Centrifuge Micro Star 17	VWR (West Chester, USA)
Centrifuge “Eppifuge” 5415R	Eppendorf AG (Hamburg, Germany)
Centrifuge 5804R	Eppendorf AG (Hamburg, Germany)
Centrifuge Sorvall Evolution RC	Thermo Fisher Scientific (Waltham, USA)
Centrifuge tube, 50 mL, 15 mL	SARSTEDT AG & Co. (Nümbrecht, Germany)

Cultivation

Erlenmeyer flask, 1000 mL, 300 mL	Schott DURAN Produktions GmbH & Co. KG (Mainz, Germany)
Erlenmeyer flask, baffled, 1000 mL, 300 mL	Schott DURAN Produktions GmbH & Co. KG (Mainz, Germany)
Fermentation system	Infors HT (Bottmingen-Basel, Switzerland)
Fermenter Labfors 2	
Software Iris NT	
pH electrode	
Shaking incubator	Infors HT (Bottmingen-Basel, Switzerland)
Shaking incubator CERTOMAT BS-1	Satorius AG (Goettingen, Germany)

Filters

Syringe filter Minisart^{R}, 0.2 µm, 0.45 µm	Satorius AG (Goettingen, Germany)
Polyamide filter Sartolon, 0.2 µm	Satorius AG (Goettingen, Germany)

HPLC/RI system	Merck – Hitachi LaChrom (Darmstadt, Germany - San Jose, USA)
Pump L-7100	
RI detector L-7490	
UV detector L-7400	
Autosampler L-7250	
HPLC system manager software D-7000	
Degasys DG-2410	UniFlows (Tokyo, Japan)
Cation H-Cartridge Micro-Guard 125-0129	Biorad (Hercules, USA)
Column Aminex HPX-87H	Biorad (Hercules, USA)
HPLC glass vials incl. glass inlets, 200 µL	Markus Bruckner Analysentechnik (Linz, Austria)

HPLC/MS system	Thermo Fisher Scientific (Waltham, USA)
HPLC Dionex Ultimate3000	
Autosampler WPS-3000	
Solvent rack SRD-3600	
Pump LGP-3600 (LPG-3000)	
Flow manager FLM-3300	
Xcalibur software , version 2.2 SP1	
Pre-column Atlantis T3 C18, 3 µM, 100 A, 10 x 2.1 mm	Waters Corporation (Milford, USA)
Column Atlantis T3 C18, 3 µm, 100 A, 150 x 2.1 mm	Waters Corporation (Milford, USA)
HPLC vials, 200 µL , TopSert TPX-Short Thread Vial, 32x11.6	VWR (West Chester, USA)
Heated electrospray ionization source (HESI)	Thermo Fisher Scientific (Waltham, USA)
Mass spectrometer Exactive™	Thermo Fisher Scientific (Waltham, USA)
Photospectrometry	
WPA CO 8000 Biowave Cell Density Meter	Biochrom (Cambridge, UK)
Spectrophotometer DU800	Beckman Coulter Inc. (Fullerton, USA)
Peltier temperature controller	
System and applications software version 2.0	
pH measurement	
pH meter 691	Metrohm AG (Herisau, Switzerland)
pH meter inoLab 720	WTW Wissenschaftlich-Technische Werkstätten GmbH (Weilheim, Germany)
Pipettes	
Pipette FINPIPETTE, 5 mL, 10 mL	Thermo Fisher Scientific (Waltham, USA)
Pipette tips FINNTIP, 5 mL, 10 mL	Thermo Fisher Scientific (Waltham, USA)
Pipette Pipetman, 10 µL, 100 µL, 1000 µL	Gilson, Inc. (Middleton, USA)
Pipette tips, 10 µL, 100µL, 1000 µL	Greiner Bio-One GmbH (Frickenhausen, Germany)
Pipette Biomaster, 100 µL, 1000 µL	Eppendorf AG (Hamburg, Germany)
Pipette tips, 100µL, 1000 µL	Eppendorf AG (Hamburg, Germany)
Additional equipment	
8-Channel Multi-Input Thermometer PCE-T800	PCE Instruments (Meschede, Germany)
Evaporator®	Gebr. Liebisch GmbH & Co. KG (Bielefeld, Germany)
French Pressure Cell Press	Travenol Laboratories Inc. (Deerfield, USA)
Incubator/shaker Certomat BS-1	Satorius AG (Goettingen, Germany)
Needle Sterican, Ø 0.8 mm x 120 mm	B. Braun Medical AG (Emmenbrücke, Switzerland)
Needle Sterican, Ø 0.9 mm x 40 mm	B. Braun Medical AG (Emmenbrücke, Switzerland)
Vortex shaker REAX top	Heidolph Instruments GmbH & Co. KG (Schwabach, Germany)
Water bath type 1083, ≤ 99°C	GFL Gesellschaft für Labortechnik GmbH (Burgwedel, Germany)

4.2 Chemicals

Table 4-1: General chemicals

2-Propanol, LC/MS-grade	Sigma-Aldrich (St. Louis, USA)
Acetic acid, ≥ 99 %	Sigma-Aldrich (St. Louis, USA)
Agar-Agar	Carl Roth GmbH + Co. KG (Karlsruhe, Germany)
Albumin fraction V (BSA)	Carl Roth GmbH + Co. KG (Karlsruhe, Germany)
Ammonium acetate, ≥ 98 %	Merck KGaA (Darmstadt, Germany)
Ammonium chloride, ≥ 99 %	Carl Roth GmbH + Co. KG (Karlsruhe, Germany)
Ammonium sulphate, ≥ 99.5 %	Carl Roth GmbH + Co. KG (Karlsruhe, Germany)
Antifoam 204	Sigma-Aldrich (St. Louis, USA)
D-[UL-^{13}C]-Glucose, ≥ 99 %	Omicron Biochemicals, Inc. (South Bend, USA)
Ergosterol, ≥ 95 %	Sigma-Aldrich (St. Louis, USA)
EDTA (ethylenediaminetetraacetic acid disodium dihydrate), ≥ 99 %	Carl Roth GmbH + Co. KG (Karlsruhe, Germany)
Ethanol, 99.8 %	VWR (West Chester, USA)
Glucose monohydrate, ≥ 99.5 %	Carl Roth GmbH + Co. KG (Karlsruhe, Germany)
Glycerol, ≥ 99.5 %	Carl Roth GmbH + Co. KG (Karlsruhe, Germany)
HEPES (4-(2-hydroxyethyl)-1-piperazineethanesulfonic acid), ≥ 99.5 %	Carl Roth GmbH + Co. KG (Karlsruhe, Germany)
Hydrochloric acid, 37 %	Carl Roth GmbH + Co. KG (Karlsruhe, Germany)
Magnesium chloride hexahydrate, ≥ 99 %	Carl Roth GmbH + Co. KG (Karlsruhe, Germany)
Magnesium sulphate heptahydrate, ≥ 99 %	Carl Roth GmbH + Co. KG (Karlsruhe, Germany)
Methanol, LC/MS-grade	Sigma-Aldrich (St. Louis, USA)
Peptone ex casein	Carl Roth GmbH + Co. KG (Karlsruhe, Germany)
PK/LDH enzyme mixture, Lot.nr. 051 M7405V Pyruvate kinase, 0.6-1.0 U μL^{-1} Lactate dehydrogenase, 0.9-1.4 U μL^{-1}	Sigma-Aldrich (St. Louis, USA)
Potassium dihydrogen phosphate, ≥ 99 %	Carl Roth GmbH + Co. KG (Karlsruhe, Germany)
Roti®-Quant	Carl Roth GmbH + Co. KG (Karlsruhe, Germany)
Sodium acetate, ≥ 98.5 %	Carl Roth GmbH + Co. KG (Karlsruhe, Germany)
Sodium hydroxide, ≥ 99 %	Carl Roth GmbH + Co. KG (Karlsruhe, Germany)
Sulphuric acid, 1N	Carl Roth GmbH + Co. KG (Karlsruhe, Germany)
Trace element solution, 1000 x	Supplied by I.B.B. / made according to *Jeppsson et al.* 2006 [48]
TRIS (tris(hydroxymethyl)aminomethane)	Carl Roth GmbH + Co. KG (Karlsruhe, Germany)
Tributylamine, ≥ 99.5 %	Sigma-Aldrich (St. Louis, USA)
Tween® 80	Sigma-Aldrich (St. Louis, USA)
Vitamin solution, 1000 x	Supplied by I.B.B. / made according to *Jeppsson et al.* 2006 [48]
Water, LC/MS-grade	Sigma-Aldrich (St. Louis, USA)
Xylitol, ≥ 99 %	Sigma-Aldrich (St. Louis, USA)
Xylose, ≥ 99 %	Carl Roth GmbH + Co. KG (Karlsruhe, Germany)
Xylulose, ≥ 95 %	Supplied by I.B.B. / concentration determined by HPLC, 08/2008
Yeast extract	Carl Roth GmbH + Co. KG (Karlsruhe, Germany)

Table 4-2: Metabolomics stock compounds

Compound	Purity		Supplier
2,3-Diphospho-D-glyceric acid pentasodium salt[1]	-		Sigma-Aldrich (St. Louis, USA)
6-Phosphogluconic acid trisodium salt *	≥ 97	%	Sigma-Aldrich (St. Louis, USA)
Acetyl Coenzyme A (C2:0) sodium salt	≥ 93	%	Sigma-Aldrich (St. Louis, USA)
Adenosine 5´-monophosphoric acid disodium salt dihydrate	≥ 99	%	AppliChem GmbH (Darmstadt, Germany)
Adenosine 5´-diphosphate sodium salt	≥ 95	%	Sigma-Aldrich (St. Louis, USA)
Adenosine 5´-triphosphoric acid disodium salt *	≥ 99	%	Sigma-Aldrich (St. Louis, USA)
Citric acid	≥ 99	%	Sigma-Aldrich (St. Louis, USA)
D-3-Phosphoglyceric acid disodium salt	≥ 93	%	Sigma-Aldrich (St. Louis, USA)
D-Fructose 1,6-bisphosphate trisodium salt	≥ 98	%	Sigma-Aldrich (St. Louis, USA)
D-Fructose 6-phosphate dipotassium salt	≥ 97	%	Sigma-Aldrich (St. Louis, USA)
D-Glucose 6-phosphate sodium salt *	≥ 98	%	Sigma-Aldrich (St. Louis, USA)
Dihydroxyacetone phosphate dilithium salt	≥ 95	%	Sigma-Aldrich (St. Louis, USA)
DL-Glyceraldehyde 3-phosphate[2]	-		Sigma-Aldrich (St. Louis, USA)
DL-Isocitric acid trisodium salt hydrate	≥ 93	%	Sigma-Aldrich (St. Louis, USA)
D-Mannose 6-phosphate sodium salt	≥ 98	%	Sigma-Aldrich (St. Louis, USA)
D-Ribose 5-phosphate disodium salt hydrate	≥ 98	%	Sigma-Aldrich (St. Louis, USA)
D-Ribulose 5-phosphate disodium salt	≥ 96	%	Sigma-Aldrich (St. Louis, USA)
D-Trehalose dihydrate	≥ 99	%	Sigma-Aldrich (St. Louis, USA)
Fructose 1-phosphate barium salt	≥ 97	%	Sigma-Aldrich (St. Louis, USA)
Fumaric acid	≥ 99	%	Sigma-Aldrich (St. Louis, USA)
Glyoxylic acid monohydrate	≥ 98	%	Sigma-Aldrich (St. Louis, USA)
Guanosine 5´-diphosphate sodium salt	≥ 96	%	Sigma-Aldrich (St. Louis, USA)
Guanosine 5´-monophosphate disodium salt	≥ 99	%	Sigma-Aldrich (St. Louis, USA)
Guanosine 5´-triphosphate sodium	≥ 95	%	Fluka / Sigma-Aldrich (St. Louis, USA)
L-Asparagine	≥ 98	%	Sigma-Aldrich (St. Louis, USA)
L-Aspartic acid	≥ 99	%	Sigma-Aldrich (St. Louis, USA)
L-Glutamic acid	≥ 99	%	Sigma-Aldrich (St. Louis, USA)
L-Glutamine	≥ 99.5	%	Sigma-Aldrich (St. Louis, USA)
L-Malic acid	≥ 99,5	%	Fluka / Sigma-Aldrich (St. Louis, USA)
Oxaloacetic acid	≥ 98	%	Sigma-Aldrich (St. Louis, USA)
Phospho(enol)pyruvic acid potassium salt *	≥ 99	%	Sigma-Aldrich (St. Louis, USA)
Pyruvic acid sodium salt	≥ 99	%	Sigma-Aldrich (St. Louis, USA)
sn-Glycerin 3-phosphate lithium salt	≥ 95	%	Sigma-Aldrich (St. Louis, USA)
Succinic acid	≥ 99	%	Sigma-Aldrich (St. Louis, USA)
Trehalose 6-phosphate dipotassium salt	~ 95	%	Sigma-Aldrich (St. Louis, USA)
Uridine 5´-diphosphoglucose disodium salt	≥ 95	%	Carbosynth Limited (Compton, UK)
α-D(+)Mannose 1-phosphate sodium salt	≥ 99	%	Sigma-Aldrich (St. Louis, USA)
α-D-Galactose 1-phosphate dipotassium salt pentahydrate	≥ 98	%	Sigma-Aldrich (St. Louis, USA)

[1] Purity not indicated by supplier.
[2] 45-55 mg ml^{-1}, purity not indicated by supplier.

α-D-Glucose 1-phosphate dipotassium salt	≥	98	%	Sigma-Aldrich (St. Louis, USA)
α-Ketoglutaric acid potassium salt	≥	99	%	Sigma-Aldrich (St. Louis, USA)
β-Nicotinamide adenine dinucleotide (NAD^+) *	≥	97.5	%	Carl Roth GmbH + Co. KG (Karlsruhe, Germany)
β-Nicotinamide adenine dinucleotide disodium salt (NADH) *	≥	98	%	Carl Roth GmbH + Co. KG (Karlsruhe, Germany)
β-Nicotinamide adenine dinucleotide phosphate hydrate ($NADP^+$) *	≥	95	%	Sigma-Aldrich (St. Louis, USA)
β-Nicotinamide adenine dinucleotide phosphate tetrasodium salt (NADPH)	≥	96	%	AppliChem GmbH (Darmstadt, Germany)

Chemicals marked with an * were also used for enzyme activity assays.

4.3 Yeast strains

Candida tenuis
CBS 4435[a]

Saccharomyces cerevisiae

CEN.PK 113-7D[b] [59]	*MAT*a *URA*3 *HIS*3 *LEU*2 *TRP*1 *MAL*2-8[c] *SUC*2
BP000 [43][c]	CEN.PK 113-5D ura3::(GPDp-XKS1-CYC1t, GPDp-*Ct*XRWt-CYC1t, GPDp-*Gm*XDH-CYC1t)
BP10001 [43][c]	CEN.PK 113-5D ura3::(GPDp-XKS1-CYC1t, GPDp-*Ct*XRDm-CYC1t, GPDp-*Gm*XDH-CYC1t)
IBB10B05 [49][c]	evolved out of BP10001

[a] Centraalbureau voor Schimmelcultures (Baarn, The Netherlands). [b] Provided for I.B.B. by Dr. Jochen Förster (Fluxome Sciences A/S, Lyngby, Denmark). [c] I.B.B.

4.4 Growth media

4.4.1 Yeast peptone dextrose medium

Table 4-3: Yeast peptone dextrose (YPD) medium

Solution	Component	($g\ L^{-1}$)[a]
A	Glucose	20.0
B	Yeast extract	10.0
	Peptone	20.0
	Agar-Agar	16.0

[a] Concentrations refer to the final medium composition.

Solutions A and B were prepared separately in concentrated form. Solution A was adjusted to a pH value of 5.5 with 1 M HCl. After sterilization (at 121°C and 1 bar over pressure for 20 min) solutions A and B were combined to the final concentrations (see Table 4-3).

4.4.2 Mineral medium

Composition of mineral medium (MM) 1 is listed in Table 4-4. Solution A was prepared in concentrated form and autoclaved separately from other MM components. The pH value of concentrated solution C was adjusted with 1 M NaOH or 1 M HCl prior to sterilization. Concentrates of vitamin solution (C) and trace element solution (D) were sterilized by filtering (0.2 µm) and autoclaving, respectively. Tween80 and Ergosterol (E) were dissolved in pure ethanol and boiled up briefly. Antifoam (F, excluded in MM1) was autoclaved. All media components were combined prior to inoculation.

Table 4-4: Mineral medium MM1

Solution	Component		($g\ L^{-1}$)[a]
A_1[b]	Glucose		20.0
A_2	Xylose		-
B[b]	KH_2PO_4		14.4
	$(NH_4)_2SO_4$		5
	$Mg_2SO_4x7H_20$		0.5
C[c]	Vitamins	D-Biotin	0.00005
		Ca-Pantothenate	0.001
		Thiamine-HCl	0.001
		Pyridoxine-HCl	0.001
		Nicotinic acid	0.001
		p-Aminobenzoic acid	0.002
		m-Inositol	0.025
D[c]	Trace elements	$FeSO_4x7H_2O$	0.003
		$ZnSO_4x7H_20$	0.0045
		$CaCl_2x6H_2O$	0.0045
		$MnCl_2x2H_2O$	0.00084
		$CoCl_2x6H_2O$	0.0003
		$CuSO_4x5H_2O$	0.0003
		$Na_2MoO_4x2H_2O$	0.0004
		H_3BO_3	0.001
		KI	0.0001
		Na_2EDTA	0.015

[a] Concentrations relate to the final MM composition. [b] Concentrated solutions were prepared for solution A (10-fold) and B (1.2-fold).
[c] Concentrated solutions of C (1000-fold) and D (1000-fold) were provided by I.B.B.

In addition to MM1 six different MM (MM2-MM7) were used in this work (see Table 4-5). Concentrations of compounds of solutions C and D were the same as in MM1.

Table 4-5: Mineral media MM2-MM7[a]

Solution	Component	MM2 ($g\ L^{-1}$)	MM3 ($g\ L^{-1}$)	MM4 ($g\ L^{-1}$)	MM5 ($g\ L^{-1}$)	MM6 ($g\ L^{-1}$)	MM7 ($g\ L^{-1}$)
A_1[b]	Glucose	-	-	-	-	5.0	5.0
A_2[b]	Xylose	50.0	20.0	20.0/50.0	20.0/50.0	-	-
B[b]	KH_2PO_4	14.4	14.4	0.25	1.0	0.25-3.0	0.25
	KCl	-	-	1.5	1.1	1.5-0	1.5
	$(NH_4)_2SO_4$	5.0	5.0	-	-	5.0	-
	NH_4Cl	-	-	4.0	4.0	-	4.0
	$Mg_2SO_4x7H_20$	0.5	0.5	0.5	0.5	0.5	0.5
E[b]	Ergosterol	0.01	-	0.01	0.01	-	-
	Tween80	0.42	-	0.42	0.42	-	-
F[e]	Antifoam 204	0.015	-	0.015	0.015	-	-

[a] Final concentrations are shown. [b] Concentrated solutions were prepared for A_1 (10-fold), A_2 (200 g L^{-1}), B (1.2-fold (MM2, 3), 2-fold (MM4, 5) and 10 g L^{-1} component stocks (MM6,7)) and E (1000-fold). [c] Solutions A and B were autoclaved separately. [d] pH value was adjusted in solution B prior to sterilization, for respective pH values see Table 5-1, Table 5-2 and Table 5-3. [e] Values are shown in % (*v*/*v*).

5 Methods

5.1 Yeast physiology study (performed at I.B.B.)

5.1.1 Glucose fermentation

All glucose fermentations were performed at 30°C and with CEN.PK 113-7D.

5.1.1.1 Preculture (PC)

Fifty µL of a CEN.PK 113-7D glycerol stock solution were streaked out on YPD agar plates and incubated for 48 hours. A loop full of cells was then transferred to a 300 mL baffled Erlenmeyer flask (BEF) containing 30 mL glucose-MM1 and cultured at 125 rpm. Cells obtained from overnight cultures served as inocula for fermentations. In case of media optimization (see later) yeast cells were harvested by centrifugation (5000 rpm, 10 min, 4°C) and washed once with 40 mL cold (4°C) sterile 0.9 % NaCl solution to reduce carry-over of main culture components.

5.1.1.2 Fermentation

Five different experiments were performed (G1-G5). Fermentation G1 was carried out with MM1 at different glucose concentrations (5, 10 and 20 g L^{-1}). Fermentations G2-4 were performed in MM6 supplemented with different concentrations of KH_2PO_4 (0.25, 0.5, 1.0 and 3.0 g L^{-1}). Fermentation G5 was carried out with MM7 ($(NH_4)_2SO_4$ substituted by NH_4Cl). Fermentation parameters are summarized in Table 5-1. Cultures were inoculated to optical densities (OD_{600}) between 0.1 and 0.2. Fermentation G1, G2 and G5 were carried out in duplicates.

Table 5-1: Cultivation parameters for glucose fermentations under aerobic conditions

	Fermentation				
Parameter	G1	G2	G3	G4	G5
T [°C]	30	30	30	30	30
pH	6.5	6.5	6.5	6.5	6.5
Rpm	200	150-200	150	150-200	125-200
MM	MM1	MM6	MM6	MM6	MM7
Volume (mL)	50	30	30	50	50
Flask[a]	EF	EF	BEF	EF	BEF/EF
Glucose (g L^{-1})[b]	5.0/10.0/20.0	5.0	5.0	5.0	5.0

[a] EF and BEF indicate Erlenmeyer and baffled Erlenmeyer flasks, respectively. [b] Final concentrations are shown.

5.1.2 Xylose fermentation

Xylose fermentations were performed with BP000, BP10001 and IBB10B05 at 30 °C and with *C. tenuis* at 25°C.

5.1.2.1 Preculture

A two-step cultivation protocol was used. Preparation of preculture 1 (PC 1) was carried out as described in Section 5.1.1.1. Aliquots of PC 1 were used to inoculate PC 2. Initial OD_{600} values were between 0.05 and 0.1. *C. tenuis*, BP000 and BP10001 were grown overnight aerobically in 1 L BEF containing 300 mL of MM1 (BP000, BP10001) or MM3 (*C. tenuis*). PC 2 of IBB10B05 was carried out under anaerobic conditions in 100 mL sealed flasks containing 90 mL of MM2 for 48 to 72 hours (at least to an OD_{600} of 1.0). To ensure anaerobic conditions flasks were sparged with sterile nitrogen (filtered, 0.2 µm) for 15 minutes before and after inoculation.

Yeast cells from PC 2 were harvested by centrifugation (5000 rpm, 10 min, 4°C), washed once (45 mL) and resuspended (40 mL) in sterile 0.9 % NaCl solution. To ensure metabolizing ability in the subsequent fermentation *C. tenuis* was harvested at an OD_{600} of 3.5-4.0 [54]. PC conditions are summarized in Table 5-2.

Table 5-2: Cultivation parameters for xylose fermentation precultures

	Preculture 1				Preculture 2			
Parameter	*C. tenuis* *aerobic*	BP000 *aerobic*	BP10001 *aerobic*	IBB10B05 *aerobic*	*C. tenuis* *aerobic*	BP000 *aerobic*	BP10001 *aerobic*	IBB10B05 *anaerobic*
T [°C]	25	30	30	30	25	30	30	30
pH	5.5	6.5	6.5	6.5	5.5	6.5	6.5	6.5
Rpm	125	125	125	125	125	125	125	200
MM	MM1	MM1	MM1	MM1	MM3	MM1	MM1	MM2

5.1.2.2 Fermentation

Each xylose fermentation was carried out twice in a 1L-batch Labfors 2 bioreactor equipped with two six bladed Rushton disk impellers (both d = 4.6 cm) and a three baffled element. Two different MM conditions (MM4, MM5) were applied. Parameter settings for fermentations 1-4 (F1-F4) and F5-F8 are shown in Table 5-3. Temperature and rpm were controlled by a PID controller and monitored online. PID-regulated addition of 0.5 M NaOH was used to keep pH at a constant value during fermentation. Anaerobic conditions were maintained by sparging the bioreactor with 0.16 vvm nitrogen. Cultivation temperature, pH and xylose concentration were varied in dependence of the strain cultivated.

Table 5-3: Cultivation parametes for xylose fermentations under anaerobic conditions

	Fermentation							
	F1	F3	F5	F7	F2	F4	F6	F8
Parameter	*C. tenuis*	BP000	BP10001	IBB10B05	*C. tenuis*	BP000	BP10001	IBB10B05
T [°C]	25	30	30	30	25	30	30	30
pH	4.5	5.5	6.5	6.5	4.5	5.5	6.5	6.5
Rpm	200	200	200	200	200	200	200	200
MM	MM4	MM4	MM4	MM4	MM5	MM5	MM5	MM5
Xylose ($g\ L^{-1}$)	20.0	20.0	50.0	50.0	20.0	20.0	50.0	50.0

5.1.2.3 Cell harvest

Biomass was separated from cultivation medium by centrifugation (5000 rpm, 15 min, 4°C). Cell pellets from 800 mL fermentation medium were combined and washed once with 400 mL precooled (to 4°C) sterile 0.9 % NaCl solution. After centrifugation at 5000 rpm and at 4°C for 5 minutes, the resulting cell pellet was resuspended in 40 mL sterile 0.9 % NaCl solution, transferred to a 50 mL Sarstedt tube and once again centrifuged (5000 rpm, 5 min, 4°C). The final cell pellet was stored at -20°C.

5.1.3 French press

Cell pellets from xylose fermentations were resuspended in ice cold 50 mM potassium phosphate buffer pH 7.0 before disruption at 15000 psi in a French Press chamber (precooled to < 0°C). The ratio of wet cell mass to buffer volume was ~3. Cell disruption was repeated thrice and cell free extracts were obtained by centrifugation (5000 rpm, 45 min, 4°C). French Press elements were cooled on ice between disruption repeats. Aliquots (1 mL) of cell-free extracts were stored at -20°C.

5.1.4 Monitoring

5.1.4.1 Sampling

In case of metabolizing strains 1 mL aliquots of xylose fermentation broth were drawn aseptically at cultivation start, after 24 and 48 hours and at the end of fermentation. For IBB10B05 and glucose fermentations aliquots were taken at shorter time intervals to record growth. Samples were centrifuged for 10 minutes at 13000 rpm and 4°C. Supernatants were stored at -20°C.

5.1.4.2 Determination of the cell density

Cell density was determined spectrophotometrically at 600 nm (OD_{600}). A Biowave Cell Density Meter was used. Dilutions were made with 0.9 % NaCl solution. Cell dry weight (CDW) was calculated by applying known g_{CDW}/OD_{600} relations [54]–[56]. Corrections were made in dependence of the instrument used (OD_{600} (Beckmann spectrophotometer) x 1.77 =

OD_{600} (Biowave cell density meter)). One OD_{600} unit (Biowave) represents 0.23 g_{CDW} L^{-1} for strain *C. tenuis*, CEN.PK113-7D, BP000 and BP10001 and 0.29 g_{CDW} L^{-1} for IBB10B05. The logarithmic plotting of OD_{600} values versus time served for cell growth monitoring and further determination of specific growth rates (μ).

5.1.4.3 HPLC/RI analysis

Substrate consumption and product formation was monitored via HPLC/RI analysis. Components were separated by an isocratic eluent flow of 0.6 mL min^{-1} (5 mM H_2SO_4, degassed and filtered) and at a constant temperature of 65°C. The total run time was 30 min and 20 µL were injected. Samples were, if required, diluted with 5 mM H_2SO_4 prior to the analysis. A 5-component standard was used for calibration (see Table 5-4). The set of standards was measured before and after fermentation samples. A Merck-Hitachi system application software was used for quantitation.

Table 5-4: HPLC/RI calibration standard components and concentrations

	Xylose	Xylitol	Glycerol	Acetate	Ethanol
Standard			($g L^{-1}$)		
STD 1	20.01	9.94	1.00	2.00	15.00
STD 2	15.00	7.45	0.75	1.50	11.25
STD 3	10.00	4.97	0.50	1.00	7.50
STD 4	5.00	2.48	0.25	0.50	3.75
STD 5	2.50	1.24	0.13	0.25	1.87
STD 6	1.26	0.63	0.06	0.13	0.94

5.1.5 Determination of physiological parameters (μ, Y, q)

The specific growth rate μ was determined by linear regression from the linear part of a $logOD_{600}$-vs.-time plot. Product yields (Y) were calculated by the relation $([P]_{t1}-[P]_{t0})/([S]_{t0}-[S]_{t1})$. Subscripts t_0 and t_1 indicate start and end point of cultivation, respectively. Specific xylose uptake rates q_{xylose} for non-growing strains were calculated by the relation $([S]_{t1}-[S]_{t0})/g_{CDW}/(t_1-t_0)$. q_{xylose} for growing strains was calculated by the relation $\mu/Y_{biomass}$ [60].

5.1.6 Determination of specific enzyme activities

Protein concentrations were determined according to the Bradford method [61]. The Roti®-Quant dye was used. Albumin fraction V (BSA) served as reference for calibration (concentration range was 0.1-1.0 g L^{-1}). If necessary, samples were diluted with double-distilled water ($^{dd}H_2O$). Samples were measured at room temperature.

Initial rates were recorded at 25°C under saturating substrate and coenzyme conditions using a Beckmann DU800 spectrophotometer equipped with a thermocontroller. The change of NAD(P)H was measured at a wavelength of 340 nm. A molar extinction coefficient of 6.22 L $mmol^{-1}$ cm^{-1} was used [62]. Volumetric activities (µmol min^{-1} mL^{-1}) and specific activities (µmol min^{-1} $mg^{-1}_{protein}$) were determined. Samples were appropriately diluted with 50 mM potassium phosphate buffer (PPB pH 7.0). Protein concentrations and enzyme activities were measured in duplicates.

Specific activities of XR, XDH, XK, glucose 6-phosphate dehydrogenase (G6PDH), 6-phosphogluconate dehydrogenase (6PGDH) and alcohol dehydrogenase (ADH) were determined in cell free extracts. All assays, but the XK assay, were initiated by the addition of coenzyme. The XK reaction was started by simultaneous addition of NADH and enzyme sample. If not indicated otherwise 10 µL of coenzyme solution was added to a reaction mixture containing 480 µL of a buffer/substrate solution and 10 µL of sample. Reference measurements were carried out under identical conditions but lacking either sample or substrate.

5.1.6.1 Xylose reductase (XR)

XR assays were carried out in 50 mM PPB pH 7.0. Xylose (700 mM) served as substrate. Initial concentration of NADH was 0.2 mM.

Reaction

$$\text{Xylose} + \text{NADH} + H^+ \rightarrow \text{xylitol} + NAD^+ \qquad \text{(EC 1.1.1.307)}$$

5.1.6.2 Xylitol dehydrogenase (XDH)

XDH activities were determined at pH 7.0 (50 mM PPB) and pH 9.0 (50 mM TRIS/HCl) using xylitol (150 mM) as substrate and NAD^+ (3 mM) as coenzyme.

Reaction

Xylitol + NAD^+ → xylulose + NADH + H^+ (EC 1.1.1.9)

5.1.6.3 Xylulose kinase (XK)

For the XK assay 440 µL of 50 mM HEPES buffer pH 7.4 containing 50 mM KCl, 10 mM $MgCl_2$ and 1 g L^{-1} BSA were mixed with 10 µL of each phosphoenolpyruvic acid (PEP, 50 mM), ATP (250 mM) and xylulose (215 mM) to obtain a start concentration of 1 mM, 5 mM and 4.3 mM, respectively. Additionally 10 µL of a 1:5 diluted pyruvate kinase/lactate dehydrogenase mixture (PK 0.6-1.0 U μL^{-1}, LDH 0.9-1.4 U μL^{-1}) was added. The reaction was initiated by the addition of NADH (0.2 mM in the assay). Reference measurements were made without PEP under otherwise identical conditions. XK activity was obtained by calculating the difference between measured and reference rate (representing the XDH reaction).

Reaction

Xylulose + ATP → xylulose 5-phosphate + ADP (EC 2.7.1.17)

Coupled reactions

Phophoenol pyruvate + ADP → pyruvate + ATP (EC 2.7.1.40)
Pyruvate + NADH + H^+ → lactate + NAD^+ (EC 1.1.2.4)

5.1.6.4 Glucose 6-phosphate dehydrogenase (G6PDH)

G6PDH activity was carried out at pH 7.0. The buffer/substrate reaction mixture contained 50 mM PPB, 5 mM $MgCl_2$ and 20 mM glucose 6-phosphate (G6P) as reaction substrate. Initial concentrations of $NADP^+$ were 2 mM.

Reaction

Glucose 6-phosphate + $NADP^+$ → 6-phosphogluconate + NADPH + H^+ (EC 1.1.1.49)

5.1.6.5 6-Phospogluconate dehydrogenase (6PGDH)

Buffer and coenzyme conditions were the same as for G6PDH assay. The concentration of 6-phosphogluconate was 1 mM.

Reaction

6-Phosphogluconate + NAD^+ → Ribulose 5-phosphate + CO_2 + NADH + H^+

(EC 1.1.1.44)

5.1.6.6 Alcohol dehydrogenase (ADH)

ADH reaction was carried out in a 50 mM TRIS/HCl buffer pH 9.0 containing 0.25 mM EDTA and 200 mM ethanol as substrate. Starting molarity of NAD^+ was 3 mM.

Reaction

Ethanol + NAD^+ → acetaldehyde + NADH + H^+ (EC 1.1.1.1)

5.2 Metabolomics (performed at I.B.B. and HEALTH)

Cell cultivation, media optimization, production of ^{13}C-labeled yeast extract, sample work-up from sampling to extraction, determination of temperature/time profiles of the sample work-up and P_i assays were carried out at I.B.B..
LC/MS sample preparation beginning with sample concentration, construction of a multi-component calibration solution for quantitative analytics and LC/MS measurements were performed at HEALTH.

5.2.1 Media optimization

To minimize the amount of residual glucose in ^{13}C-labeled cell extract used for internal standardization experiments with different glucose concentrations were carried out in MM1 (see fermentation G1, Table 5-1). To identify minimal requirements of aerobic growth of *S. cerevisiae* with respect to P_i and sulphate S_i content cultivations were performed in MM6 and MM7 at different concentrations of P_i and sulphate while initial concentration of glucose was 5 g L^{-1} and not varied (see fermentations 2-5, Table 5-1). To maintain start concentrations of potassium and ammonium KCl and NH_4Cl were used as substitutes of KH_2PO_4 and $(NH_4)_2SO_4$, respectively. Furthermore to reduce the amount of P_i in LC/MS samples quenched cells were subjected to one or more washing steps with quenching solution (QS). P_i concentrations were measured at the beginning of fermentation and in the final LC/MS samples. A protocol in accordance to *Saheki et al. (1985)* [63] was applied. KH_2PO_4 was used for calibration.

5.2.2 Sample work-up

5.2.2.1 Quenching

One volumetric part of cell suspension was rapidly pipetted into a 50 mL Sarstedt tube containing at least eight volumetric parts of precooled (-76°C, on dry ice) methanol (QS (CM)). Immediately after cell transfer the cell/QS mixture was vortexed and again stored on dry ice. Replicates of four were quenched prior to centrifugation (5000 rpm, -9°C, 3 min). The supernatants were decanted as quantitatively as possible. The remaining cell pellets were shock frozen in liquid nitrogen and stored at -80°C until further treatment. Volumes of QS and sample (SV) were dependent on the cell density (see Table 5-5).

Table 5-5: Sample and quenching volumes

	C. tenuis BP000 BP10001			IBB10B05	
Time	SV (mL)	QS (mL)	Phase	SV (mL)	QS (mL)
24 h	0.5	10.0	I[c]	5.0	40.0
48 h	0.5	10.0	II[c]	1.0	10.0

[a] Four replicates per fermentation and sampling time. [b] SV: Sample volume, QS: Quenching solution (volume). [c] Phase I and II correspond to characteristic cell growth periods.

5.2.2.2 Extraction

A 75 % (*v*/*v*) ethanolic solution containing 15 mM ammonium acetate buffer pH 7.5 was used as ES (BE). One and a half mL of ES, placed in a 15 mL Sarstedt tubes, were incubated in a water bath (WB, > 90°C) for 5-10 min to adjust to extraction temperature. The 50 mL tubes containing the frozen (-78°C) cell pellets were transferred to the WB just before pouring the ES onto the pellet. In cases where absolute quantification was intended 50 µL of a precooled (on ice) ^{13}C-labeled ISTD were added to the cell pellet tube immediately prior to extraction. The cell/ES mixture was then vortexed shortly and incubated in the WB for 3 minutes at 90°C. Incubation was interrupted after 60 sec and 120 sec by short but thorough mixing. Cell extracts were cleared by centrifugation (5000 rpm, 3 min, 0°C). All extracts were stored at -80°C prior to further work up.

5.2.2.3 Concentration of samples

Metabolite extracts obtained were concentrated to complete dryness by N_2-gas-forced evaporation of the aqueous phase. Dried samples were dissolved in 100 µL LC/MS-grade water and transferred to 200 µL HPLC vials. Samples were then stored at -80°C prior to the analysis.

5.2.2.4 Determination of temperature/time profiles of critical steps along the sample work-up procedure

Temperature/time profiles were recorded for quenching and extraction. Different volumes of QS (4, 10, 20 and 40 mL), ES (1.5 and 10 mL) and sample (0.5, 1, 2, 5 and 10 mL) were tested. Biological samples were simulated with tempered (to 30°C) 0.9 % NaCl solution. The

change in temperature over time was monitored by an 8-channel multi input thermometer. Sensors were channelled through a bore hole in the tube cap and fixed at the tube wall in the middle of the cone. To simulate quenching and extraction the cap was lifted right before sampling and ES addition and closed immediately thereafter. How centrifugation affected the temperature of quenched samples was analysed by determination of the sample temperature before and after centrifugation. As starting point for the extraction experiments the thermosensor was placed in the frozen pellet simulated by 200 µL (for simulation of fermentation samples) or 400 µL (for simulation of the pellet of 10 mL cell suspension) 0.9 % NaCl solution.

5.2.3 Preparation of ^{13}C-labeled internal standard (^{13}C-ISTD)

The PC (MM1) and the glucose fermentation (MM7) were carried out as described in Section 5.1.1 with slight modifications. ^{13}C-labeled glucose was used as substrate (PC: 10 g L^{-1}, cultivation: 5 g L^{-1}). The cells from the PC were washed once with 40 mL sterile 0.9 % NaCl solution before inoculation of the main cultures. At an OD_{600} between 2.0 and 3.0 the cells were quenched (typically 10 mL were transferred to 40 mL of QS) and extracted (10 mL BE) as described in Sections 5.2.2. The cell extracts obtained were concentrated by a factor of 10 by evaporation to get a "ready-to-use" ISTD.

5.2.4 Quantification of intracellular metabolites

Forty two metabolites of the central carbon metabolism including glycolysis, TCA, PPP, energy metabolites, important amino acids and redox cofactors were addressed. The reference components were dissolved in LC/MS-grade water to obtain a concentration of 10 mM (A-stocks). In a second step the A-stocks were clustered in four groups according to their metabolic appearance (glycolysis, TCA, etc.) and combined to 4 B-stocks each containing 500 µM of the respective component. A further combination of the B-stocks led to a 42 metabolite mix of 100 µM of each component (C-stock). The C-stock was then used for preparing calibration standards (CS) by dilution with 10 mM ammonium acetate buffer pH 7.5. All stocks were stored at -80°C. The same amount of ISTD was added to the CSs as for the metabolomics samples prior to the LC/MS analysis. ISTD from the same charge was used for samples and standards. Concentration and dissolving steps were made as described in Section

5.2.2.3. Eleven CS dilutions were prepared and measured to determine calibration linearity and appropriate quantification limits.

5.2.5 HPLC/MS

All metabolomics samples were measured with a LC/MS system from Thermo Fisher Scientific™. A Dionex Ultimate 3000 HPLC setup equipped with an Atlantis T3 C18 pre- and analytical column (Waters, USA) was used for compound separation prior to the mass spectrometric detection with an Exactive™ Orbitrap system. Setup details are listed in Section 4.1.

A reversed-phase ion-pairing HPLC method was used for metabolite separation (adapted from *Buescher et al. (2010)* [13]). Tributylamine was used as ion-pairing agent [17]. A 40 minutes gradient was applied and 2-propanol and an aqueous phase (5 % methanol (*v*/*v*), 10 mM tributylamine, 15 mM acetic acid, pH 4.95) was used as eluent A and B, respectively (see Figure 5-1). The injection volume was 10 µL per sample and an injection loop of 20 µL was used.

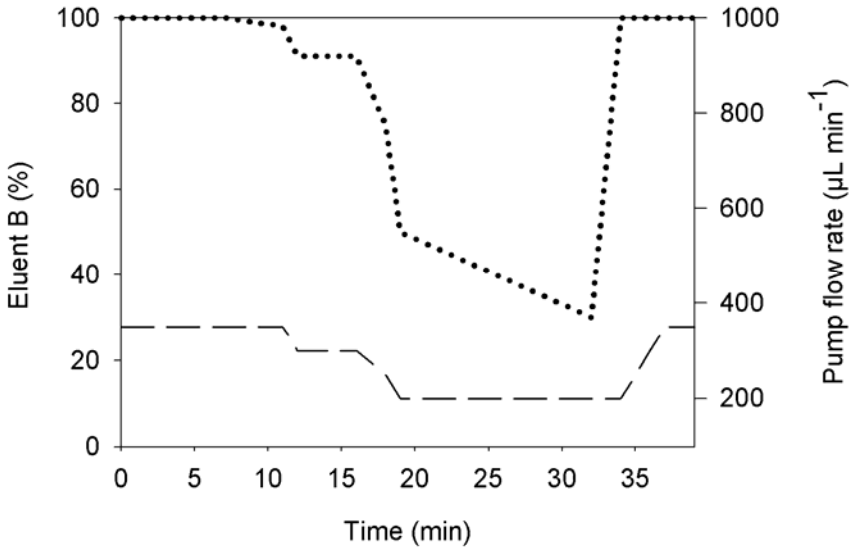

Figure 5-1: HPLC elution gradient applied. Compositions of eluent A and B are described in the main text. Dotted and dashed lines indicate the percentage of eluent B and the pumpflow (µL min^{-1}), respectively.

Equal aliquots of each biological sample measured in one analysis batch were pooled and used as a quality control (QC) sample. Biological samples were divided into 8 sample classes (SC) referring to strain (Batch 1: *C. tenuis* and BP000, Batch 2: BP10001 and IBB10B05),

fermentation (0.25 and 1.0 g L^{-1} KH_2PO_4) and sampling point (24 and 48 h). Thirty two biological samples (four replicates of every SC) were analysed, split into four run series á fourteen injections (including QC and blank samples, see Figure 5-2). Each series was thawed right before measurement and included one replicate of the eight SC. For quantification the CSs were measured twice in one analysis batch, randomized before and after the series cycles.

[a] BL: Blank, QC: Quality control, SC: Sample class 1-8 randomized;

Figure 5-2: Injection sequence of LC/MS measurement (4 x per batch).

Negative ionization of metabolites was carried out via heated electrospray ionization (HESI) prior to the mass spectrometric analysis. For the online detection of the analytes a full scan of all masses between 70 and 1100 m/z with a resolution (R) of 50000 (at *m*/z 200) was used.

5.3 Data analysis (performed at I.B.B. and HEALTH)

Data interpretation was carried out at I.B.B. for HPLC/RI measurements and at HEALTH for LC/MS measurements.

5.3.1 HPLC/RI

Automated and manual peak integration was carried out with the respective Merck-Hitachi software (see 4.1). Raw data processing was done in Microsoft Excel 2010.

5.3.2 HPLC/MS

LC/MS data acquisition was conducted with Xcalibur software (see Section 4.1) and automated peak integration with TraceFinder™ software (version 3.1, Thermo Fisher Scientific (Waltham, USA)). Screening and manual correction of peak integrations were done with the respective tools provided by the TraceFinder™ package. Raw data was further assessed with Microsoft Excel 2010.

5.3.2.1 Calibration and quantification

For the evaluation of the linearity of the calibration curves a double logarithmic presentation was used. This was done for external and internal calibrations which were then opposed in terms of lower and higher quantification limits. Further the addition of ISTD and its impact on external calibration was tested.

For quantification relative ratios of ^{12}C to ^{13}C components were used to establish calibration ranges. Linearity ranges used for the determination were dependent from the concentration range observed in the biological samples. Therefore calibration points outside the observed concentration range were eliminated. Calculated amounts of quantifiable compounds were then related to the CDW. For the correction of semi-quantitative data $^{12}C/^{13}C$ ratios were multiplied by the average ^{13}C value of the calibration standards as they represent ^{13}C compounds not degraded in the extraction step. Resulting responses were related to the CDW. In case ^{13}C signals were not detectable ^{12}C data were used.

5.3.2.2 Metabolite profiling and thermodynamic analysis

Metabolite profiles obtained were compared according to their arithmetic average of four replicates. Significances of contrasts were analysed by a t-test. Homogeneity of variances was tested by an F-test and considered in contrast analysis. Normal distribution of replicates was assumed. Statistical analysis was carried out by Excel 2010.

Free energies of a reaction (ΔG) were calculated according to the equation $\Delta G = -RT\ln K_{eq}$, where R and T are gas constant (= 8.314 kJ mol^{-1} K^{-1}) and absolute temperature (303.15 K (*S. cerevisiae*) or 298.15 K (*C. tenuis*)), respectively, while K_{eq} is the equilibrium constant. Thermodynamic contrasts to equilibrium ($\Delta\Delta G$) were determined according to the equation $\Delta\Delta G = \Delta G_{Keq} - \Delta G_{MAR}$. MAR refers to the mass action ratio of a reaction.

6 Results

6.1 Improving the sample work-up for *S. cerevisiae* metabolomics

The carry-over of cultivation media components in the LC/MS sample causes significant drawbacks in subsequent metabolite analysis. For that reason optimization of the cultivation media and the sample work-up in order to fit in with the requirements of a LC/MS system is a prerequisite. Beside that the quick and reproducible sampling, quenching and extraction under metabolite conserving conditions affect the accuracy of metabolomic analysis mostly. In particular the temperature courses over all sample treatment steps have to be considered critically. For this temperature profiles were monitored for the quenching and extraction step. Improvements of the sample work-up procedure were applied based on the monitoring findings to obtain metabolomic results as close as possible to real physiological conditions.
The work-flow for quenching and extraction of *S. cerevisiae* cells as established at the I.B.B. prior to this thesis is shown in Table 6-1 and Table 6-2, respectively.

Table 6-1: Quenching workflow of the the original protocol

Step	
1	Four volumetric parts of QS, transferred in 15 mL Sarstedt tubes, are pre-cooled in an -78°C ethanol bath embedded in dry ice.
2	One volumetric part of cell suspension is quenched rapidly into the QS by pipetting. Tubes are screwed, mixed gently and embedded in the dry ice-cooled ethanol bath again.
3	Centrifugation for 3 minutes at 5000 rpm and -9°C is conducted to separate the cell pellet from the solution.
4	The centrifugation supernatant is discarded and the cell pellet re-suspended in four volumetric parts of washing solution (= QS).
5	The centrifugation step is repeated and the supernatant discarded.
6	The screwed tubes are then immediately shock frozen in liquid nitrogen.
7	Shock frozen pellets are then stored at -80°C for further treatment.

Table 6-2: Extraction workflow of the original protocol

Step	
1	One mL of BE (> 80°C) per OD_{600} unit of quenched cells is poured rapidly onto the frozen cell pellet. (Optional: Addition of ISTD prior to the extraction)
2	The suspension is mixed gently and incubated in a > 90°C WB for 3 minutes.
3	Every 60 seconds the suspension is mixed gently.
4	The cell fragments are separated from the extract by centrifugation for 5 minutes at 5000 rpm and 0°C.
5	The extract is stored at -80°C for further treatment.

6.1.1 Reduction of residual salt components in LC/MS samples by additional washing steps in the quenching process

Residual P_i and S_i cause significant interfering effects in LC/MS analytics, as can be seen in Figure 6-1 for phosphate. In order reduce the residual salt content in LC/MS samples, additional washing steps with QS were carried out after the centrifugation step. Cells at mid-exponential growth of glucose fermentations G2-4 were used in these experiments. The QS volume and SV were 40 mL and 10 mL, respectively. Unwashed or washed (once or twice) samples were used. The cell pellets were extracted with 10 mL BE as described in Section 5.2.2.2. One and a half mL of metabolite extract were concentrated to complete dryness and dissolved in 100 µL LC/MS-grade water. The P_i concentrations in the final metabolomics samples and the expected P_i concentrations (a residual QS volume of ~400 µL was assumed after decanting) are listed in Table 6-3.

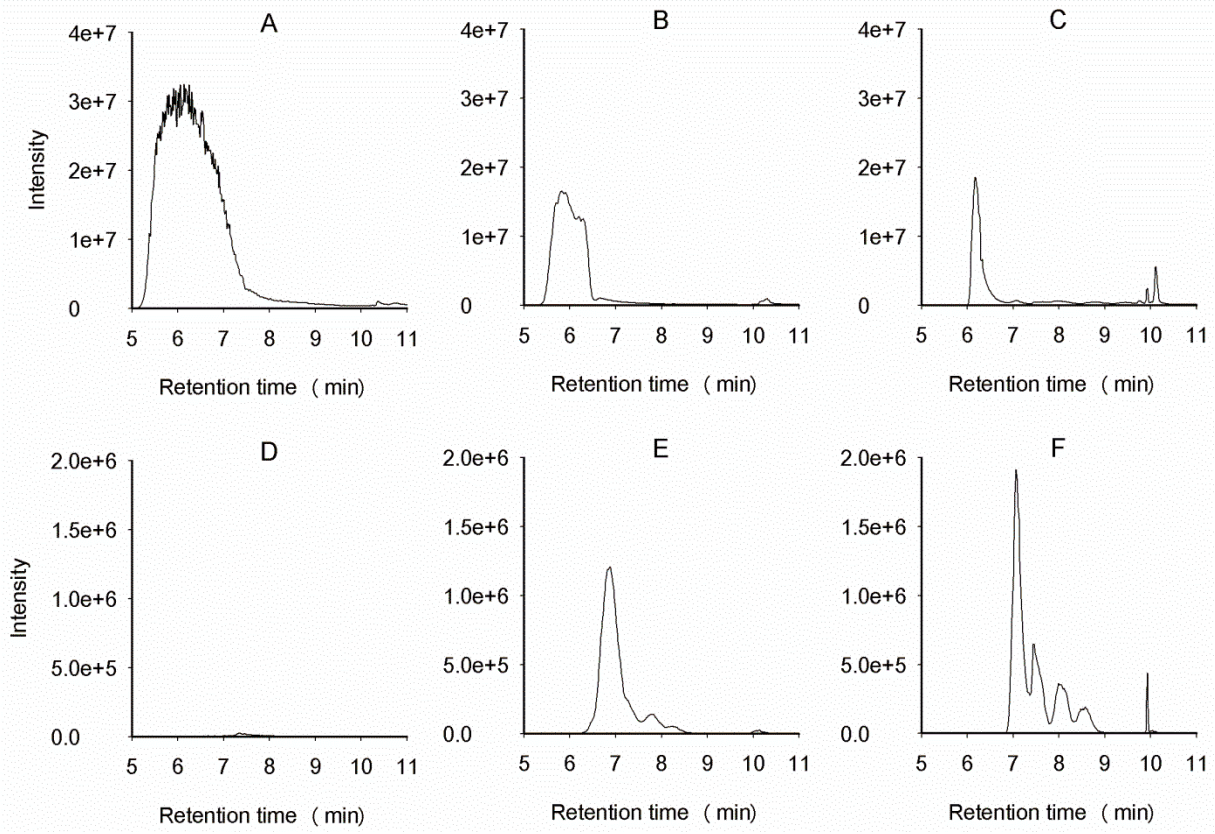

Figure 6-1: Impact of phosphate on LC/MS performance illustrated for hexose phosphates. On top Pi signals and below HXP signals are presented. LC/MS samples contained ~130 mM (A), 1.6 mM (B) and 0.5 mM Pi (C). Corresponding HXP signals (D-F) originate from CEN.PK 113-7D cells grown aerobically on 5 g L^{-1} glucose sampled at an OD_{600} of 2.1-2.6.

From Figure 6-1 it can be seen that the lowering of P_i concentration in the LC/MS samples lead to (i) improved chromatographic separation and to (ii) enhanced ion signals for HXPs. Further the analysis proofed that yeast samples cultivated in standard phosphate buffered mineral media (14.4 g L^{-1} (= 106 mM) KH_2PO_4) were incompatible with the LC/MS measurement when applying the current sample work-up protocol. Hence a threshold value of 1 mM P_i in the LC/MS samples was introduced to maintain the analysis quality.

Table 6-3: Impact of applied washing steps after quenching on the residual phosphate concentration in metabolomics samples

				Fermentation				
				G2		G3	G4	
				Washing steps				
	0 x	1 x	2 x	1 x	2 x	2 x	0 x	1 x
$[P_i]$ of MM	Expected residual $[P_i]$			Residual $[P_i]$				
				(mM)				
22.04	2.54	0.025	0.0002	1.16	1.47	1.64		
				1.40	1.54	1.24		
7.35	0.85	0.008	0.0001	0.73	0.72	0.60	1.00	0.39
				0.70	0.65	0.40	0.85	0.32
3.67	0.42	0.004	0.00004	0.43	0.43	0.20		
				0.45	0.44	0.24		
1.83	0.21	0.002	0.00002	0.26	0.26	0.18	0.39	0.23
				0.26	0.27	0.19	0.51	0.29

[a] $[P_i]$ of the first column reflects the molarity of KH_2PO_4 (mM) corresponding to 3.0, 1.0, 0.5 and 0.25 g L^{-1} in the MM.

The P_i concentrations in metabolomics samples correlated with the P_i content in the mineral medium. Introducing a washing step led to 40-60 % reduction of the P_i concentration (see fermentation G4 in Table 6-3). However, a second washing step did not further improve the metabolite extract with respect to final P_i concentration. In any case the final P_i content was by far above a value one would have expected. Evidenced by the observation that the addition of cell sample to QS caused massive precipitation these findings could be best explained by the insolubility of P_i in pure MeOH [64]. Hence to further decrease the P_i content experiments were performed in which the amount of aqueous portion (water or 10 mM (final concentration) NH_4Ac buffer pH 7.5 was used) in the QS was varied (10 and 20 % (*v*/*v*)). However, neither the increase of the aqueous portion nor the addition of buffer led to a decrease of the residual P_i content in the metabolomics samples (corresponding data are collected in Additional File 01 (see G6)). The S_i content was not determined in this study.

6.1.2 Reduction of LC/MS interfering components in mineral medium

As described in the previous section the introduction of washing steps after quenching and centrifugation did not lead to the expected salt reduction. As an alternative the reduction of salt content in the MM and the resulting effects on cell growth were tested. Therefore the

growth of CEN.PK 113-7D was studied in glucose containing mineral media differing in their P_i and S_i contents. Growth was monitored for 8 h by measuring OD_{600}. Typically OD_{600} of 2-3 could be achieved and specific growth rates were calculated. Results are listed in Table 6-4. From the results it is clear that the specific growth rate of CEN.PK 113-7D is not affected by both, P_i and S_i, in the concentration ranges studied. Consequently based on these findings following experiments were conducted with MM containing 0.25 or 1.0 g L^{-1} KH_2PO_4 and 0.5 g L^{-1} $Mg_2SO_4x7H_20$ as P_i and S_i source, respectively.

Beside that μ was also not influenced by the working volume (30 mL or 50 mL), the flask (EF or BEF) and/or the rpm value in the fermentation approaches. But it turned out that the cultivation in BEF at high rpm values (≥ 150) and low working volume of 30 mL was problematic due to sputtering and the risk of volume loss and contamination.

Table 6-4: Specific growth rates (μ) of *S. cerevisiae* growing on 5 g L^{-1} glucose

	Fermentation[a,c]					
	G2	G3	G4		G5	
Start OD_{600}	0.12-0.13	0.17-0.18	0.21	0.18	0.14-0.15	0.24-0.25
	μ (h^{-1})[d]					
KH_2PO_4 concentration[b]						
3.0 g L^{-1}	0.39	0.34	-	-	-	-
1.0 g L^{-1}	0.37	0.33	0.35	0.35	-	-
0.5 g L^{-1}	0.38	0.34	-	-	-	-
0.25 g L^{-1}	0.38	0.35	0.35	-	0.35	0.35

[a] Fermentations G2, G4 (150 rpm) and G5 were carried out in duplicates for each headed KH_2PO_4 concentration. [b] For S_i concentrations see compounds of MM6 (G2-4) and MM7 (G5) in Table 4-5. [c] Fermentation experiments were stopped at an OD_{600} value of 2.0 to 3.0 after 7 to 8 h of cultivation. [d] μ values ± 0.01 and $R^2 > 0.99$. [e] Raw data is shown in Additional File 02.

6.1.3 Temperature/time profiles of biological samples along the sample work-up procedure

There is no information available in literature concerning critical temperatures during the sample work-up process. As temperature impacts quenching and extraction strongly in terms of efficiency, metabolite stability and reproducibility, it is inevitable to improve handling to prevent critical temperature ranges. Thus temperature courses were monitored continuously over time for quenching (CM) and extraction (BE) in order to verify whether the established protocol is suitable. Volumes of QS, BE and samples were varied in dependence on expected cell densities (see Section 5.2.2).

6.1.3.1 Quenching

The quenching process (see Table 6-1) was considered in three phases: Pre-cooling of QS (I), quenching of biological sample (II) and removal of media components (III). A typical temperature-vs.-time profile is shown in Figure 6-2. Parameters used to characterize the phases were for phase I T_{IC} (initial temperature of the QS prior to cooling), t_C (cooling time (sec) of the QS on dry ice to reach a temperature < -70°C) and T_{EC} (the end temperature of QS after t_C (< -70°C)), for phase II T_{IQ} (initial QS-temperature prior to the quenching (= T_{EC})), T_{EQ} (end temperature after quenching and mixing) and T_{EQ60} (T_{EQ} + 60 sec resting on dry ice) and for phase III T_{ICF} and T_{ECF} (initial and end temperature of centrifugation). The tubes were directly embedded in dry ice for the experiments. No ethanol bath was used in order to simplify the handling. The experiments were carried out at least twice.

Phase I shows a two-phasic cooling process of QS in which QS rapidly (within 80 sec of incubation on dry ice) cooled down from room temperature (= T_{IC} (I)) to -60°C. The temperature of QS further decreased but slowly reaching -75°C (T_{EC} (I)) after ~350 sec of incubation. Phase II was initiated by the addition of cell suspension (T = 30°C). This caused an immediate rise in temperature up to -35°C (= T_{EQ} (II)). Resting the sample on dry ice for 60 seconds (represents the average time biological samples rest on dry ice before centrifugation) decreased the temperature of QS < -60°C (= T_{EQ60} (II)). Phase III imitates the increase in temperature provoked by centrifugation at -9°C, whereby T_{ICF} (III) and T_{ECF} (III) in Figure 6-2 indicate the temperature of QS prior to and after centrifugation, respectively.

Results obtained for the tested parameters (15 or 50 mL Sarstedt tubes, QS volume and SV) were summarized in Table 6-5 (phase I), Table 6-6 (phase II) and Table 6-7 (phase III).

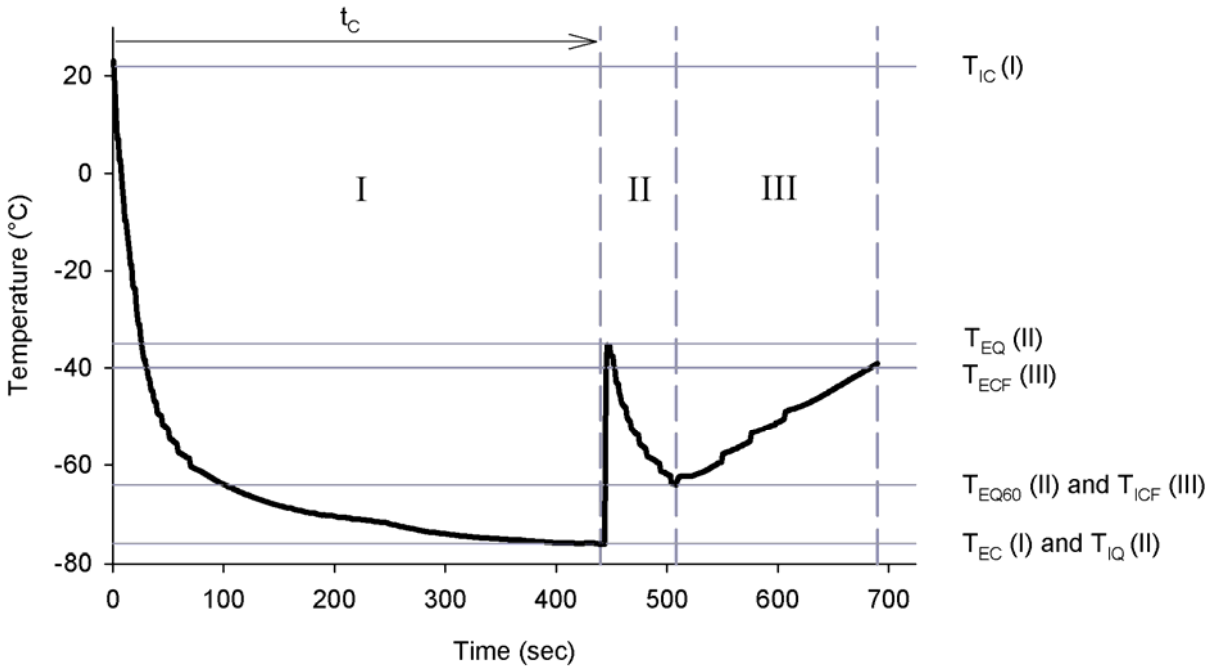

Figure 6-2: Exemplified phases of quenching process. I, II, III refer to phase I (cooling of QS), phase II (quenching and resting on dry ice), phase III (centrifugation at -9°C), respectively. T_I and T_E refer to the initial and end temperature of cooling (T_{IC}, T_{EC}), quenching (T_{IQ}, T_{EQ}, T_{EQ60}) and centrifugation (T_{ICF}, T_{ECF}) and t_c refers to the cooling time. Data presented were obtained from an experiment in which 50 mL Sarstedt tube, 10 mL QS and 2 mL SV were used.

In Table 6-5 cooling responses in dependence of QS volume (4, 10, 20 and 40 mL) and the volume of the tube used for quenching (15 mL or 50 mL Sarstedt tubes) are shown. The SV was varied between 0.5 and 10 mL resulting in SV/QS ratios of 4, 5, 8, 10 and 20. The cooling time to reach a T < -70°C was dependent on the QS. Nevertheless even 40 mL of QS could be cooled down within 11 min. In the original protocol 15 mL Sarstedt tubes were used which led to a quicker temperature decrease down to -70°C on dry ice. The required cooling time (t_C) was 2- to 4-fold shorter than for the approaches where 50 mL tubes were used. Beside the lower QS volume this could be explained by the bigger surface/volume ratio [65] of 15 mL tubes (not tested).

QS/SV ratios of 4/1, commonly used in yeast metabolomics, led to a T_{EQ} of < -25°C (see Table 6-6). The T_{EQ} could be significantly reduced to below -40°C by increasing the QS/SV ratios. The subsequent resting on dry ice for at least 60 sec (T_{EQ60}) led to temperatures below -50°C throughout all tested QS/SV ratios.

However the greater surface/volume ratio of 15 mL tubes showed negative effects concerning the temperature stability in the centrifugation step (180 sec at -9°C, see Table 6-7). Even at higher T_{ICF} the usage of 50 mL tubes showed advantages and lower T_{ECF}. While for the 15 mL tubes the temperature rose to about -13°C, T_{ECF}s obtained for 50 mL tubes were always lower. Depending on the SV/QS ratio T_{ECF}s between -20°C and below -50°C were obtained.

Table 6-5: Summary of temperature-vs.-time profiles - Phase I[a]

	15 mL tube	50 mL tube		
QS (mL)	4	10	20	40
T_{IC} (°C)	22	22	22	22
T_{EC} (°C)	-70	-70	-70	-70
t_C (sec)	150	370	400	620

[a] T_{IC}: Initial temperature of QS prior to cooling on dry ice, T_{EC}: End temperature of cooling (at least < -70°C), t_C: Cooling time of QS on dry ice to reach < -70°C. Data presented was optained from single determinations.

Table 6-6: Summary of temperature-vs.-time profiles - Phase II[a]

	15 mL tube	50 mL tube					
QS (mL)	4	10	10	10	20	40	40
SV (mL)	1	0.5	1	2	5	5	10
MeOH (%)	80	95.2	90.9	83.3	80	88.9	80
T_{IQ} (°C)	-75	-70	-70	-70	-70	-70	-70
T_{EQ} (°C)	-30	-57	-54	-40	-30	-40	-25
T_{EQ60} (°C)	-65	-65	-65	-60	-50	-55	-50

[a] T_{IQ}: Initial temperature of QS prior to quechning, T_{EQ}: End temperature after quechning and vortexing, T_{EQ60}: Temperature after a resting time of 60 sec on dry ice prior to centrifugation. Data presented was optained from single determinations.

Table 6-7: Summary of temperature-vs.-time profiles - Phase III[a]

	15 mL tube	50 mL tube					
QS (mL)	4	10	10	10	20	40	40
SV (mL)	1	0.5	1	2	5	5	10
MeOH (%)	80	95.2	90.9	83.3	80	88.9	80
T_{ICF} (°C)	-65	-65	-65	-60	-50	-55	-50
T_{ECF} (°C)	-13	-50	-45	-40	-20	-40	-

[a] T_{ICF}: Initial temperature prior to centrifugation, T_{ECF}: End temperature after 180 sec of centrifugation at -9°C. Data presented was optained from single determinations.

6.1.3.2 Extraction with boiling ethanol

The extraction process is marked by an initial rapid temperature rise, a brief homogenization step (vortexing), which leads to the extraction initial temperature (T_{IEX}) and the extraction time (t_{EX}) above a distinct temperature. Three different approaches were tested for 1.5 mL (A1-A3) and 10 mL (B1-B3) BE. The frozen cell pellet was simulated as described in Section 5.2.2.4. In approach A1 and B1 BE was poured via the cold tube wall on the pellet. In A2 and B2 BE was directly poured onto the pellet and in A3 and B3 the tube (including the pellet) was preheated in the water bath straight before BE addition (< 1 sec). All experiments were carried out in 50 mL Sarstedt tubes, at least twice.

Resultant temperature time profiles were analysed with respect to characteristic temperatures measured as T_{IEX}, T_{EEX} and the times above 60°C and 70°C (t_{EX}). The complete set of characteristic parameters is shown in Table 6-8. Representative time courses obtained for approach A1 and B2 are shown in Figure 6-3. As it turned out for 1.5 mL BE addition only approach A3 showed a T_{IEX} (~50°C) within the desired temperature range. In comparison A1 showed a surprisingly low T_{IEX} (5°C, see Figure 6-3), which led to more than 40 sec in a critical temperature range below 50°C (t_{CRIT}) and nearly 60 sec below 60°C. In case of 10 mL BE addition minor differences occurred in the approaches. Only in B1 a T_{IEX} below 50°C was observed (27°C).

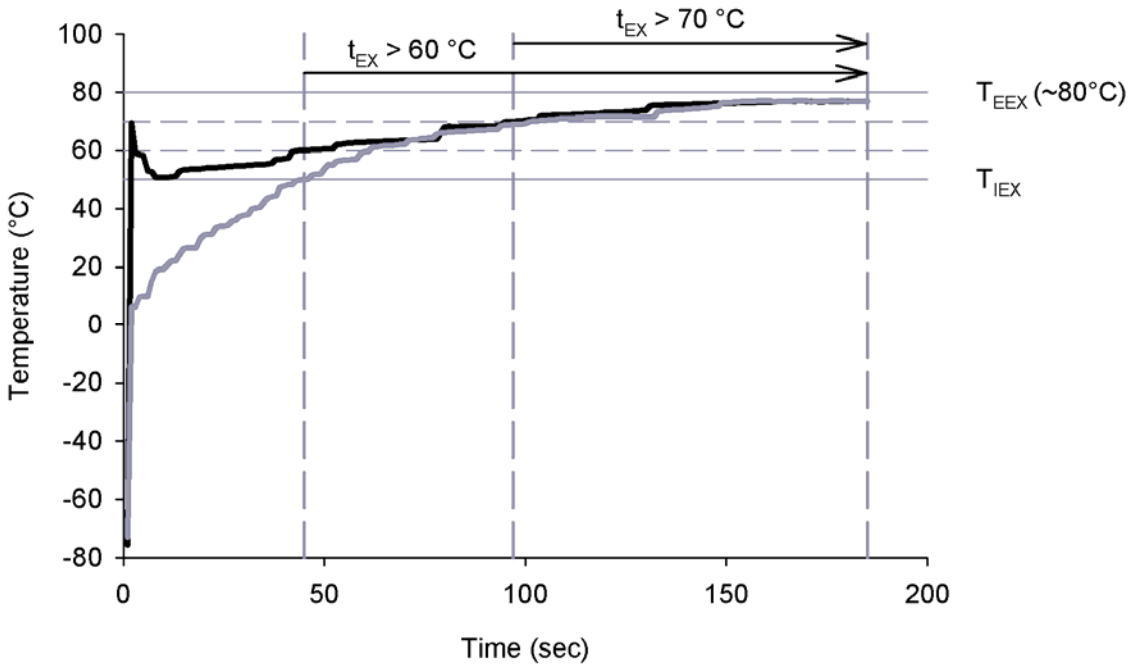

Figure 6-3: Typical temperature profile of the extraction. T_{IEX} refers to the initial temperature of extraction (after vortexing), T_{EEX} to the end temperature of extraction and t_{EX} to the extraction time above a defined temperature (60 and 70°C). Data presented were obtained from an experiment in which 50 mL Sarstedt tube and 10 mL BE were used (B2, black line). The dark grey line represents another typical extraction temperature profile where T_{IEX} is extremely low (~5°C) due to wrong handling (A1, 50 mL Sarstedt, 1.5 mL BE).

Table 6-8: Initial extraction temperature and extraction time

	Approach[a]					
	A1	A2	A3	B1	B2	B3
BE > 80°C (mL)	1.5	1.5	1.5	10	10	10
T_{IEX} (°C)	5	13	50	27	50	66
T_{EEX} (°C)	80	80	80	80	80	80
t_{CRIT} < 50°C (sec)	45	50	-	35	-	-
t_{EX} > 60°C (sec)	120	125	160	115	135	180
t_{EX} > 70°C (sec)	75	90	140	70	85	160

[a] Approaches A1-3 and B1-3 are explained in the text. Data presented was optained from single determinations. [b] T_{IEX}: Initial temperature after addition of BE and vortexing, T_{EEX}: End temperature of extraction, t_{CRIT}: Time in a critical temperature range below 50°C, t_{EX}: Extraction time where the temperature excesses a distinct temperature (> 60°C or > 70°C).

6.1.4 Preparation of ^{13}C-labeled internal standard

In order to obtain an ISTD with large pools of uniformly ^{13}C-labeled metabolites in a short time span of a work day (~8 h) exponential growth of the cultivated cells is aimed. As ^{13}C-labeled glucose is an expensive substrate, residual glucose concentration at the time point of cell harvesting should be minimal. Therefore initial glucose concentrations of 5, 10 and 20 g L^{-1} were tested (see Figure 6-4). Results are summarized in Table 6-9. Biomass formation and μ were not dependent on initial concentration of glucose within the first 8 h of cultivation. After 26 h of fermentation CDW levels reached ~8.4, ~4.2 and ~2.1 g L^{-1} in case of 20, 10 and 5 g L^{-1} glucose, respectively, implying formed ethanol was utilized too. Glucose concentrations were not determined. Based on the results obtained a glucose concentration of 5 g L^{-1} was chosen as appropriate for the subsequent production of ISTD.

Table 6-9: Influence of glucose concentration on cell growth

	Fermentation[a]					
	G1a			G1b		
Glucose (g L^{-1})	5.0	10.0	20.0	5.0	10.0	20.0
Start OD_{600}	0.07	0.07	0.07	0.06	0.06	0.06
End OD_{600}	9.4	n.d.[b]	36	8.8	18.4	36.8
Fermentation duration (h)	26	7	26	28	28	28
μ (h^{-1})[c]	0.38	0.39	0.39	0.40	0.40	0.39

[a] Raw data are shown in Additional File 02. [b] n.d.: Not determined, Batch was stopped after 7 h of fermentation. [c] μ was determined for fermentation G1a between 0 and 9.5 h (between 0 and 7 h for 10 g L^{-1}), for G1b between 3 h and 11.5 h. Standard error of μ was ± 0.01 h^{-1} and $R^2 > 0.99$.

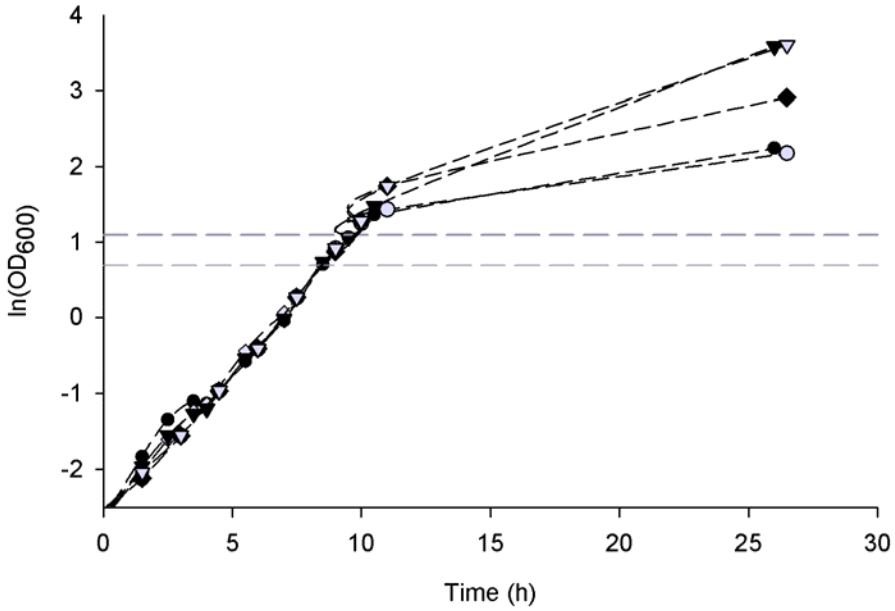

Figure 6-4: Influence of glucose concentration on cell growth. Initial concentrations of glucose were 5 g L^{-1} (black and grey circles), 10 g L^{-1}, (black and grey diamonds) and 20 g L^{-1} (black and grey triangles). Cells were harvested at OD_{600} values between 2.0 and 3.0 (indicated by grey dashed lines).

6.1.5 Improvements implemented into the work-flow

Based on results obtained in the Sections 6.1.1 to 6.1.4 following modifications were introduced:

- LC/MS interfering components $H_2PO_4^-$ and HSO_4^- could be reduced in the MM by 58-fold and 20-fold, respectively, without altering fermentation capability of CEN.PK-7D on glucose. $(NH_4)_2SO_4$ was completely substituted by NH_4Cl leaving MgSO4 as the sole sulphur source.
- The quenching setup was simplified by replacing the ethanol bath with fine grained dry ice. The problem of hydrostatic uplift of tubes could be prohibited. Tubes could be placed deeper in the dry ice which led to a quick and sufficient cooling response (below -70°C) of the QS. Using dry ice instead of an ethanol bath precluded contamination risk due to ethanol sputtering.
- Independent of the SV to be quenched 50 mL tubes are to be preferred over commonly used 15 mL tubes. Due to larger liquid surface/volume ratio sample transfer was relieved but more important the temperature of the sample/QS mixture could be stably

maintained below -20°C during resting on dry ice and separation of cells by centrifugation (see Table 6-7).

- In order to decrease residual salt components of the cultivation an additional washing step was used in the original quenching protocol (see point 4, Table 6-1). Whether the washing step was skipped or not, the P_i concentrations did not excess the acceptable level of 1 mM in the appropriate LC/MS samples for cultivation relevant KH_2PO_4 concentrations of 0.25 and 1.0 g L^{-1} (see Table 6-3). Therefore additional washing steps with toxic QS were omitted.
- According to the obtained temperature profiles the handling in the extraction step was modified. As both T_{IEX} after BE addition (avoiding t_{CRIT}) and t_{EX} could be increased significantly by preheating the cooled tube (< 1 sec in the water bath) prior to the BE addition (see Table 6-8), approaches A3 and B3 were chosen for the extraction procedure.
- Furthermore centrifugation time after extraction could be decreased from 5 min to 3 min without affecting separation efficiency.

All metabolomics samples were processed by applying the new sample work-up protocol (see Section 5.2.1 and 5.2.2).

6.2 Metabolomics

To fathom out sources for differences in the phenotypes of a natural xylose metabolizing strain (*C. tenuis*) and a recombinant xylose assimilating yeast strain (BP000) a metabolite analysis was carried out with focus on the quantification of metabolites of the central carbon metabolism (comparison 1). In a second study metabolite profiles of a xylose metabolizing (BP10001) and a (IBB10B05) *S. cerevisiae* strain that can grow on xylose were compared based on a more global approach (comparison 2).

6.2.1 Metabolization of xylose by *C. tenuis*, BP000, BP10001 and IBB10B05

Xylose fermentations were performed under anaerobic conditions for *C. tenuis*, BP000, BP10001 and IBB10B05. Corresponding fermentation parameters are summarized in Table 6-10 and Table 6-11. Ethanol and CO_2 yields were not determined as fermentations were carried out without off-gas analysis. Xylose consumption rates and product yields obtained for BP000, BP10001 and *C. tenuis* were in reasonable agreement with those reported elsewhere [14], [43], [50].

Table 6-10: Physiological parameters obtained from xylose fermentations of *C. tenuis*, BP000 and BP10001

Strain and fermentation[a]		OD_{600}	Parameter[b] q_{xylose} ($g\ g^{-1}_{CDW}\ h^{-1}$)	$Y_{xylitol}$ ($g\ g^{-1}$)	$Y_{glycerol}$ ($g\ g^{-1}$)	$Y_{acetate}$ ($g\ g^{-1}$)
C. tenuis						
	1	4.2	0.11	0.11	0.05	n.d.[b]
	2	3.9	0.08	0.10	0.05	n.d.[b]
BP000						
	3	6.1	0.08	0.43	0.08	0.03
	4	5.6	0.07	0.44	0.05	0.04
BP10001						
	5	3.4	n.d.[b]	0.28	0.06	0.05
	6	3.9	n.d.[b]	0.30	0.04	0.04

[a] Numbering of fermentations in accordance with Table 5-3. [b] Parameters were calculated from two time points (q_{xylose}, t_1 = 24 h and t_2 = 48 h; $Y_{product}$, t_1 = 0 h and t_2 = 48 h). [b] n.d, not determined.

Table 6-11: Physiological parameters obtained from xylose fermentations of IBB10B05

Fermentation[a]		Parameters					
		q_{xylose} ($g\ g^{-1}_{CDW}\ h^{-1}$)	μ (h^{-1})	$Y_{biomass}$ ($g\ g^{-1}$)	$Y_{xylitol}$ ($g\ g^{-1}$)	$Y_{glycerol}$ ($g\ g^{-1}$)	$Y_{acetate}$ ($g\ g^{-1}$)
	Phase						
7	I	0.62 ± 0.02	0.015 ± 0.001	0.020 ± 0.003	0.07 ± 0.01	0.22 ± 0.05	0.05 ± 0.02
	II	0.70 ± 0.05	0.0260 ± 0.0003	0.04 ± 0.01	0.14 ± 0.02	0.04 ± 0.01	0.020 ± 0.004
8	I	0.58 ± 0.04	0.019 ± 0.001	0.03 ± 0.01	0.05 ± 0.003	0.14 ± 0.02	0.06 ± 0.01
	II	0.52 ± 0.02	0.027 ± 0.001	0.06 ± 0.01	0.09 ± 0.01	0.020 ± 0.002	0.0142 ± 0.0002

[a] Numbering of fermentations in accordance with Table 5-3.

Time courses of substrate utilization and product formation for IBB10B05 are displayed in Figure 6-5A. As indicated in Figure 6-5B IBB10B05 showed a two phasic growth on xylose which can be further distinguished by the extent of side-product formation of glycerol and xylitol. This phase-specific phenotype is in good agreement with findings reported recently for IBB10B05 [49]. Growth phase I was characterized by predominant glycerol production while xylitol was formed instead in growth phase II. In contrast to cultivation in sealed flasks where μ was constant over time [49] the specific growth rate of IBB10B05 in a bioreactor was dependent on the growth phase such that μ at phase II was 1.4- to 1.7-fold higher than that at phase I. The specific growth rate per se was lower by a factor of > 2 when IBB10B05 was cultivated in a bioreactor. Specific xylose consumption rates in turn were not prone to fermentation phase and cultivation conditions.

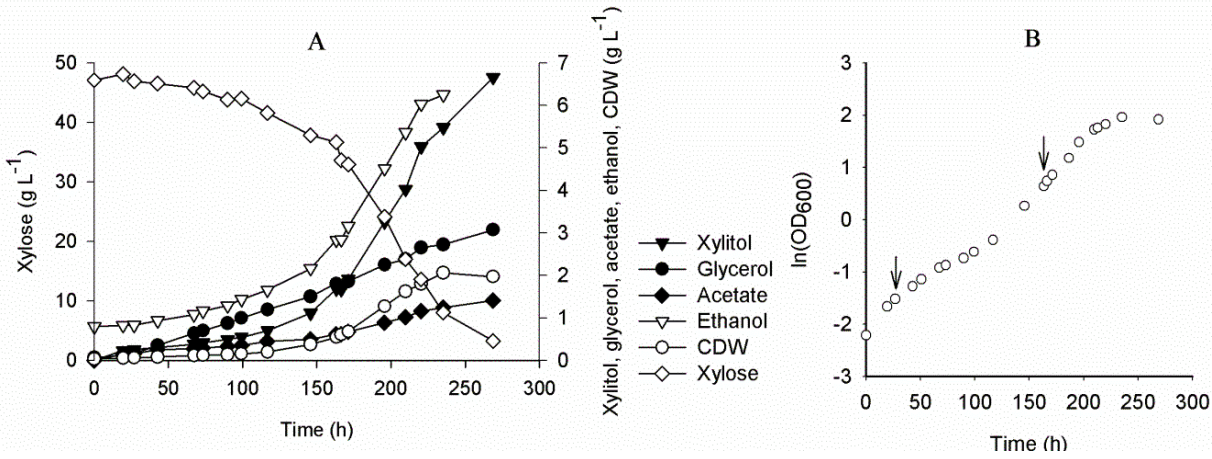

Figure 6-5: Xylose fermentation by IBB10B05 in a stirred bioreactor under anaerobic conditions. Panel A shows representative time courses of xylose utilization and product formation. Panel B shows the two-phasic growth of IBB10B05 and metabolomics sampling points are indicated by arrows.

6.2.1.1 Specific enzyme activities

Specific enzyme activities of the xylose assimilation and pentose phosphate pathway were determined from cell free extracts. Cells of *C. tenuis* (F2), BP000 (F4) and BP10001 (F6) applied to cell disruption were harvested after 51 h of fermentation. IBB10B05 (F8) cells were harvested in growth phase II after 210 h of fermentation. Results obtained are summarized in Table 6-12. Specific enzyme activities of XR, XDH and XK were in good agreement with findings described in literature [43], [49], [58]. The extraordinary low ADH activity of *C. tenuis* points to a degeneration of activity in cell free extract.

Table 6-12: Specific enzyme activities of xylose fermenting strains

	Specific enzyme activities (μmol min^{-1} mg^{-1})[a]						
Strain	XR	XDH (pH 7.0)	XDH (pH 9.0)	XK	G6PDH	6PGDH	ADH
C. tenuis	0.66 ± 0.04	0.39 ± 0.04	0.4 ± 0.1	1.2 ± 0.1	0.4 ± 0.1	0.7 ± 0.2	0.04 ± 0.01
BP000	0.07 ± 0.03	0.3 ± 0.1	0.6 ± 0.2	1.1 ± 0.2	0.3 ± 0.1	0.4 ± 0.1	1.9 ± 0.2
BP10001	0.08 ± 0.01	0.3 ± 0.1	0.6 ± 0.1	1.1 ± 0.1	0.29 ± 0.02	0.29 ± 0.02	2.0 ± 0.1
IBB10B05	1.2 ± 0.1	0.6 ± 0.1	0.9 ± 0.1	1.9 ± 0.5	0.4 ± 0.1	0.17 ± 0.02	3.4 ± 0.2

[a] Experiments were carried out in duplicates, standard deviations are shown (error propagation was considered) .

6.2.2 External and internal calibration for quantitative metabolomics

Calibration of intracellular metabolites was performed by applying two approaches. Calibration A included only ^{12}C standard components, whereas for calibration B standard component mixtures were spiked with ^{13}C-ISTD to compensate for matrix effects in the biological samples. To this end 11 standards covering a concentration range of about 2 nM to 100 µM were prepared that contained 42 different compounds. In analogy to *Buescher et al. 2010* [13] double logarithmic presentation was used to equal the influence of all dilution points on calibration linearity. Components had to show a linear correlation of at least four neighbouring concentrations with a R^2 greater than 0.99. The lowest standard concentration within the linear range had to show a larger response area than the response area of blank injections (lower limit of calibration). Results are summarized in Table 6-13.

No significant differences in calibration quality were observed at logarithmic presentation. 6-Phosphogluconic acid (6PG) showed minor improvement in linearity through internal calibration, especially at higher concentrations. Further compounds which were influenced positively through internal calibration were X,3-bisphosphoglyceric acid (BPG, X stands for the isomeric forms 1,3BPG and 2,3BPG which cannot be separated by LC), ATP, fructose X,6-bisphosphate (FBP, X stands for the isomeric forms F1,6BP and F2,6BP which cannot be separated by LC) and trehalose 6-phosphate (T6P). Compounds which showed minor negative effects on linearity at the lower concentration range when calibrated internally were AMP, ASN, ASP, dihydroxyacetone phosphate (DHAP), GLN, GLU, α-ketoglutaric acid (αKG), phosphoenolpyruvic acid (PEP), ribose 5-phosphate (R5P) and ribulose 5-phosphate (Ru5P). Glyoxylic acid (GlyoxA) and glyceraldehyde 3-phosphate (GAP) could only be calibrated externally as there were no appropriate ^{13}C signals. Oxaloacetic acid (OxalA) was detectable in the absence of ISTD. The ISTD interfered with the ^{12}C signal of OxalA so that no peak was analysable. Six components showed a maximum calibration range over all eleven concentrations at calibration A (AMP, glucose 6-phosphate (G6P, not separable in approach B), glycerol 3-phosphate (G3P), mannose 6-phosphate (M6P, not separable in approach B), PEP, Ru5P). Only G3P showed the same calibration range at the internal approach B. As not all applied hexose phosphates (HXP where X stands for a monophosphate residue at the C1 or the C6 of the hexose backbone) were separable by the LC (F6P/M1P/Gal1P and G6P/M6P in calibration A and B, respectively) they were analysed as one signal and the area was referred to the G6P area (calibration A) and the G6P/M6P area (calibration B) for the determination of

the linear concentration range. Significant carry-over effects observed for carboxylic acids (e.g. for citric acid (CitrA), fumaric acid (FumA), malic acid (MalA), succinic acid (SuccA)) limited the linearity ranges to high concentrations (see Figure 6-6 B for MalA). SuccA did not fit the acceptance criteria ($R^2 > 0.99$ of at least four neighbouring standards).

Highest concentrations at the external calibration often failed the linearity criteria of $R^2 > 0.99$ (14 metabolites at calibration A). This is shown in a decrease of the slope of the calibration curve indicating an overloading of the MS leading to ion suppression (see Figure 6-6 A and B). In particular this effect is apparent in a non-logarithmic presentation of external calibration (see A) and could be widely compensated by internal calibration (see C and D in Figure 6-6). This effect was observed for all applied metabolites although they passed the linearity criteria in many cases (see comparison of external calibration A and B in Table 6-13). Metabolites in biological samples were quantified by using internal calibration in analogy to calibration approach C of Figure 6-6.

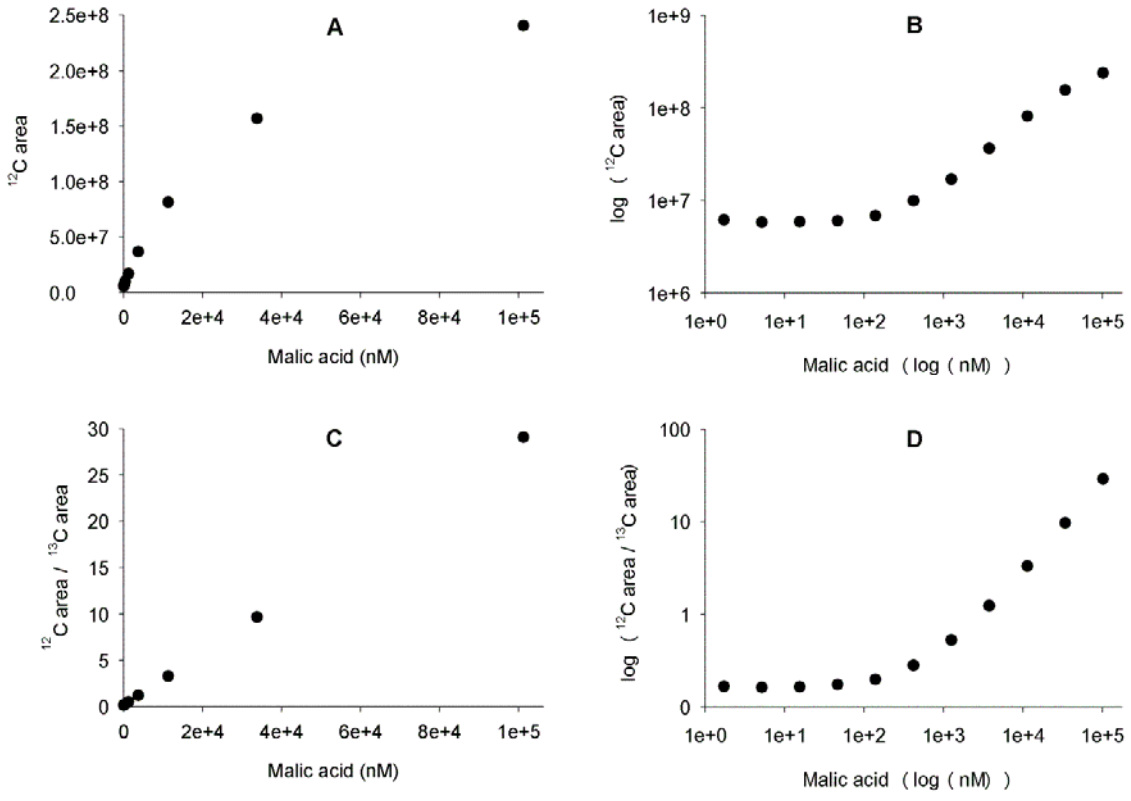

Figure 6-6: External and internal calibration curves of malic acid. In A the ^{12}C area vs. the concentration is illustrated, B reveals to the double logarithmic presentation of A. C shows the ratio of the ^{12}C area/^{13}C area vs. the concentration and D shows the double logarithmic presentation of C.

Table 6-13: Linear ranges of calibration compounds and influence of isotope-labeled internal standard on linearity

	Calibration A				Calibration B							
		Area ^{12}C				^{12}C			Area	$^{12}C/^{13}C$		
Metab.[e]	Linear range (log_3)	Higher limit (µM)	-	Lower limit (µM)	Linear range (log_3)	Higher limit (µM)	-	Lower limit (µM)	Linear range (log_3)	Higher limit (µM)	-	Lower limit (µM)
BPG	5	33.46	-	0.14	5	33.46	-	0.14	6	100.39	-	0.14
XPG	6	33.75	-	0.05	7	101.24	-	0.05	7	101.24	-	0.05
6PG	4	8.8	-	0.1	6	26.41	-	0.04	8	79.23	-	0.01
AcCoA	6	11.111	-	0.015	7	100.00	-	0.05	7	100.00	-	0.05
ADP	7	35.02	-	0.02	7	105.05	-	0.05	6	105.05	-	0.14
AMP	10	107.328	-	0.002	9	107.328	-	0.005	9	107.328	-	0.005
ASN	8	110.20	-	0.02	6	110.20	-	0.15	5	110.20	-	0.45
ASP	8	105.86	-	0.02	6	105.86	-	0.15	6	105.86	-	0.15
ATP	4	105.6	-	1.3	7	105.65	-	0.05	8	105.65	-	0.02
CitrA/ IcitrA	4	205.4	-	2.5	4	205.4	-	2.5	3	205.4	-	7.6
DHAP	9	100.218	-	0.005	6	100.22	-	0.14	6	100.22	-	0.14
FBP	6	11.43	-	0.02	7	102.85	-	0.05	7	102.85	-	0.05
F1P	9	113.25	-	0.01	9	113.25	-	0.01	9	113.25	-	0.01
F6P		n.s.[a]			8	98.82	-	0.02	8	98.82	-	0.02
FumA	5	100.4	-	0.4	5	33.5	-	0.1	5	100.4	-	0.4
GDP	7	12.03	-	0.01	7	108.30	-	0.05	6	108.30	-	0.15
G1P	7	35.55	-	0.02	9	106.652	-	0.005	8	106.65	-	0.02
G6P	10	101.640	-	0.002		n.s.[a]				n.s.[a]		
GLU	8	102.14	-	0.02	6	102.14	-	0.14	6	102.14	-	0.14
GLN	8	103.06	-	0.02	6	103.06	-	0.14	6	103.06	-	0.14
GAP	7	117.61	-	0.05	7	117.61	-	0.05		n.d.[a,b]		
G3P	10	106.555	-	0.002	10	106.555	-	0.002	10	106.555	-	0.002
GlyoxA	6	108.99	-	0.15	7	108.99	-	0.05		n.d.[a,b]		
GMP	9	104.878	-	0.005	8	104.88	-	0.02	8	104.88	-	0.02
GTP	4	105.3	-	1.3	7	105.29	-	0.05	7	105.29	-	0.05
MalA	5	101.2	-	0.4	6	101.21	-	0.14	5	101.2	-	0.4
M6P	10	105.299	-	0.002		n.s.[a]				n.s.[a]		
NAD^+	7	35.06	-	0.02	9	105.179	-	0.005	9	105.179	-	0.005
NADH	6	11.92	-	0.02	9	107.259	-	0.005	6	3.973	-	0.005
$NADP^+$	8	11.891	-	0.002	9	107.020	-	0.005	9	107.020	-	0.005
NADPH	7	31.131	-	0.014	8	93.393	-	0.014	6	31.13	-	0.04
OxalA	7	98.022	-	0.045		n.d.[a,c]				n.d.[a,c]		
αKG	9	77.717	-	0.004	8	77.72	-	0.01	8	77.72	-	0.01
PEP	10	83.972	-	0.001	7	83.97	-	0.04	8	83.97	-	0.01
PYR	6	105.53	-	0.15	6	105.53	-	0.15	6	105.53	-	0.15
R5P	9	108.00	-	0.01	7	108.0	-	0.1	7	108.0	-	0.1
Ru5P	10	100.000	-	0.003	9	100.000	-	0.003	8	100.00	-	0.02
SuccA		n.d.[a,d]				n.d.[a,d]				n.d.[a,d]		
Treha	8	107.76	-	0.02	5	107.8	-	0.4	4	35.92	-	0.44
T6P	6	11.11	-	0.02	7	33.33	-	0.02	8	100.00	-	0.02
UDPGlc	8	36.39	-	0.01	9	109.17	-	0.01	9	109.17	-	0.01
F6P/M1P/ Gal1P	9	101.339	-	0.005		n.d.[a]				n.d.[a]		
G6P/M6P		n.d.[a]			8	206.94	-	0.03	8	206.94	-	0.03

[a] n.s.: Not separable, n.a.: Not available in calibration stock, n.d.: Not determined. [b] Not determinable due to weak or missing ^{13}C signal. [c] Not detectable due to matrix effects. [d] Linearity criteria of $R^2 > 0.99$ not fulfilled. [e] Metabolites abbreviated, see List of Abbreviations.

6.2.3 Quantification of metabolites of the CCM in metabolite extracts obtained from yeasts fermenting xylose

Metabolite extracts generated from samples withdrawn either at the pseudo-steady state (24 h and 48 h) of xylose metabolization (*C. tenuis*, BP000 and BP10001) or at by-product-specific mid-exponential growth (phase I: dominated by glycerol; phase II: dominated by xylitol) of IBB10B05 on xylose were subjected to quantitative metabolite analysis. $^{12}C/^{13}C$ ratios were calculated from the automatically integrated peak areas (manually controlled and corrected in case of miss-integration) obtained from LC/MS measurements for biological samples and standards. Of the 42 selected metabolites (the same collection of metabolites as described in Table 4-2 (calibration B) was analysed) 32 could be individually quantified, 30 by internal standardization. GAP and NADH were calibrated externally due to low signal-to-noise (S/N) of the ^{13}C signals. Resultant molar concentrations of metabolites were based on the respective cell dry weight. Values obtained are summarized in Table 6-14, Table 6-15, Table 6-16 and Table 6-17 for *C. tenuis*, BP000, BP10001 and IBB10B05, respectively.

Among the 10 metabolites that could not be individually quantified HXPs (G6P, F6P, M6P, G1P, F1P) as well as CitrA and IcitrA could not be baseline-separated by LC (see Figure 6-7 B and C). Hence HXPs were collectively addressed in the analysis and referred to the G6P-peak of the standard mixture for quantification (see Figure 6-7 A). Similarly CitrA and IcitrA were quantified together against the integrated area of both compounds due to chromatographic inseparability and termed as citric acid.

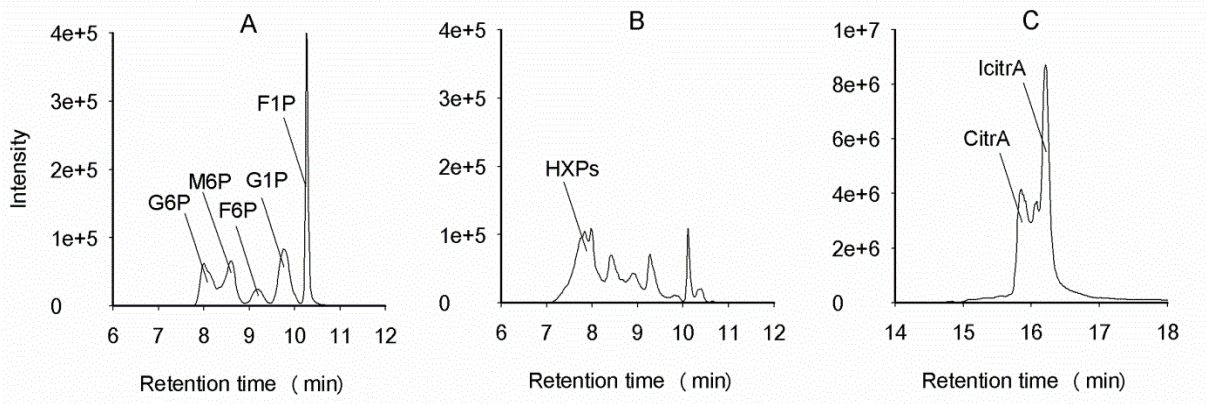

Figure 6-7: Typical chromatographic separation of hexose phosphates and citric acid species. A represents a HXP chromatogram of the standard mixture and B represents a typical elution profile of a biological sample where HXPs are not chromatographically separable. Both samples include ISTD. C shows the chromatographic inseperability of CitrA and IcitrA of a biological sample.

Neither ^{12}C signals nor ^{13}C signals could be detected for T6P, GlyoxA and OxalA in the biological samples. No ^{13}C signals could be found for GAP. Therefore GAP was calibrated externally for the quantification in IBB10B05 and *C. tenuis*. GAP could not be quantified for samples of BP000 and BP10001 due to high variation in ^{12}C signals. NADH was calibrated externally for BP10001 and IBB10B05 due to high variation in ^{13}C signals. Quantification results for NADH when calibrated externally were roughly corrected with a factor of 2.4 to compensate for degradation effects in the sample work-up. The factor was determined by dividing the mean ^{13}C areas of the CSs by the mean ^{13}C areas of the biological samples (values over a threshold area of 2000 were used for calculation). For the quantification of NADH in *C. tenuis* and BP000 internal calibrations were used as they showed acceptable ^{13}C signals. Carboxilic acids, especially CitrA, FumA, MalA and SuccA, caused significant carry-over effects, but were not influencing the quantification as the signals represented a constant background below the concentration range used for quantification.

In contrast to the calibration experiments (see Section 6.2.2) only six standards with a concentration from 400 nM to 100 µM were measured for the quantification of intracellular metabolites. The lowest standard concentration applied correlated to 0.06 - 0.10 µmol g^{-1}_{CDW} depending on the observed yeast strain. Quantification results below that point were accepted if the linearity of the calibration in this concentration range was proven by the calibration experiments (see Table 6-13). This rule was applied to 6PG, PEP, αKG, GMP, $NADP^+$, NADPH and acetyl-CoA (AcCoA). In case of BPG which did not fulfil the criteria the quantification was accepted as the peaks showed good signals and the semi-quantitative analysis confirmed the results (see Additional File 04).

Metabolite levels in µmol g^{-1}_{CDW} for *C. tenuis*, BP000, BP10001 and IBB10B05 are displayed in Figure 6-8. Corresponding values and standard deviations are shown in Table 6-14 to Table 6-17. Abbreviations are clarified in the List of Abbreviations.

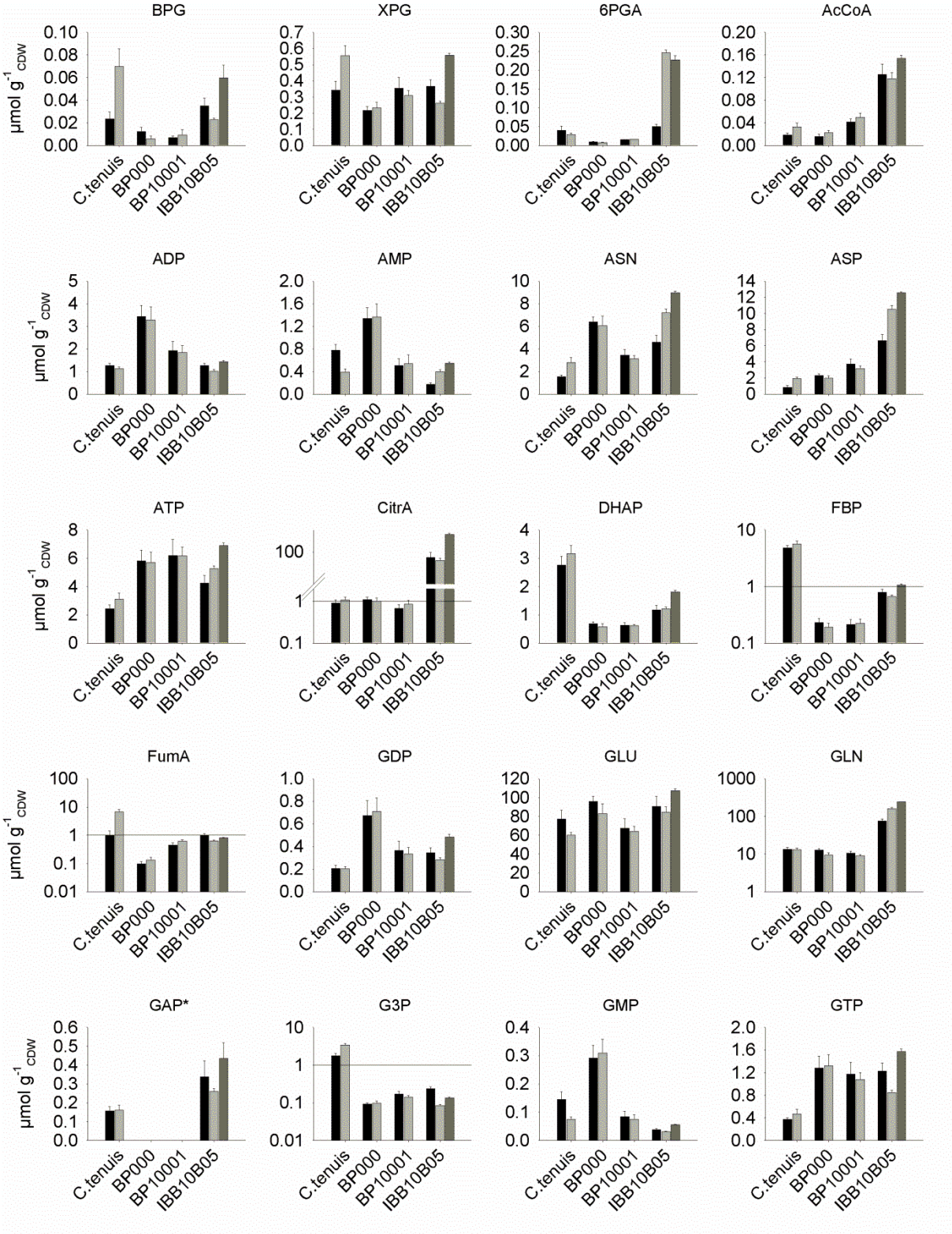
BPG
XPG
6PGA
AcCoA
ADP
AMP
ASN
ASP
ATP
CitrA
DHAP
FBP
FumA
GDP
GLU
GLN
GAP*
G3P
GMP
GTP
µmol g-1 CDW
C.tenuis
BP000
BP10001
IBB10B05

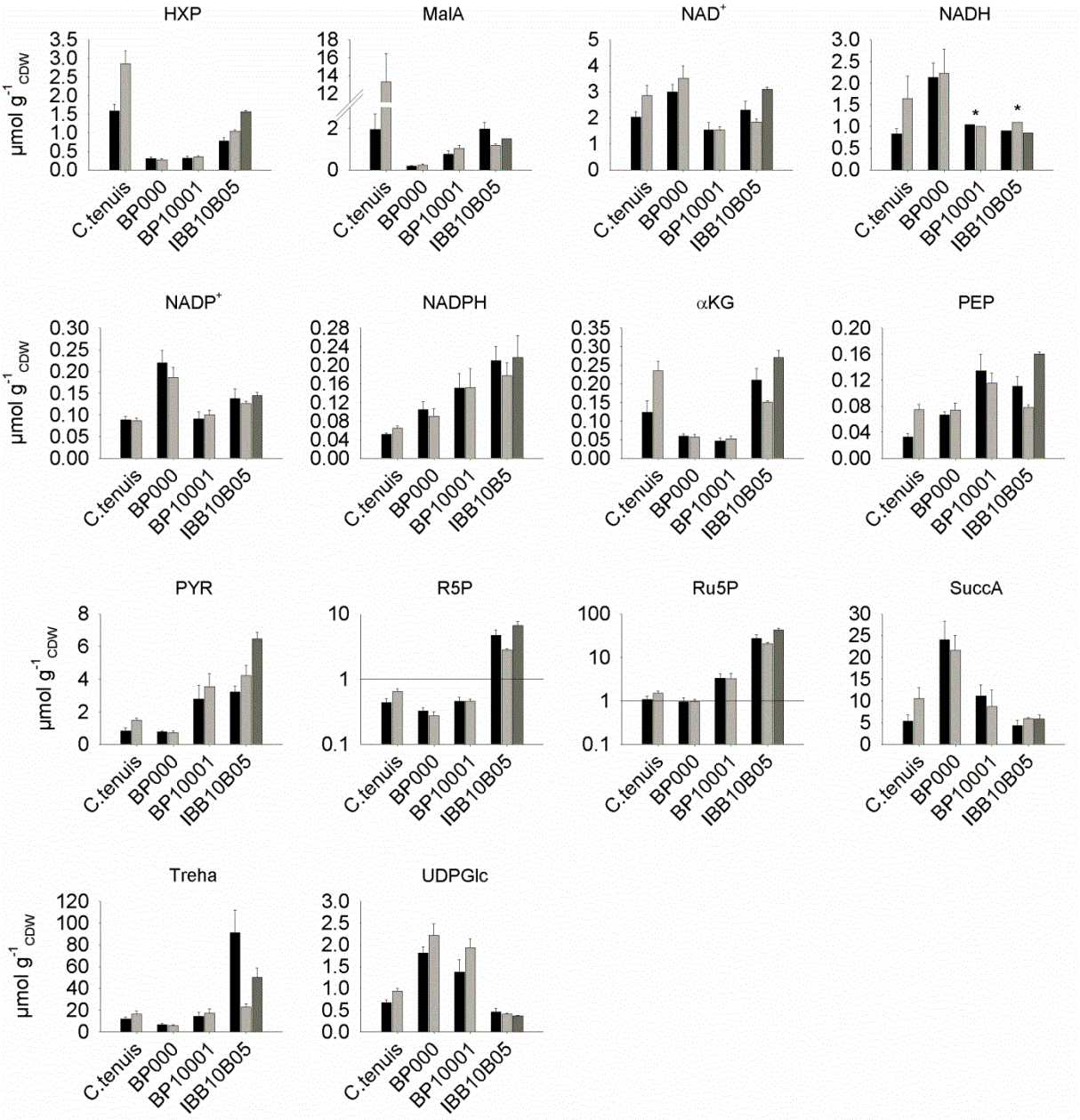

Figure 6-8: Intracellular metabolite levels of *C. tenuis*, BP000, BP10001 and IBB10B05. Average specific metabolite concentrations of two fermentations for each strain are shown. Bars for 24 h and phase I (IBB10B05) samples are displayed in black, 48 h and phase II samples of F7 in light grey and phase II samples of F8 in dark grey. Metabolite levels determined based on external calibration are tagged with an asterix (*). Note logarithmic scale for the y-axis was used to display CitrA, FBP, FumA, G3P, Ru5P and R5P.

Table 6-14: Metabolite pools of *C. tenuis* fermentations on xylose[a]

	C. tenuis			
	Fermentation 1		Fermentation 2	
Metabolite	24 h	48 h	24 h	48 h
Central carbon metabolism				
HXP	1.72 ± 0.03	3.2 ± 0.2	1.4 ± 0.2	2.6 ± 0.1
FBP	5.0 ± 0.1	6.2 ± 0.3	4.8 ± 0.7	5.0 ± 0.7
DHAP	2.9 ± 0.2	3.4 ± 0.2	2.6 ± 0.4	2.9 ± 0.1
GAP	0.17 ± 0.02	0.17 ± 0.02	0.14 ± 0.02	0.15 ± 0.03
G3P	2.0 ± 0.1	3.7 ± 0.2	1.6 ± 0.2	3.1 ± 0.1
BPG	0.029 ± 0.003	0.083 ± 0.004	0.018 ± 0.003	0.06 ± 0.01
XPG	0.39 ± 0.00	0.61 ± 0.03	0.29 ± 0.03	0.51 ± 0.04
PEP	0.038 ± 0.001	0.081 ± 0.005	0.027 ± 0.002	0.069 ± 0.005
PYR	0.9 ± 0.2	1.6 ± 0.1	0.8 ± 0.2	1.39 ± 0.04
6PG	0.031 ± 0.001	0.026 ± 0.001	0.05 ± 0.01	0.032 ± 0.003
R5P	0.24 ± 0.05	0.37 ± 0.03	0.24 ± 0.03	0.33 ± 0.02
Ru5P	0.9 ± 0.1	1.1 ± 0.1	0.66 ± 0.03	1.0 ± 0.2
Carbon acids				
CitrA	0.9 ± 0.2	1.1 ± 0.2	0.9 ± 0.1	1.0 ± 0.2
FumA	1.4 ± 0.1	8.0 ± 0.5	0.6 ± 0.1	5.3 ± 0.2
MalA	2.6 ± 0.1	16 ± 1	1.2 ± 0.1	10.5 ± 0.3
αKG	0.15 ± 0.01	0.26 ± 0.02	0.10 ± 0.02	0.21 ± 0.01
SuccA	6 ± 1	12 ± 3	5 ± 1	9 ± 1
Energy metabolism				
AMP	0.7 ± 0.1	0.35 ± 0.03	0.8 ± 0.1	0.43 ± 0.05
ADP	1.30 ± 0.03	1.17 ± 0.05	1.2 ± 0.1	1.10 ± 0.05
ATP	2.6 ± 0.1	3.4 ± 0.2	2.2 ± 0.2	2.9 ± 0.5
GMP	0.125 ± 0.005	0.066 ± 0.003	0.16 ± 0.03	0.082 ± 0.005
GDP	0.20 ± 0.01	0.21 ± 0.01	0.22 ± 0.04	0.19 ± 0.02
GTP	0.37 ± 0.01	0.52 ± 0.02	0.37 ± 0.05	0.4 ± 0.1
Redox metabolism				
NAD^+	2.1 ± 0.1	3.2 ± 0.2	2.0 ± 0.3	2.5 ± 0.1
NADH	0.9 ± 0.1	2.0 ± 0.5	0.8 ± 0.1	1.3 ± 0.4
$NADP^+$	0.091 ± 0.001	0.090 ± 0.003	0.09 ± 0.01	0.08 ± 0.01
NADPH	0.051 ± 0.003	0.068 ± 0.001	0.052 ± 0.004	0.062 ± 0.005
Amino acids				
ASN	1.6 ± 0.1	3.2 ± 0.1	1.5 ± 0.2	2.4 ± 0.1
ASP	1.0 ± 0.1	2.11 ± 0.01	0.6 ± 0.2	1.8 ± 0.1
GLN	12 ± 1	14 ± 1	14 ± 2	12.1 ± 0.4
GLU	79 ± 6	61 ± 3	75 ± 12	59 ± 2
AcCoA	0.019 ± 0.004	0.03 ± 0.01	0.018 ± 0.004	0.032 ± 0.004
Treha	13 ± 1	18 ± 3	11 ± 2	15 ± 1
UDPGlc	0.72 ± 0.01	1.0 ± 0.1	0.62 ± 0.05	0.90 ± 0.04

[a] Values are shown in μmol g^{-1}_{CDW} as average of quadruplicate samples ± standard deviation.

Table 6-15: Metabolite pools of BP000 fermentations on xylose[a]

	BP000			
	Fermentation 3		Fermentation 4	
Metabolite	24 h	48 h	24 h	48 h
Central carbon metabolism				
HXP	0.32 ± 0.01	0.26 ± 0.05	0.30 ± 0.04	0.28 ± 0.02
FBP	0.25 ± 0.01	0.19 ± 0.05	0.21 ± 0.05	0.19 ± 0.01
DHAP	0.70 ± 0.02	0.6 ± 0.1	0.7 ± 0.1	0.5 ± 0.1
GAP	n.q.[b]	n.q.[b]	n.q.[b]	n.q.[b]
G3P	0.093 ± 0.004	0.10 ± 0.02	0.09 ± 0.01	0.09 ± 0.01
BPG	0.014 ± 0.005	0.007 ± 0.002	0.011 ± 0.003	0.005 ± 0.002
XPG	0.23 ± 0.01	0.22 ± 0.04	0.21 ± 0.03	0.25 ± 0.01
PEP	0.067 ± 0.003	0.07 ± 0.01	0.07 ± 0.01	0.080 ± 0.004
PYR	0.8 ± 0.1	0.8 ± 0.1	0.73 ± 0.03	0.64 ± 0.03
6PG	0.010 ± 0.001	0.007 ± 0.001	0.009 ± 0.001	0.008 ± 0.001
R5P	0.19 ± 0.02	0.15 ± 0.03	0.17 ± 0.02	0.15 ± 0.02
Ru5P	0.7 ± 0.2	0.7 ± 0.1	0.6 ± 0.1	0.7 ± 0.1
Carbon acids				
CitrA	1.2 ± 0.1	1.0 ± 0.2	1.1 ± 0.2	1.0 ± 0.2
FumA	0.10 ± 0.02	0.11 ± 0.02	0.09 ± 0.02	0.16 ± 0.01
MalA	0.20 ± 0.03	0.19 ± 0.04	0.16 ± 0.02	0.27 ± 0.04
αKG	0.06 ± 0.01	0.06 ± 0.01	0.056 ± 0.002	0.055 ± 0.001
SuccA	25 ± 5	20 ± 1	24 ± 3	23 ± 4
Energy metabolism				
AMP	1.4 ± 0.1	1.5 ± 0.2	1.3 ± 0.3	1.2 ± 0.1
ADP	3.6 ± 0.2	3.4 ± 0.8	3.2 ± 0.7	3.2 ± 0.2
ATP	6.3 ± 0.3	5.5 ± 1.1	5.4 ± 0.9	5.9 ± 0.2
GMP	0.31 ± 0.004	0.34 ± 0.05	0.3 ± 0.1	0.28 ± 0.04
GDP	0.7 ± 0.1	0.7 ± 0.2	0.6 ± 0.2	0.7 ± 0.1
GTP	1.4 ± 0.1	1.3 ± 0.3	1.2 ± 0.2	1.4 ± 0.1
Redox metabolism				
NAD^+	3.1 ± 0.1	3.6 ± 0.7	2.9 ± 0.4	3.4 ± 0.2
NADH	2.3 ± 0.1	2.4 ± 0.8	2.0 ± 0.4	2.1 ± 0.4
$NADP^+$	0.23 ± 0.01	0.19 ± 0.03	0.21 ± 0.04	0.19 ± 0.01
NADPH	0.11 ± 0.01	0.09 ± 0.02	0.10 ± 0.02	0.09 ± 0.02
Amino acids				
ASN	6.4 ± 0.3	6.2 ± 1.2	6.4 ± 0.6	6.0 ± 0.5
ASP	2.4 ± 0.1	1.9 ± 0.4	2.3 ± 0.2	2.1 ± 0.1
GLN	14 ± 1	10 ± 2	12 ± 1	9 ± 1
GLU	97 ± 5	86 ± 13	95 ± 7	81 ± 7
AcCoA	0.016 ± 0.003	0.023 ± 0.005	0.016 ± 0.004	0.022 ± 0.004
Treha	7.5 ± 1.7	5.3 ± 0.7	5.6 ± 0.8	6.3 ± 0.4
UDPGlc	1.8 ± 0.1	2.3 ± 0.4	1.8 ± 0.2	2.2 ± 0.2

[a] Values are shown in µmol g^{-1}_{CDW} as average of quadruplicate samples ± standard deviation.
[b] n.q.: Not quantified (signal too low).

Table 6-16: Metabolite pools of BP10001 fermentations on xylose[a]

	BP10001			
	Fermentation 5		Fermentation 6	
Metabolite	24 h	48 h	24 h	48 h
Central carbon metabolism				
HXP	0.30 ± 0.05	0.34 ± 0.02	0.33 ± 0.05	0.35 ± 0.03
FBP	0.19 ± 0.06	0.19 ± 0.03	0.23 ± 0.03	0.25 ± 0.03
DHAP	0.62 ± 0.14	0.62 ± 0.04	0.63 ± 0.07	0.61 ± 0.04
GAP	n.q.[b]	n.q.[b]	n.q.[b]	n.q.[b]
G3P	0.19 ± 0.03	0.14 ± 0.02	0.15 ± 0.02	0.14 ± 0.01
BPG	0.007 ± 0.001	0.014 ± 0.003	0.007 ± 0.001	0.006 ± 0.002
XPG	0.38 ± 0.09	0.33 ± 0.02	0.33 ± 0.02	0.29 ± 0.03
PEP	0.15 ± 0.03	0.13 ± 0.01	0.12 ± 0.01	0.10 ± 0.01
PYR	3.4 ± 0.5	4.1 ± 0.5	2.2 ± 0.5	3.0 ± 0.6
6PG	0.016 ± 0.001	0.017 ± 0.001	0.015 ± 0.001	0.016 ± 0.001
R5P	0.25 ± 0.05	0.26 ± 0.01	0.25 ± 0.03	0.25 ± 0.03
Ru5P	2.6 ± 0.7	2.7 ± 0.7	1.9 ± 0.2	1.7 ± 0.3
Carbon acids				
CitrA	0.8 ± 0.1	0.9 ± 0.1	0.6 ± 0.1	0.8 ± 0.3
FumA	0.51 ± 0.06	0.65 ± 0.08	0.39 ± 0.06	0.56 ± 0.05
MalA	0.9 ± 0.1	1.1 ± 0.1	0.6 ± 0.1	0.9 ± 0.1
αKG	0.05 ± 0.01	0.058 ± 0.005	0.045 ± 0.005	0.048 ± 0.003
SuccA	10 ± 2	10 ± 4	12 ± 3	8 ± 3
Energy metabolism				
AMP	0.6 ± 0.2	0.6 ± 0.2	0.5 ± 0.1	0.5 ± 0.1
ADP	2.0 ± 0.5	2.0 ± 0.4	1.8 ± 0.3	1.7 ± 0.2
ATP	6.3 ± 1.6	6.0 ± 0.6	6.1 ± 0.7	6.3 ± 0.7
GMP	0.09 ± 0.02	0.08 ± 0.02	0.08 ± 0.01	0.07 ± 0.01
GDP	0.39 ± 0.11	0.35 ± 0.08	0.34 ± 0.05	0.32 ± 0.03
GTP	1.2 ± 0.3	1.1 ± 0.1	1.2 ± 0.1	1.1 ± 0.1
Redox metabolism				
NAD^+	1.6 ± 0.3	1.5 ± 0.1	1.5 ± 0.3	1.6 ± 0.1
NADH[c]	0.8	1.0	1.2	1.0
$NADP^+$	0.10 ± 0.02	0.11 ± 0.01	0.08 ± 0.01	0.09 ± 0.01
NADPH	0.16 ± 0.04	0.13 ± 0.01	0.15 ± 0.03	0.18 ± 0.05
Amino acids				
ASN	3.6 ± 0.6	3.3 ± 0.3	3.3 ± 0.4	3.0 ± 0.2
ASP	3.9 ± 0.7	3.4 ± 0.3	3.6 ± 0.5	2.9 ± 0.2
GLN	11 ± 2	9 ± 1	10 ± 1	9 ± 1
GLU	71 ± 12	66 ± 6	64 ± 8	62 ± 5
AcCoA	0.041 ± 0.003	0.05 ± 0.01	0.04 ± 0.01	0.046 ± 0.003
Treha	17 ± 4	20 ± 3	11 ± 2	15 ± 4
UDPGlc	1.2 ± 0.3	1.8 ± 0.1	1.5 ± 0.2	2.1 ± 0.2

[a] Values are shown in µmol g^{-1}_{CDW} as average of quadruplicate samples ± standard deviation.
[b] n.q.: Not quantified (signal too low). [c] NADH concentrations were estimated based on external calibration.

Table 6-17: Metabolite pools of IBB10B05 fermentations xylose[a]

	IBB10B05			
	Fermentation 7		Fermentation 8	
Metabolite	Phase I	Phase II	Phase I	Phase II
Central carbon metabolism				
HXP	0.8 ± 0.1	1.04 ± 0.04	0.74 ± 0.04	1.56 ± 0.03
FBP	0.8 ± 0.2	0.67 ± 0.04	0.8 ± 0.1	1.1 ± 0.1
DHAP	1.2 ± 0.2	1.2 ± 0.1	1.1 ± 0.1	1.8 ± 0.1
GAP	0.4 ± 0.1	0.26 ± 0.01	0.28 ± 0.04	0.5 ± 0.1
G3P	0.25 ± 0.04	0.08 ± 0.01	0.22 ± 0.01	0.14 ± 0.01
BPG	0.039 ± 0.003	0.023 ± 0.001	0.031 ± 0.008	0.06 ± 0.01
XPG	0.36 ± 0.05	0.26 ± 0.01	0.37 ± 0.03	0.56 ± 0.01
PEP	0.11 ± 0.02	0.08 ± 0.01	0.11 ± 0.01	0.16 ± 0.003
PYR	3.3 ± 0.5	4.2 ± 0.6	3.2 ± 0.2	6.5 ± 0.4
6PG	0.05 ± 0.01	0.25 ± 0.01	0.049 ± 0.004	0.23 ± 0.01
R5P	2.3 ± 0.5	1.5 ± 0.1	2.9 ± 0.2	3.6 ± 0.6
Ru5P	21 ± 4	14 ± 1	17 ± 3	30 ± 3
Carbon acids				
CitrA	90 ± 15	84 ± 4	87 ± 5	145 ± 4
FumA	1.09 ± 0.13	0.63 ± 0.04	0.87 ± 0.07	0.80 ± 0.04
MalA	2.2 ± 0.3	1.2 ± 0.1	1.7 ± 0.1	1.49 ± 0.02
αKG	0.19 ± 0.02	0.151 ± 0.004	0.24 ± 0.02	0.27 ± 0.02
SuccA	5.3 ± 0.6	6.0 ± 0.1	3.4 ± 0.6	5.8 ± 0.9
Energy metabolism				
AMP	0.17 ± 0.04	0.40 ± 0.03	0.18 ± 0.01	0.55 ± 0.02
ADP	1.2 ± 0.2	1.0 ± 0.1	1.28 ± 0.04	1.4 ± 0.1
ATP	4.4 ± 0.8	5.3 ± 0.2	4.1 ± 0.3	6.9 ± 0.2
GMP	0.036 ± 0.004	0.031 ± 0.002	0.040 ± 0.001	0.055 ± 0.002
GDP	0.33 ± 0.06	0.28 ± 0.02	0.36 ± 0.03	0.48 ± 0.02
GTP	1.24 ± 0.19	0.85 ± 0.04	1.21 ± 0.11	1.57 ± 0.05
Redox metabolism				
NAD^+	2.4 ± 0.5	1.8 ± 0.1	2.2 ± 0.2	3.1 ± 0.1
NADH[b]	0.8	1.1	1.0	0.9
$NADP^+$	0.15 ± 0.03	0.13 ± 0.01	0.13 ± 0.01	0.14 ± 0.01
NADPH	0.22 ± 0.04	0.18 ± 0.03	0.21 ± 0.03	0.22 ± 0.05
Amino acids				
ASN	4.5 ± 0.8	7.2 ± 0.4	4.7 ± 0.4	9.0 ± 0.1
ASP	6.7 ± 1.1	10.5 ± 0.5	6.6 ± 0.4	12.6 ± 0.1
GLN	70 ± 11	161 ± 9	80 ± 4	241 ± 3
GLU	91 ± 16	85 ± 5	90 ± 4	107 ± 2
AcCoA	0.12 ± 0.02	0.12 ± 0.01	0.13 ± 0.02	0.15 ± 0.01
Treha	100 ± 28	23 ± 3	82 ± 6	50 ± 9
UDPGlc	0.51 ± 0.08	0.41 ± 0.02	0.41 ± 0.02	0.37 ± 0.01

[a] Values are shown in µmol g^{-1}_{CDW} as average of quadruplicate samples ± standard deviation.

[b] NADH concentrations were estimated based on external calibration.

6.2.4 Comparison of intracellular metabolite levels of investigated yeasts

Two-sided independent two sample t-tests were performed based on the specific metabolite concentrations to identify differences between the compared groups. The approach comprised (i) the influence of the fermentation time (24 h vs. 48 h and phase I vs. phase II) for every fermentation conducted, (ii) the comparison of the fermentation replicates for every strain and sampling time and (iii) the strain comparison between *C. tenuis* and BP000 and between BP10001 and IBB10B05 for every sampling time and phase. Normal distribution of replicates was presumed, F-tests were performed to check for variance homogeneity within the groups. Results which showed a p value below the chosen 0.05 were listed in bold in the following tables (Table 6-18 to Table 6-25).

6.2.4.1 Influence of fermentation time on metabolite pools

Table 6-18 and Table 6-22 show the influence of the fermentation time on the metabolite concentrations. Based on t-test analysis no major changes in metabolite concentrations over time were observed for BP000 and BP10001, except for F4 (BP000) where the concentration of BPG was ~2.3-fold lower in 48 h samples and MalA and FumA were ~1.5-fold higher in 48 h.

In contrast metabolite levels of *C. tenuis* and IBB10B05 cells fermenting xylose showed a significant dependency on time. Levels of most of the quantified metabolites (20-26 out of 34) of *C. tenuis* were higher at 48 h compared to 24 h. In particular MalA and FumA were 6- to 9-fold higher at 48 h. Concentrations of BPG were ~3-fold and concentrations of PEP, glycerol 3-phosphate (G3P), HXP, pyruvic acid (PYR), SuccA and α-ketoglutaric acid (αKG) were ~2-fold higher. ASP and ASN accumulated 2- to 3-fold, while the concentration of AMP and GMP decreased ~2-fold with time.

In IBB10B05 fermentations an increase of glycolytic metabolites was observable by advanced fermentation time (HXP pool and PYR 2-fold higher). AMP and GLN showed up to 3-fold higher concentrations with time, ASP and ASN up to 2-fold larger pools. The G3P-pool was decreased 1.6- to 3-fold in phase II compared to phase I. Trehalose (Treha) was reduced 1.6- to 4.5-fold at phase II.

6.2.4.2 Comparison of fermentation replicates

To analyse the reproducibility of metabolite pools of the CCM fermentation replicates were compared. Results are listed in Table 6-19 (*C. tenuis* (F1, F2) and BP000 (F3, F4)) and Table 6-23 (BP10001 (F5, F6) and IBB10B05 (F7, F8)). Metabolite pools showed no discrepancies for BP000 and BP10001 fermentation replicates at 24 h and 48 h.

Differences in metabolite levels obtained for *C. tenuis* fermentations were low. With the exception of MalA and FumA (both ~2-fold lower in F2) for 24 h samples highest metabolite levels were within ± 1.6-fold.

Phase I of IBB10B05 fermentations demonstrated no considerable disparities in metabolite concentrations as well. Beside that significant larger pools throughout the quantified metabolites were observed in phase II for F8 compared to F7. This is most probably explained by differences in the time of sampling (for F7 after 167 h (OD600 2.2) and for F8 after 115 h (OD600 1.3) of fermentation).

6.2.4.3 Metabolite pools of C. tenuis compared to those of BP000

In Table 6-20 and Table 6-21 results obtained for comparison of metabolite levels at 24 h and at 48 h, respectively, are listed. Generally glycolytic metabolite and carbon acid pools were larger in *C. tenuis* throughout all comparisons and differences were intensified at 48 h of fermentation. Only for PEP (1.8- to 2.5-fold lower at 24 h and equally concentrated at 48 h), CitrA (no significant differences between all compared classes) and SuccA (4- to 5-fold lower at 24 h and 1.7- to 2.5-fold lower at 48 h) lower metabolite pools were observed in *C. tenuis*. Large differences were determined for G3P (16- to 40-fold higher), FBP (20- to 33-fold higher), BPG (up to 17-fold higher at 48h), HXP (5- to 12-fold higher), MalA (6- to 80-fold higher) and FumA (6- to 75-fold higher). Metabolites of the energy metabolism were significantly lower in *C. tenuis* in a range of 1.6- (ATP) to 5-fold (GMP) independent of the fermentation time. The same tendency was observed for redox metabolites at 24 h and 48 h samples (1.4-fold (NAD^+) to 3-fold (NADH) lower in *C. tenuis*). Differences in amino acid levels of ASP and ASN were higher in the comparison at 24 h (2.3- to 3.7-fold lower for ASP and ~4-fold lower for ASN in *C. tenuis*). While similar ASP concentrations were found in both strains after 48 h of xylose metabolization, concentrations of ASN were 1.9- to 2.5-fold lower in *C. tenuis*. Treha pools were larger in *C. tenuis* throughout all comparisons, from ~2-

fold (24 h) to ~3-fold (48 h). UDP-glucose (UDPGlc) concentrations were significantly lower in *C. tenuis* (2.3- to 3-fold).

6.2.4.4 Metabolite pools of IBB10B05 compared to those of BP10001

Results of IBB10B05/BP10001-comparisons are listed in Table 6-24 and Table 6-25. Except for the energy metabolites, SuccA and UDPGlc, which were lower, metabolite pools were higher in IBB10B05 samples independent of the fermentation time. As the metabolite pools did not significantly change over time for BP10001 and the growth phase dependency of IBB10B05 was already considered (see section 6.2.4.1), the following section is focused on the comparison of phase I (IBB10B05) and 24 h (BP10001) of fermentation. When looking at the CCM biggest differences were observed for CitrA (up to ~150-fold higher in IBB10B05), R5P and Ru5P (4- to 16-fold higher), BPG (~5-fold higher) and GAP (not determinable in BP10001). FumA (2- to 3-fold), MalA (2- to 3.5-fold) and αKG (4- to 5-fold) were higher concentrated in IBB10B05. Energy metabolites had lower levels (~3-fold for AMP, 2- to 2.5-fold for GMP) and redox metabolites were higher concentrated (1.4- to 1.8-fold) compared to BP10001. Looking at the amino acid pools GLN showed larger pools in IBB10B05 (6- to 8-fold), followed by ASP levels (1.7- to 1.9-fold higher). These differences intensified in phase II compared to 48 h of fermentation of BP10001 (GLN 20- to 25-fold higher, ASP 3.0- to 4.4-fold higher and ASN 2.2- to 3-fold higher). Significantly larger metabolite pools were also observed for Treha (5- to 9-fold) and AcCoA (~3-fold) and lower pools for UDPGlc (2.4- to 3.7-fold). Differences in Treha and AcCoA levels declined with advanced fermentation time, while differences in UDPGlc intensified (4.4- to 5.6-fold lower in IBB10B05 phase II).

Table 6-18: Influence of fermentation time on metabolite pools of *C. tenuis* and BP000

	C. tenuis				BP000			
	log (C_{Met}^{48h} / C_{Met}^{24h})[a]							
Metabolite	F1	p value	F2	p value	F3	p value	F4	p value
Central carbon								
BPG	**0.46**	4.5E-07	**0.49**	5.1E-04	-0.29	7.9E-02	**-0.36**	2.6E-02
PEP	**0.33**	2.2E-06	**0.40**	3.6E-06	0.01	8.8E-01	**0.08**	1.1E-02
G3P	**0.27**	9.0E-06	**0.30**	1.4E-05	0.04	3.4E-01	0.00	9.4E-01
HXP	**0.26**	3.4E-04	**0.25**	4.1E-05	-0.09	8.9E-02	-0.03	4.5E-01
PYR	**0.25**	5.8E-04	**0.26**	8.3E-03	-0.01	7.6E-01	**-0.06**	2.7E-03
XPG	**0.19**	6.8E-04	**0.24**	1.3E-04	-0.01	7.6E-01	0.08	5.9E-02
R5P	**0.19**	3.6E-03	**0.15**	2.0E-03	-0.09	8.3E-02	-0.05	1.9E-01
FBP	**0.10**	3.4E-04	0.02	5.9E-01	-0.11	1.0E-01	-0.06	3.7E-01
Ru5P	**0.09**	4.8E-02	**0.18**	3.0E-02	-0.04	5.7E-01	0.03	4.9E-01
DHAP	**0.07**	1.0E-02	0.05	1.9E-01	-0.06	2.8E-01	-0.08	1.1E-01
GAP	0.01	8.1E-01	0.02	6.9E-01	n.d.[b]		n.d.[b]	
6PG	**-0.08**	7.7E-05	**-0.19**	1.6E-03	**-0.13**	1.3E-03	-0.06	7.3E-02
Carbon acids								
MalA	**0.79**	1.1E-07	**0.93**	2.6E-09	0.00	9.5E-01	**0.22**	2.7E-03
FumA	**0.76**	1.2E-07	**0.92**	8.1E-09	0.02	7.7E-01	**0.24**	8.2E-04
SuccA	**0.30**	2.1E-02	**0.29**	9.2E-04	-0.09	2.0E-01	-0.01	8.9E-01
αKG	**0.23**	7.7E-05	**0.35**	1.3E-05	-0.02	5.6E-01	-0.01	2.5E-01
CitrA	0.10	1.7E-01	0.05	3.4E-01	-0.08	1.7E-01	-0.01	8.9E-01
Energy metabolism								
GTP	**0.15**	2.6E-05	0.05	4.0E-01	-0.04	4.7E-01	0.07	1.6E-01
ATP	**0.11**	1.1E-03	0.11	5.1E-02	-0.06	2.6E-01	0.04	3.2E-01
GDP	**0.03**	2.7E-02	-0.05	2.8E-01	0.00	9.8E-01	0.05	4.1E-01
ADP	**-0.05**	3.5E-03	-0.05	1.5E-01	-0.03	6.5E-01	-0.01	8.6E-01
GMP	**-0.28**	6.8E-07	**-0.30**	9.7E-04	0.04	3.1E-01	0.01	9.0E-01
AMP	**-0.33**	3.7E-05	**-0.27**	1.5E-03	0.03	4.9E-01	-0.01	8.0E-01
Redox metabolism								
NADH	**0.35**	4.2E-03	0.25	5.1E-02	0.02	8.5E-01	0.02	8.0E-01
NAD^+	**0.18**	7.9E-05	**0.11**	7.6E-03	0.07	2.0E-01	0.07	5.2E-02
NADPH	**0.13**	1.4E-05	**0.08**	2.1E-02	-0.10	8.6E-02	-0.03	6.1E-01
$NADP^+$	0.00	5.6E-01	-0.02	6.3E-01	-0.09	6.1E-02	-0.05	2.7E-01
Amino acids								
ASP	**0.31**	2.0E-04	**0.44**	3.6E-05	-0.08	7.5E-02	-0.05	9.2E-02
ASN	**0.31**	4.3E-07	**0.20**	2.4E-04	-0.02	6.9E-01	-0.03	3.5E-01
GLN	**0.06**	1.8E-02	-0.07	1.5E-01	**-0.14**	6.8E-03	**-0.12**	2.8E-03
GLU	**-0.11**	1.7E-03	-0.10	8.1E-02	-0.05	1.6E-01	**-0.07**	2.8E-02
AcCoA	**0.24**	2.0E-02	**0.26**	3.7E-03	0.16	7.4E-02	0.13	9.8E-02
Treha	**0.16**	1.2E-02	**0.13**	9.9E-03	-0.15	1.0E-01	0.05	1.8E-01
UDPGlc	**0.13**	2.4E-03	**0.17**	9.0E-05	0.09	9.7E-02	**0.08**	2.7E-02

[a] C_{Met} is the metabolite concentration in µmol g^{-1}_{CDW}. Bold values represent a significant difference with a p value < 0.05. A p value > 0.05 indicates a non-significance with 90 % statistical propability.
[b] n.d.: Not determined.

Table 6-19: Comparison of fermentation replicates of *C. tenuis* and BP000

	C. tenuis				BP000			
	log (C_{Met}^{F2} / C_{Met}^{F1})				log (C_{Met}^{F4} / C_{Met}^{F3})			
Metabolite	24 h	p value	48 h	p value	24 h	p value	48 h	p value
Central carbon metabolism								
6PG	**0.21**	7.2E-03	**0.09**	2.1E-02	-0.01	6.0E-01	0.05	1.2E-01
R5P	-0.01	8.4E-01	-0.05	9.2E-02	-0.06	1.3E-01	-0.02	7.3E-01
FBP	-0.02	6.1E-01	**-0.09**	2.8E-02	-0.07	2.5E-01	-0.01	8.2E-01
DHAP	-0.04	2.9E-01	**-0.06**	1.2E-02	-0.04	3.6E-01	-0.05	3.5E-01
PYR	-0.07	4.1E-01	**-0.06**	1.1E-02	**-0.05**	4.4E-02	-0.09	1.2E-01
GAP	-0.07	9.6E-02	-0.06	2.3E-01	n.d.[b]		n.d.[b]	
HXP	**-0.08**	3.5E-02	**-0.09**	1.5E-03	-0.04	2.7E-01	0.03	5.7E-01
G3P	**-0.11**	1.4E-02	**-0.08**	2.3E-03	-0.01	8.0E-01	-0.05	3.1E-01
Ru5P	**-0.11**	8.8E-03	-0.02	6.6E-01	-0.08	2.6E-01	-0.02	7.1E-01
XPG	**-0.12**	8.2E-03	**-0.08**	6.4E-03	-0.03	3.7E-01	0.06	2.2E-01
PEP	**-0.14**	2.2E-04	**-0.07**	1.3E-02	-0.01	8.3E-01	0.07	1.4E-01
BPG	**-0.19**	4.0E-03	**-0.16**	4.3E-03	-0.11	3.3E-01	-0.18	1.7E-01
Carbon acids								
CitrA	0.01	8.9E-01	-0.03	5.5E-01	-0.04	3.4E-01	0.03	6.9E-01
SuccA	-0.12	2.3E-01	-0.12	1.3E-01	-0.02	7.2E-01	0.06	2.6E-01
αKG	**-0.20**	1.0E-03	**-0.08**	8.4E-03	-0.05	6.8E-02	-0.04	3.8E-01
MalA	**-0.33**	2.8E-06	**-0.19**	2.3E-05	-0.08	1.1E-01	**0.14**	3.9E-02
FumA	**-0.34**	2.9E-05	**-0.18**	2.9E-05	-0.07	2.8E-01	**0.16**	9.8E-03
Energy metabolism								
GMP	0.12	6.0E-02	**0.09**	1.7E-03	-0.05	4.0E-01	-0.08	1.2E-01
AMP	0.04	3.8E-01	**0.09**	2.2E-02	-0.04	3.7E-01	-0.08	1.1E-01
GDP	0.04	4.0E-01	-0.05	7.7E-02	-0.08	1.8E-01	-0.03	5.3E-01
GTP	0.00	9.9E-01	**-0.10**	4.6E-02	-0.09	6.8E-02	0.02	6.8E-01
ADP	-0.02	3.9E-01	-0.02	1.3E-01	-0.05	3.5E-01	-0.03	6.0E-01
ATP	**-0.07**	3.5E-02	-0.07	1.1E-01	-0.07	9.3E-02	0.03	5.5E-01
Redox metabolism								
NADPH	0.01	5.3E-01	-0.04	1.2E-01	-0.03	6.2E-01	0.04	5.1E-01
$NADP^+$	-0.02	5.3E-01	-0.03	1.4E-01	-0.04	3.9E-01	0.00	9.6E-01
NAD^+	-0.04	2.8E-01	**-0.10**	1.9E-03	-0.03	3.6E-01	-0.03	5.3E-01
NADH	-0.07	1.7E-01	-0.17	7.9E-02	-0.05	3.9E-01	-0.05	6.3E-01
Amino acids								
GLN	0.06	1.7E-01	**-0.07**	4.2E-03	-0.05	5.4E-02	-0.04	4.3E-01
ASN	-0.01	8.2E-01	**-0.12**	4.5E-05	0.00	8.6E-01	-0.01	7.8E-01
GLU	-0.02	5.9E-01	-0.01	5.2E-01	-0.01	5.9E-01	-0.03	5.2E-01
ASP	**-0.21**	7.6E-03	**-0.07**	1.2E-02	-0.01	6.7E-01	0.02	6.1E-01
AcCoA	-0.04	5.4E-01	-0.02	7.6E-01	0.01	8.8E-01	-0.02	8.0E-01
UDPGlc	**-0.07**	2.2E-02	-0.03	7.2E-02	-0.01	6.2E-01	-0.02	6.2E-01
Treha	-0.07	1.3E-01	**-0.10**	5.0E-02	-0.13	1.0E-01	0.08	5.7E-02

[a] C_{Met} is the metabolite concentration in µmol g^{-1}_{CDW}. Bold values represent a significant difference with a p value < 0.05. A p value > 0.05 indicates a non-significance with 90 % statistical propability.
[b] n.d.: Not determined.

Table 6-20: Comparison *C. tenuis* and BP000 at 24 h of fermentation

	log ($C_{Met}^{C.\ tenuis\ 24h}$ / $C_{Met}^{BP000\ 24h}$)							
Metabolite	F1 / F3	p value	F1 / F4	p value	F2 / F3	p value	F2 / F4	p value
Central carbon								
G3P	**1.32**	8.0E-05	**1.33**	9.2E-08	**1.22**	8.3E-04	**1.23**	8.1E-04
FBP	**1.30**	6.6E-11	**1.37**	1.4E-10	**1.28**	8.2E-04	**1.35**	8.6E-06
HXP	**0.73**	1.4E-10	**0.77**	2.1E-09	**0.65**	7.9E-04	**0.69**	9.5E-06
DHAP	**0.61**	2.4E-07	**0.65**	4.9E-07	**0.57**	2.2E-03	**0.61**	6.8E-05
6PG	**0.51**	1.3E-08	**0.52**	4.1E-08	**0.71**	8.2E-04	**0.73**	1.1E-05
GAP	n.d.[b]		n.d.[b]		n.d.[b]		n.d.[b]	
BPG	**0.30**	4.4E-03	**0.41**	1.3E-03	0.11	2.4E-01	**0.22**	1.8E-02
XPG	**0.24**	5.0E-05	**0.27**	1.3E-03	**0.12**	5.9E-03	**0.15**	8.2E-03
R5P	0.11	8.2E-02	**0.17**	2.5E-02	**0.10**	3.1E-02	**0.16**	6.5E-03
Ru5P	0.06	3.1E-01	**0.15**	6.5E-03	-0.05	4.7E-01	0.03	2.5E-01
PYR	0.04	4.7E-01	0.09	1.9E-01	-0.03	6.6E-01	0.02	7.8E-01
PEP	**-0.25**	3.0E-06	**-0.25**	1.0E-04	**-0.39**	9.5E-07	**-0.38**	2.2E-05
Carbon acids								
MalA	**1.13**	6.2E-09	**1.20**	5.1E-09	**0.80**	4.6E-06	**0.88**	3.6E-06
FumA	**1.12**	8.3E-08	**1.19**	8.0E-08	**0.78**	6.5E-05	**0.85**	5.6E-05
αKG	**0.38**	4.0E-06	**0.43**	1.1E-06	**0.18**	8.8E-03	**0.23**	1.5E-02
CitrA	-0.11	1.1E-01	-0.07	3.0E-01	**-0.11**	3.2E-02	-0.06	2.4E-01
SuccA	**-0.61**	2.4E-03	**-0.59**	3.9E-04	**-0.72**	1.7E-03	**-0.70**	2.5E-04
Energy metabolism								
AMP	**-0.28**	3.2E-05	-0.23	3.5E-01	**-0.24**	3.5E-04	**-0.20**	1.6E-02
ATP	**-0.38**	1.8E-07	**-0.31**	7.7E-03	**-0.45**	4.2E-07	**-0.38**	4.9E-04
GMP	**-0.39**	1.7E-09	**-0.34**	1.6E-02	**-0.27**	1.6E-03	**-0.23**	1.6E-02
ADP	**-0.44**	1.1E-07	**-0.40**	4.13E-08	**-0.47**	4.9E-07	**-0.42**	1.1E-03
GDP	**-0.57**	2.7E-04	**-0.49**	1.5E-02	**-0.53**	4.5E-06	**-0.45**	3.4E-03
GTP	**-0.58**	7.3E-05	**-0.49**	6.4E-03	**-0.58**	3.3E-07	**-0.49**	5.5E-04
Redox metabolism								
NAD^+	**-0.16**	1.8E-07	**-0.13**	3.1E-02	**-0.20**	2.7E-03	**-0.17**	8.3E-03
NADPH	**-0.33**	1.0E-04	**-0.30**	0.0E+00	**-0.32**	1.5E-04	**-0.29**	4.7E-03
$NADP^+$	**-0.40**	3.0E-04	**-0.36**	8.2E-03	**-0.42**	4.8E-06	**-0.38**	8.2E-04
NADH	**-0.41**	1.3E-05	**-0.36**	8.2E-03	**-0.48**	6.8E-05	**-0.43**	4.7E-03
Amino acids								
GLN	-0.04	5.6E-02	0.01	6.2E-01	0.02	5.7E-01	0.07	1.3E-01
GLU	**-0.09**	3.5E-03	**-0.08**	1.6E-02	**-0.11**	1.7E-02	**-0.10**	3.5E-02
ASP	**-0.36**	2.9E-06	**-0.35**	3.6E-05	**-0.57**	3.4E-06	**-0.56**	1.8E-05
ASN	**-0.62**	7.6E-08	**-0.61**	4.8E-04	**-0.62**	2.1E-07	**-0.62**	5.7E-06
Treha	**0.23**	5.2E-03	**0.35**	7.8E-05	0.16	7.4E-02	**0.28**	2.6E-03
AcCoA	0.08	2.4E-01	**0.07**	1.3E-03	0.04	5.4E-01	0.03	6.9E-01
UDPGlc	**-0.41**	8.7E-05	**-0.39**	1.7E-03	**-0.48**	2.4E-07	**-0.46**	2.7E-05

[a] C_{Met} is the metabolite concentration in µmol g^{-1}_{CDW}. Bold values represent a significant difference with a p value < 0.05. A p value > 0.05 indicates a non-significance with 90 % statistical propability.
[b] n.d.: Not determined.

Table 6-21: Comparison *C. tenuis* and BP000 at 48 h of fermentation

	log ($C_{Met}^{C.\ tenuis\ 48h}$ / $C_{Met}^{BP000\ 48h}$)							
Metabolite	F1 / F3	p value	F1 / F4	p value	F2 / F3	p value	F2 / F4	p value
Central carbon								
G3P	**1.55**	4.8E-08	**1.60**	4.7E-08	**1.47**	3.0E-09	**1.52**	2.8E-09
FBP	**1.50**	2.8E-08	**1.52**	2.6E-08	**1.42**	1.0E-05	**1.43**	8.6E-04
HXP	**1.08**	5.5E-08	**1.06**	4.7E-08	**0.99**	6.2E-08	**0.96**	4.8E-08
BPG	**1.05**	4.9E-07	**1.23**	4.7E-07	**0.89**	6.2E-04	**1.07**	5.0E-04
DHAP	**0.74**	5.8E-07	**0.79**	2.2E-07	**0.68**	2.7E-07	**0.73**	3.7E-08
6PG	**0.56**	1.1E-08	**0.51**	1.8E-08	**0.65**	2.4E-06	**0.60**	3.0E-06
XPG	**0.44**	5.5E-06	**0.39**	7.0E-07	**0.37**	5.1E-05	**0.31**	1.4E-05
GAP	n.d.[b]		n.d.[b]		n.d.[b]		n.d.[b]	
R5P	**0.39**	4.8E-05	**0.41**	1.0E-05	**0.34**	8.7E-05	**0.36**	1.3E-05
PYR	**0.30**	9.7E-05	**0.40**	1.9E-06	**0.25**	2.1E-03	**0.34**	9.3E-08
Ru5P	**0.20**	3.0E-03	**0.21**	1.9E-03	**0.17**	1.8E-02	**0.19**	1.2E-02
PEP	0.07	1.2E-01	0.01	7.5E-01	0.01	9.0E-01	**-0.06**	1.3E-02
Carbon acids								
MalA	**1.92**	3.9E-08	**1.78**	4.0E-08	**1.73**	8.8E-10	**1.59**	9.1E-10
FumA	**1.87**	3.7E-08	**1.71**	5.2E-05	**1.69**	1.8E-09	**1.53**	1.8E-09
αKG	**0.63**	2.2E-06	**0.67**	2.7E-04	**0.55**	3.9E-07	**0.59**	3.6E-05
CitrA	0.06	3.1E-01	0.03	5.6E-01	0.03	6.7E-01	0.00	9.9E-01
SuccA	**-0.22**	1.8E-03	**-0.28**	5.7E-03	**-0.35**	2.6E-06	**-0.40**	7.6E-03
Energy metabolism								
ATP	**-0.22**	7.7E-03	**-0.24**	4.5E-06	**-0.28**	4.0E-03	**-0.31**	2.3E-05
GTP	**-0.39**	1.3E-02	**-0.41**	2.6E-07	**-0.49**	1.1E-03	**-0.51**	1.7E-06
ADP	**-0.47**	1.2E-02	**-0.44**	2.8E-06	**-0.49**	1.1E-02	**-0.46**	2.3E-06
GDP	**-0.54**	7.6E-03	**-0.50**	2.7E-06	**-0.59**	6.4E-03	**-0.55**	2.7E-06
AMP	**-0.63**	7.5E-05	**-0.55**	1.4E-05	**-0.54**	1.2E-04	**-0.46**	3.0E-05
GMP	**-0.71**	1.4E-03	**-0.63**	1.4E-03	**-0.61**	1.6E-03	**-0.54**	4.4E-05
Redox metabolism								
NAD^+	-0.06	2.5E-01	-0.03	1.8E-01	**-0.16**	4.3E-02	**-0.13**	1.2E-04
NADH	-0.08	4.4E-01	-0.03	6.4E-01	-0.25	6.6E-02	**-0.20**	3.4E-02
NADPH	-0.10	1.5E-01	-0.14	5.3E-02	-0.14	5.3E-02	**-0.18**	1.2E-02
$NADP^+$	**-0.31**	1.2E-02	**-0.32**	1.1E-06	**-0.35**	1.2E-03	**-0.35**	2.1E-06
Amino acids								
GLN	**0.16**	3.9E-03	**0.19**	8.8E-05	0.09	7.2E-02	**0.13**	3.1E-04
ASP	0.03	4.3E-01	0.01	4.3E-01	-0.04	4.0E-01	**-0.06**	2.4E-02
GLU	**-0.15**	1.1E-02	**-0.12**	2.1E-03	**-0.16**	2.8E-02	**-0.13**	1.1E-03
ASN	**-0.28**	1.5E-02	**-0.27**	2.8E-05	**-0.40**	8.0E-03	**-0.39**	6.2E-06
Treha	**0.54**	7.5E-04	**0.46**	3.5E-03	**0.44**	2.3E-05	**0.36**	2.4E-06
AcCoA	0.17	7.1E-02	**0.18**	4.9E-02	**0.14**	4.6E-02	**0.16**	2.2E-02
UDPGlc	**-0.37**	5.1E-03	**-0.35**	1.1E-05	**-0.40**	4.7E-03	**-0.38**	6.3E-06

[a] C_{Met} is the metabolite concentration in µmol g^{-1}_{CDW}. Bold values represent a significant difference with a p value < 0.05. A p value > 0.05 indicates a non-significance with 90 % statistical propability.

[b] n.d.: Not determined.

Table 6-22: Influence of fermentation time on metabolite pools of BP10001 and IBB10B05

	BP10001				IBB10B05			
	log (C_{Met}^{48h} / C_{Met}^{24h})				log (C_{Met}^{II} / C_{Met}^{I})			
Metabolite	F5	p value	F6	p value	F7	p value	F8	p value
Central carbon metabolism								
6PG	0.02	4.0E-01	0.02	1.0E-01	0.67	4.4E-01	0.67	9.7E-01
HXP	0.06	1.8E-01	0.03	4.7E-01	**0.11**	1.1E-02	**0.32**	8.4E-08
PYR	0.08	9.8E-02	0.13	7.7E-02	**0.11**	4.8E-02	**0.31**	7.9E-06
BPG	0.32	3.0E-01	-0.10	2.0E-01	-0.23	3.6E-01	0.28	7.5E-01
Ru5P	0.01	8.8E-01	-0.05	3.1E-01	**-0.17**	1.1E-02	**0.25**	5.6E-04
DHAP	0.00	9.8E-01	-0.01	6.5E-01	0.00	9.9E-01	**0.21**	2.7E-06
GAP	n.d.[b]		n.d.[b]		-0.18	5.8E-02	**0.19**	1.7E-02
XPG	-0.06	4.8E-01	-0.05	9.7E-02	-0.14	4.4E-01	0.18	3.4E-01
PEP	-0.06	3.2E-01	**-0.08**	4.9E-02	**-0.15**	2.5E-02	**0.16**	5.0E-06
FBP	0.00	9.8E-01	0.04	3.7E-01	-0.08	1.3E-01	**0.14**	7.5E-04
R5P	0.01	8.6E-01	-0.01	8.8E-01	-0.16	5.3E-02	0.09	7.4E-02
G3P	-0.11	8.1E-02	-0.05	2.2E-01	**-0.47**	4.8E-03	**-0.21**	7.8E-06
Carbon acids								
SuccA	0.00	9.9E-01	-0.22	6.9E-02	0.05	1.3E-01	**0.24**	6.2E-03
CitrA	0.08	1.8E-01	0.14	2.7E-01	-0.03	4.0E-01	**0.22**	2.2E-06
αKG	0.07	1.6E-01	0.03	3.4E-01	**-0.09**	2.9E-02	**0.06**	3.5E-02
FumA	**0.11**	3.6E-02	**0.16**	5.4E-03	**-0.24**	5.7E-04	-0.04	1.4E-01
MalA	**0.12**	2.1E-02	**0.17**	6.5E-03	**-0.27**	4.1E-04	**-0.07**	1.4E-02
Energy metabolism								
AMP	0.04	6.6E-01	0.00	9.6E-01	**0.38**	6.9E-05	**0.48**	1.9E-08
ATP	-0.02	7.6E-01	0.01	7.3E-01	0.08	1.0E-01	**0.23**	3.2E-06
GMP	-0.05	5.7E-01	-0.05	3.2E-01	-0.07	6.5E-02	**0.14**	2.0E-05
GDP	-0.04	6.2E-01	-0.04	3.8E-01	-0.07	1.4E-01	**0.13**	6.2E-04
GTP	-0.05	4.5E-01	-0.02	5.4E-01	**-0.17**	2.5E-02	**0.11**	8.8E-04
ADP	-0.01	9.1E-01	-0.03	4.8E-01	-0.09	5.2E-02	**0.05**	3.6E-03
Redox metabolism								
NAD^+	-0.03	6.0E-01	0.02	5.9E-01	-0.11	7.2E-02	**0.14**	8.5E-05
$NADP^+$	0.03	5.0E-01	0.06	1.4E-01	-0.07	1.9E-01	**0.06**	8.5E-03
NADPH	-0.09	3.5E-01	0.08	3.0E-01	-0.08	1.6E-01	0.02	7.0E-01
NADH	n.d.[b]		n.d.[b]		n.d.[b]		n.d.[b]	
Amino acids								
GLN	-0.08	1.3E-01	-0.07	7.0E-02	**0.36**	1.3E-05	**0.48**	8.1E-10
ASP	-0.06	2.2E-01	**-0.09**	4.5E-02	**0.20**	6.4E-04	**0.28**	1.8E-05
ASN	-0.04	3.2E-01	-0.04	2.4E-01	**0.21**	9.5E-04	**0.28**	7.3E-05
GLU	-0.03	4.7E-01	-0.01	7.5E-01	-0.03	5.0E-01	**0.08**	2.6E-04
AcCoA	0.11	8.6E-01	0.04	4.0E-01	-0.01	2.1E-01	0.08	4.4E-01
UDPGlc	**0.17**	8.2E-03	**0.13**	8.5E-03	-0.09	5.4E-02	**-0.04**	3.0E-03
Treha	0.06	2.8E-01	0.13	1.1E-01	**-0.64**	1.0E-02	**-0.21**	9.0E-04

[a] C_{Met} is the metabolite concentration in µmol g^{-1}_{CDW}. Bold values represent a significant difference with a p value < 0.05. A p value > 0.05 indicates a non-significance with 90 % statistical propability.
[b] n.d.: Not determined.

Table 6-23: Comparison of fermentation replicates of BP10001 and IBB10B05

	BP10001				IBB10B05			
	log (C_{Met}^{F6} / C_{Met}^{F5})				log (C_{Met}^{F8} / C_{Met}^{F7})			
Metabolite	24 h	p value	48 h	p value	Phase I	p value	Phase II	p value
Central carbon								
BPG	0.05	4.8E-01	-0.37	4.1E-01	-0.10	2.6E-01	0.42	1.2E-01
R5P	0.00	9.8E-01	-0.01	5.8E-01	**0.12**	3.6E-02	**0.37**	5.2E-03
XPG	-0.06	3.3E-01	-0.05	8.4E-02	0.01	7.7E-02	**0.33**	4.0E-02
Ru5P	-0.14	1.2E-01	-0.20	5.3E-02	-0.10	1.1E-01	**0.32**	4.9E-05
PEP	-0.07	2.6E-01	**-0.09**	1.1E-02	0.00	9.6E-01	**0.31**	1.1E-07
GAP	n.d.[b]		n.d.[b]		-0.14	6.8E-02	**0.22**	2.3E-02
G3P	-0.09	1.3E-01	-0.03	4.4E-01	-0.04	3.5E-01	**0.21**	1.4E-05
FBP	0.07	3.4E-01	**0.11**	3.6E-02	-0.02	6.2E-01	**0.20**	2.1E-05
PYR	**-0.20**	1.2E-02	**-0.14**	1.9E-02	-0.02	6.6E-01	**0.18**	9.0E-04
HXP	0.04	4.4E-01	0.01	6.1E-01	-0.04	3.7E-01	**0.18**	9.2E-07
DHAP	0.01	8.8E-01	0.00	8.8E-01	-0.03	4.9E-01	**0.17**	9.6E-06
6PG	-0.01	2.2E-01	-0.01	1.5E-01	-0.03	3.9E-01	-0.04	3.6E-01
Carbon acids								
αKG	-0.05	3.5E-01	**-0.09**	1.5E-02	**0.10**	8.6E-03	**0.25**	1.8E-05
CitrA	-0.12	1.8E-01	-0.07	4.5E-01	-0.02	6.6E-01	**0.24**	4.2E-07
MalA	**-0.14**	2.8E-02	**-0.09**	4.0E-02	**-0.10**	2.4E-02	**0.10**	2.1E-03
FumA	**-0.12**	3.4E-02	-0.07	8.9E-02	**-0.10**	2.6E-02	**0.10**	1.5E-03
SuccA	0.09	2.0E-01	-0.13	3.8E-01	**-0.20**	3.2E-03	-0.01	8.3E-01
Energy metabolism								
GTP	-0.02	7.6E-01	0.01	8.4E-01	-0.01	8.0E-01	**0.27**	4.9E-07
GMP	-0.08	2.5E-01	-0.08	3.3E-01	0.04	1.8E-01	**0.26**	4.3E-06
GDP	-0.05	4.8E-01	-0.05	3.9E-01	0.03	5.0E-01	**0.23**	1.0E-05
ADP	-0.04	5.6E-01	-0.06	2.5E-01	0.02	6.0E-01	**0.16**	1.9E-04
AMP	-0.06	4.5E-01	-0.11	2.7E-01	0.04	4.9E-01	**0.14**	1.5E-04
ATP	-0.01	8.9E-01	0.02	5.0E-01	-0.03	5.0E-01	**0.12**	2.2E-05
Redox metabolism								
NAD^+	-0.02	7.1E-01	0.03	3.0E-01	-0.03	5.5E-01	**0.22**	3.7E-06
NADPH	-0.02	7.8E-01	0.15	1.1E-01	-0.02	6.9E-01	0.09	2.1E-01
$NADP^+$	-0.08	1.8E-01	-0.05	9.9E-02	-0.08	1.4E-01	**0.06**	5.8E-03
NADH	n.d.[b]		n.d.[b]		n.d.[b]		n.d.[b]	
Amino acids								
GLN	-0.01	7.8E-01	0.00	9.8E-01	0.06	1.3E-01	**0.18**	2.3E-06
GLU	-0.05	3.5E-01	-0.02	3.7E-01	0.00	9.5E-01	**0.10**	2.3E-04
ASN	-0.04	3.6E-01	-0.04	1.4E-01	0.02	6.0E-01	**0.10**	8.3E-05
ASP	-0.04	4.1E-01	**-0.07**	2.3E-02	-0.01	8.2E-01	**0.08**	2.4E-03
Treha	**-0.18**	3.0E-02	-0.11	1.1E-01	-0.08	2.9E-01	**0.34**	1.4E-02
AcCoA	0.02	7.4E-01	-0.06	5.1E-01	0.02	6.2E-01	0.11	3.2E-01
UDPGlc	0.09	1.5E-01	**0.06**	4.4E-02	-0.09	8.5E-02	**-0.05**	7.8E-03

[a] C_{Met} is the metabolite concentration in µmol g^{-1}_{CDW}. Bold values represent a significant difference with a p value < 0.05. A p value > 0.05 indicates a non-significance with 90 % statistical propability.
[b] n.d.: Not determined.

Table 6-24: Comparison IBB10B05 and BP10001 at phase I and 24 h, respectively

	log ($C_{Met}^{IBB10B05}{}_{i}$ / $C_{Met}^{BP10001\ 24h}$)							
Metabolite	F7 / F6	p value	F8 / F6	p value	F7 / F5	p value	F8 / F5	p value
Central carbon								
R5P	**0.95**	3.2E-03	**1.07**	2.2E-07	**0.95**	1.4E-04	**1.07**	2.4E-07
Ru5P	**1.05**	1.7E-03	**0.95**	1.6E-03	**0.91**	5.1E-05	**0.81**	5.7E-05
BPG	**0.72**	1.2E-05	**0.63**	1.1E-03	**0.77**	3.3E-03	**0.67**	4.6E-03
GAP	n.d.[b]		n.d.[b]		n.d.[b]		n.d.[b]	
FBP	**0.55**	3.0E-04	**0.52**	1.7E-05	**0.62**	2.8E-04	**0.59**	2.6E-05
6PG	**0.53**	1.8E-03	0.50	1.6E-01	0.52	9.5E-02	**0.49**	2.9E-02
HXP	**0.39**	3.5E-04	**0.35**	1.4E-05	**0.43**	2.7E-04	**0.39**	1.3E-05
DHAP	**0.28**	2.3E-03	**0.25**	3.6E-05	**0.29**	3.8E-03	**0.26**	5.1E-04
G3P	**0.21**	7.8E-03	**0.17**	6.0E-04	0.12	7.6E-02	0.08	8.6E-02
XPG	0.04	3.4E-01	0.05	3.5E-01	-0.02	8.8E-01	-0.01	9.2E-01
PYR	**0.18**	1.5E-02	**0.16**	9.6E-03	-0.02	7.1E-01	-0.03	4.0E-01
PEP	-0.05	3.3E-01	-0.05	1.2E-01	-0.12	1.2E-01	-0.12	1.2E-01
Carbon acids								
CitrA	**2.20**	1.2E-03	**2.18**	1.4E-06	**2.07**	1.2E-03	**2.05**	1.4E-06
αKG	**0.62**	6.0E-06	**0.72**	1.1E-06	**0.57**	1.1E-05	**0.67**	1.8E-06
MalA	**0.54**	4.9E-05	**0.44**	6.5E-06	**0.40**	1.3E-04	**0.30**	3.5E-05
FumA	**0.45**	7.5E-05	**0.35**	6.0E-05	**0.33**	2.2E-04	**0.23**	3.3E-04
SuccA	**-0.36**	2.9E-03	**-0.56**	8.1E-04	**-0.27**	3.2E-03	**-0.47**	4.8E-04
Energy metabolism								
GTP	0.03	4.5E-01	0.02	4.7E-01	0.01	8.3E-01	0.00	9.5E-01
GDP	-0.01	7.9E-01	0.02	6.7E-01	-0.07	4.0E-01	-0.04	5.9E-01
ATP	**-0.15**	1.6E-02	**-0.18**	2.0E-03	-0.16	7.5E-02	-0.19	6.8E-02
ADP	**-0.17**	1.1E-02	**-0.16**	2.9E-02	**-0.21**	2.8E-02	-0.20	6.5E-02
GMP	**-0.32**	9.3E-04	**-0.28**	9.4E-03	**-0.41**	2.7E-03	**-0.37**	1.8E-02
AMP	**-0.46**	8.0E-04	**-0.42**	7.4E-03	**-0.52**	2.6E-03	**-0.48**	1.6E-02
Redox metabolism								
NADPH	**0.16**	2.6E-02	**0.14**	2.0E-02	0.14	1.0E-01	0.12	1.0E-01
NAD^+	**0.20**	1.7E-02	**0.17**	2.7E-03	**0.18**	3.4E-02	**0.15**	1.3E-02
$NADP^+$	**0.26**	3.8E-03	**0.18**	4.8E-04	**0.18**	2.3E-02	**0.10**	4.2E-02
NADH	n.d.[b]		n.d.[b]		n.d.[b]		n.d.[b]	
Amino acids								
GLN	**0.83**	3.7E-05	**0.89**	4.7E-08	**0.82**	4.0E-05	**0.88**	6.7E-08
ASP	**0.28**	1.7E-03	**0.27**	5.7E-05	**0.23**	5.1E-03	**0.22**	6.0E-04
ASN	**0.13**	4.5E-02	**0.16**	2.2E-03	0.09	1.6E-01	**0.11**	2.4E-02
GLU	**0.15**	2.2E-02	**0.15**	9.1E-04	0.11	9.7E-02	**0.10**	2.6E-02
Treha	**0.95**	7.4E-03	**0.87**	6.1E-07	**0.77**	9.7E-04	**0.69**	1.7E-06
AcCoA	**0.46**	4.0E-04	**0.48**	2.2E-05	**0.48**	1.2E-03	**0.50**	6.0E-05
UDPGlc	**-0.48**	2.1E-04	**-0.57**	2.6E-03	**-0.38**	2.2E-03	**-0.48**	8.9E-03

[a] C_{Met} is the metabolite concentration in µmol g^{-1}_{CDW}. Bold values represent a significant difference with a p value < 0.05. A p value > 0.05 indicates a non-significance with 90 % statistical propability.
[b] n.d.: Not determined.

Table 6-25: Comparison IBB10B05 and BP10001 at phase II and 48 h, respectively

	log ($C_{Met}^{IBB10B05\ II}$ / $C_{Met}^{BP10001\ 48h}$)							
Metabolite	F7 / F6	p value	F8 / F6	p value	F7 / F5	p value	F8 / F5	p value
Central carbon								
R5P	**0.79**	1.0E-07	**1.16**	1.4E-03	**0.78**	6.7E-05	**1.15**	1.4E-03
6PG	**1.18**	9.2E-10	**1.15**	3.4E-02	1.17	5.6E-02	1.13	1.9E-01
Ru5P	**0.93**	1.1E-05	**1.25**	1.2E-05	**0.73**	2.5E-06	**1.04**	1.3E-06
GAP	n.d.[b]		n.d.[b]		n.d.[b]		n.d.[b]	
FBP	**0.42**	5.0E-06	**0.62**	1.5E-07	**0.54**	1.6E-06	**0.74**	7.2E-08
HXP	**0.47**	1.3E-07	**0.65**	3.0E-09	**0.48**	4.7E-08	**0.66**	1.0E-09
BPG	**0.60**	4.2E-06	**1.01**	2.1E-05	**0.22**	1.6E-02	**0.64**	1.2E-02
DHAP	**0.30**	5.2E-06	**0.47**	2.1E-08	**0.29**	5.9E-06	**0.47**	2.5E-08
XPG	-0.04	1.4E-01	0.28	8.7E-01	-0.09	3.4E-01	0.23	8.8E-01
PYR	**0.16**	2.1E-02	**0.34**	5.2E-05	0.01	7.8E-01	**0.20**	3.1E-04
PEP	**-0.13**	3.3E-03	**0.19**	7.7E-04	**-0.21**	4.8E-05	**0.10**	3.2E-04
G3P	**-0.21**	2.3E-04	0.00	9.9E-01	**-0.24**	5.8E-04	-0.03	3.7E-01
Carbon acids								
CitrA	**2.02**	2.4E-07	**2.26**	1.8E-08	**1.96**	2.4E-05	**2.20**	1.8E-08
αKG	**0.50**	1.7E-08	**0.75**	4.5E-07	**0.41**	1.6E-07	**0.67**	6.9E-07
MalA	**0.10**	7.4E-03	**0.20**	1.1E-03	0.01	6.5E-01	**0.12**	9.9E-03
FumA	0.05	5.9E-02	**0.16**	3.0E-04	-0.02	6.3E-01	**0.09**	2.3E-02
SuccA	-0.10	4.4E-01	-0.11	4.6E-01	-0.22	1.5E-01	-0.23	1.6E-01
Energy metabolism								
GTP	**-0.11**	1.6E-02	**0.16**	7.1E-04	**-0.10**	1.2E-02	**0.17**	2.5E-04
GDP	-0.05	1.2E-01	**0.18**	1.3E-04	-0.10	1.2E-01	**0.14**	1.7E-02
ATP	**-0.08**	2.7E-02	0.04	1.7E-01	-0.06	5.4E-02	**0.06**	2.7E-02
AMP	-0.07	1.7E-01	0.07	1.8E-01	-0.18	1.3E-01	-0.04	6.2E-01
ADP	**-0.23**	1.9E-04	**-0.08**	1.3E-02	**-0.29**	2.7E-03	-0.14	6.7E-02
GMP	**-0.35**	1.9E-04	**-0.09**	3.1E-02	-0.43	6.5E-02	-0.17	1.9E-01
Redox metabolism								
NAD^+	**0.07**	1.9E-02	**0.29**	8.5E-07	**0.09**	6.9E-03	**0.32**	1.0E-06
NADPH	0.00	9.8E-01	0.08	2.9E-01	**0.15**	3.3E-02	**0.23**	3.2E-02
$NADP^+$	**0.13**	8.6E-04	**0.19**	1.0E-04	**0.07**	1.3E-02	**0.13**	6.8E-04
NADH	n.d.[b]		n.d.[b]		n.d.[b]		n.d.[b]	
Amino acids								
GLN	**1.26**	3.9E-08	**1.43**	3.6E-12	**1.26**	3.9E-08	**1.43**	4.0E-12
ASP	**0.56**	1.1E-07	**0.64**	2.0E-10	**0.49**	2.2E-07	**0.57**	2.9E-07
ASN	**0.38**	9.4E-07	**0.47**	8.2E-09	**0.34**	1.7E-06	**0.44**	1.8E-08
GLU	**0.13**	8.8E-04	**0.24**	2.5E-06	**0.11**	2.9E-03	**0.21**	7.8E-06
AcCoA	**0.41**	1.1E-05	**0.52**	1.1E-05	**0.35**	1.0E-06	**0.46**	4.0E-06
Treha	0.18	6.3E-02	**0.52**	2.8E-04	0.07	2.2E-01	**0.41**	4.6E-04
UDPGlc	**-0.70**	6.3E-07	**-0.75**	1.9E-04	**-0.64**	9.7E-07	**-0.69**	2.3E-04

[a] C_{Met} is the metabolite concentration in µmol g^{-1}_{CDW}. Bold values represent a significant difference with a p value < 0.05. A p value > 0.05 indicates a non-significance with 90 % statistical propability.
[b] n.d.: Not determined.

6.2.5 Thermodynamic analysis of the central carbon metabolism

The reactant concentrations for thermodynamic analysis were taken from Table 6-14 to Table 6-17. A value of 2.38 mL g^{-1}_{CDW} was used to calculate molar concentrations [66]. Respective equilibrium constants were found in the literature [14]. Concentrations of P_i an d CO_2 used (5 mM and 28.6 mM, respectively) were taken from Ref. [14]. Glucose 6-phosphate isomerase (G6P > F6P) and phosphoglycerate mutase reaction (3PG > 2PG) were assumed to be at equilibrium. The HXP pool was interpreted as the sum of G6P and F6P (other HXPs were neglected). Resultant ΔΔG are shown in Table 5-26. Representative results for C. tenuis (F1), BP000 (F3), BP10001 (F5) and IBB10B05 (F7) at 24 h and at phase I, respectively, are listed.
Results obtained for PFK, PYK, G3PDH, G3PDH-laconase and ADK1 were in good agreement with data reported for BP000 and BP10001 [14]. Differences to the published data were determined for the reaction of ENO, GND and RKI. While the published data implied reactions near the equilibria the results showed discrepancies. For GND and RKI this was most probably due to incorrect Ru5P and CO2 concentrations. Values for the FBA, GAPDH-PGK and TPI reactions were not calculated for BP000 and BP10001 due to unknown reactant concentrations.
For C. tenuis it was observed that the reactions for PFK and GND moved away from equilibrium while GA3PDH-PGK and ADK1 reaction converged to the equilibrium over time. ΔΔG values for IBB10B05 reactions approached in the direction of a balance for PYK and GND in phase II. At the same time values for ADK1 switched from slightly negative to positive. ΔΔG values of reactions in BP000 and BP10001 remained constant over time. All reaction data and additional thermodynamic calculations according to strain and sampling point are provided in Additional File 03.

Table 6-26: Summary of thermodynamic analysis.

		C. tenuis	BP000	BP10001	IBB10B05
Enzyme[a]	Keq	ΔΔG[b]	ΔΔG[b]	ΔΔG[b]	ΔΔG[b]
PFK	800	-12.3 ± 0.1	-15.2 ± 0.2	-20.9 ± 1.3	-20.0 ± 0.8
FBA	0.099 mM	-2.2 ± 0.2	n.d.[c]	n.d.[c]	2.2 ± 0.8
GAPDH-PGK	1.83 mM^{-1}	-4.4 ± 0.4	n.d.[c]	n.d.[c]	-7.2 ± 1.5
ENO	4.5	-5.1 ± 0.0	-2.2 ± 0.0	-5.7 ± 0.0	-6.3 ± 0.1
PYK	6500	-12.3 ± 0.3	-14.2 ± 0.1	-10.1 ± 0.5	-9.6 ± 0.4
TPI	22	-0.6 ± 0.2	n.d.[c]	n.d.[c]	-4.9 ± 0.5
G3PDH	4300	-19.8 ± 0.3	-25.4 ± 0.2	-22.3 ± 1.1	-22.2 ± 1.1
G6PDH-lactonase	100000	-38.9 ± 0.1	-38.0 ± 0.3	-33.6 ± 0.9	-33.2 ± 0.8
GND	77 mM	4.4 ± 0.3	6.5 ± 0.6	11.4 ± 0.9	13.6 ± 0.8
RKI	1.2	-3.7 ± 0.4	-3.8 ± 0.5	-6.3 ± 0.55	-6.1 ± 0.5
ADK1	0.8	0.9 ± 0.2	-0.4 ± 0.3	0.1 ± 1.3	-1.4 ± 0.8
FUM	4.3	-2.1 ± 0.1	-2.1 ± 0.4	-2.4 ± 0.3	-1.9 ± 0.3

[a] Substrates and products according to the enzymatic reaction are provided in Additional File 03.
[b] ΔΔG values are shown in kJ mol^{-1}. [c] n.d., not determined.

6.2.6 Semi-quantitative metabolomics

A set of 127 compounds was analysed semi-quantitatively for *C. tenuis*, BP000, BP10001 and IBB10B05 to identify metabolic differences beyond quantified metabolites. Thereof signals for 114 metabolites of comparison 1 (*C. tenuis*/BP000) and 113 metabolites of comparison 2 (BP10001/IBB10B05) were analysable. Metabolite responses (^{12}C areas/^{13}C areas multiplied by the average ^{13}C area of the calibration standard for correction) per g_{CDW} were compared by applying two sided independent t-tests. In case of too high variance of ^{13}C signals (low S/N and high relative S.D. (> 40 %)) ^{12}C area per g_{CDW} were compared. Areas were not corrected in this case as it was supposed that the variation of the metabolite responses was effected equally by randomization of the LC/MS samples. This was applied to 14 and 15 metabolites of comparison 1 and comparison 2, respectively. Figure 6-10 shows the semi-quantitative results at 24 h of xylose fermentation of *C. tenuis* (F1) and BP000 (F3). A comparison of BP10001 (F6, 24 h) and IBB10B05 (F8, phase I) is presented in Figure 6-11. Metabolites which are analysed exclusively based on their ^{12}C areas are marked by a dagger ("†"). For the clarification of abbreviations see List of Abbreviations. Additional comparisons as illustrated for the quantitative approach can be found in Additional File 04.

It has to be considered that metabolites of the same concentration differ in their MS response due to diverse ionization efficiencies and/or high carry-over associated background signals. In Figure 6-9 the mean response of the ^{12}C area of the quantified metabolites normalized to a concentration of 10 µM is shown. MS responses were taken from the calibration of the *C. tenuis*/BP000 comparison. The calculation can be found in Additional File 05.

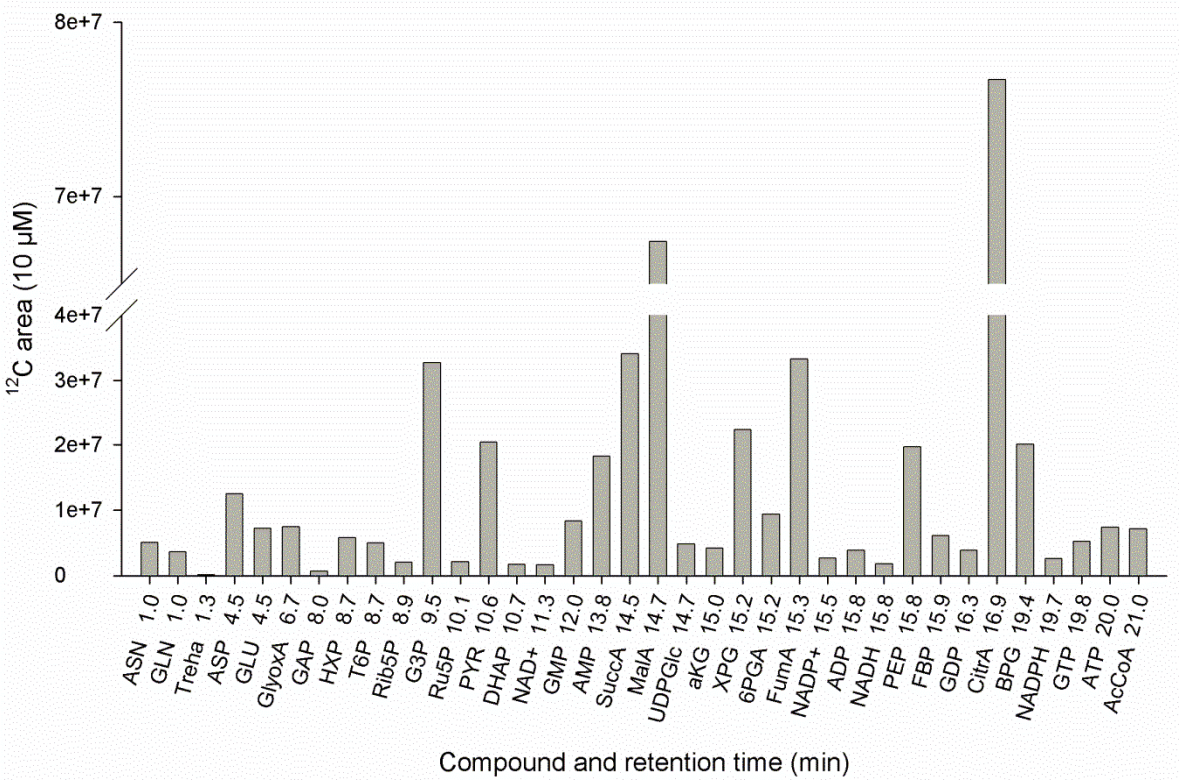

Figure 6-9: Mean MS response of the ^{12}C areas of the quantified metabolites normalized to a concetration of 10 µM.

6.2.6.1 Semi-quantitative compared to quantitative results

For the *C. tenuis*/BP000 approach (F1/F3) a comparison of the semi-quantitative and quantitative approach based on the t-test analysis results was made representatively for all other comparisons. Of the 34 metabolites opposed only 5 (excluding GAP as it was not determined quantitatively for BP000) showed differences of greater than 30 % when looking at the determined ratios based on metabolite responses or the specific concentrations obtained for *C. tenuis* and BP000. 6PG (4.5-fold compared to 3.2-fold higher in *C. tenuis*), NADPH (3.1-/2.1-fold lower) and UDPGlc (4.4-/2.6-fold lower) showed greater differences in the semi-quantitative analyses, while FumA (8.5-/13.3-fold higher) and MalA (8.5-/13.4-fold higher) showed lower differences in the semi-quantitative compared to the quantitative data. NADH was the only metabolite which showed an insignificant difference in the semi-quantitative (p value of 0.13) analysis although determined as significant (p value of $1.3x10^{-5}$) in the quantitative analysis. The complete dataset is presented in Additional File 06.

As implied by Figure 6-9 semi-quantitative data was not suited for the calculation of energy and anabolic/catabolic reduction charges and further thermodynamic investigations.

6.2.6.2 Influence of fermentation time on metabolite responses

While metabolite responses obtained from BP000 and BP10001 remained stable with fermentation time, *C. tenuis* and IBB10B05 metabolite levels showed a significant dependency on fermentation time. In the following a short overview of changes in *C. tenuis* and IBB10B05 is given. A detailed comparison of all individual fermentations can be seen in Additional File 04.

Of the analysed metabolites 76 (F2) to 100 (F1) metabolites showed significant differences over time in *C. tenuis* fermentations, most of them accumulated. About 30 metabolites were more than factor two higher at 48 h, one third to half of it more than factor three. Biggest effects were observed for acetyllysine (AcLYS, 7.1- to 7.8-fold), 2-isopropylmalic acid (5.6- to 7.7-fold), MalA (5.7- to 7.3-fold), FumA (5.4- to 7.3-fold), TYR (4.2- to 6.7-fold) and phosphoribosylpyrophosphate (PRPP, 2.8- to 5.4-fold). Two- to 4-fold higher responses at 48 h were observed for PHE, ALA, uridine, citraconic acid, citramalic acid, TRP, X5P, uracil, LEU, SER, BPG, S7P, CTP, dTTP, PEP, NADH, UTP, ASP, SuccA, CDP, G3P and HXP. Metabolite responses which lowered over time more than 2- to 3-fold were dAMP, GMP, adenine and N-carbamoylaspartic acid (NCarbASP).

IBB10B05 fermentations resulted in 74 (F7) to 100 (F8) metabolites that changed in concentration significantly over time. 26 (F7) and 43 (F8) of them were ~2-fold and above enhanced in phase II, 13 (F7) and 3 (F8) metabolite lowered in the signal more than 2-fold. Highest increasing metabolite responses were observed for inosine (14- to 34-fold), CDP-ethanolamine (12- to 17-fold), xanthine (10- to 15-fold), dAMP (7.3- to 9.7-fold), 6PG (~6,5-fold), deoxyguanosine (6- to 15.7-fold), THR (6.1- to 6.7-fold), adenosine (5.4- to 18.2-fold), GLY (5- to 12.2-fold), cytidine (3.8- to 11.7-fold), guanosine (3.3- to 9.7-fold), orotic acid (3.3- to 5.2-fold) and N-acetylglutamine (NAcGLN, 4- to 4.5-fold). Metabolite responses lowered in both fermentations were quinolinic acid (4.1- to 5.8-fold), creatine (1.9- to 4.7-fold) and CYS (2.1- to 4.5-fold).

6.2.6.3 Metabolite responses of C. tenuis compared to those of BP000

Beside the quantified metabolites (G3P, FBP, HXP, DHAP, 6PG) gluconic acid (GlcA, 9.4-fold), N-carbamoylaspartic acid (NCarbASP, 9.4-fold), inosine (8.5-fold), sedoheptulose 1,7-bisphosphate (S1,7BP, 5.1-fold), guanosine (4.8-fold), pantothenic acid (4.2-fold) and creatine (3.9-fold) showed the highest differences at metabolite levels of *C. tenuis* compared

to BP000 at 24 h. Metabolite levels of *C. tenuis* were lower for xanthine (61-fold), ILE (30-fold), LEU (23.5-fold) and VAL (20-fold). dTDP and taurine were not determinable in *C. tenuis*. Seven-fold to 13-fold lower responses were observed for TYR, THR, UDP, CMP, PHE, Uracil, dTTP and TRP.

6.2.6.4 Metabolite responses of IBB10B05 compared to those of BP10001

The largest differences for metabolites higher concentrated in IBB10B05 compared to BP10001 were observed for the signals of sedoheptulose 1,7-bisphosphate (S1,7BP, 186-fold), sedoheptulose 7-phosphate (S7P, 36-fold), IMP (36-fold), 2-isopropylmalic acid (23-fold), PRPP (18-fold), N-acetyl-glutamine (NAcGLN, 8.1-fold) and inosine (7.7-fold). Lower signal responses were observed for IBB10B05 in metabolites pools of lysine (LYS, 176-fold), CDP-ethanolamine (57-fold), cytidine (48-fold), xanthine (27-fold), UMP (16-fold), uracil (15-fold), dAMP (11-fold), citrulline (10-fold), ornithine (8.5-fold) and CMP (8.4-fold).

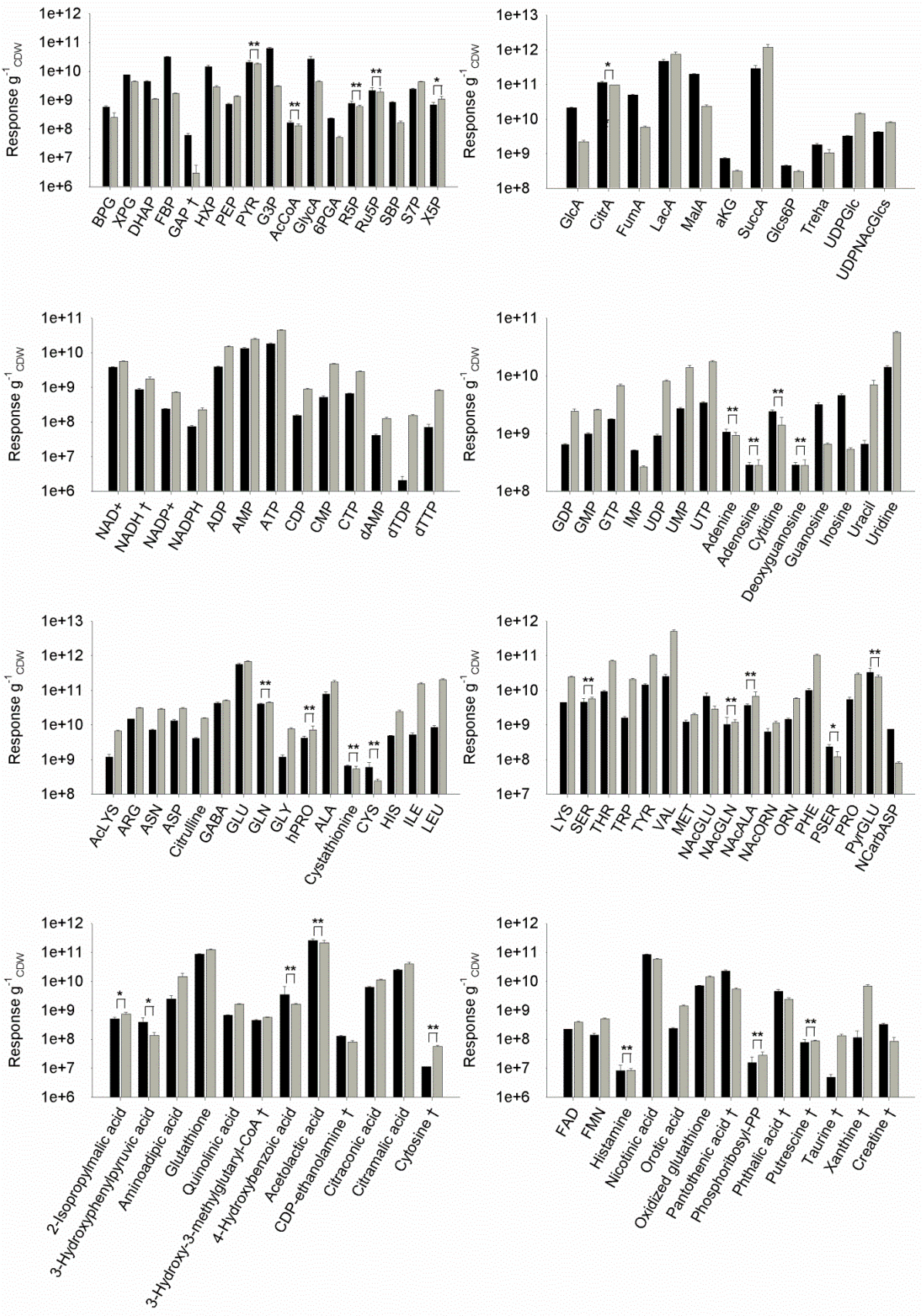

Figure 6-10: Semi-quantitatve comparison of metabolite pools in *C. tenuis* and BP000. Metabolite response per g_{CDW} of *C. tenuis* (black, F1, 24h) and BP000 (grey, F3, 24h), * p value < 0.05 and > 0.01, ** p value > 0.05, unmarked pairs represent significant differences (p value < 0.01); "†" marks metabolite responses based on ^{12}C signals.

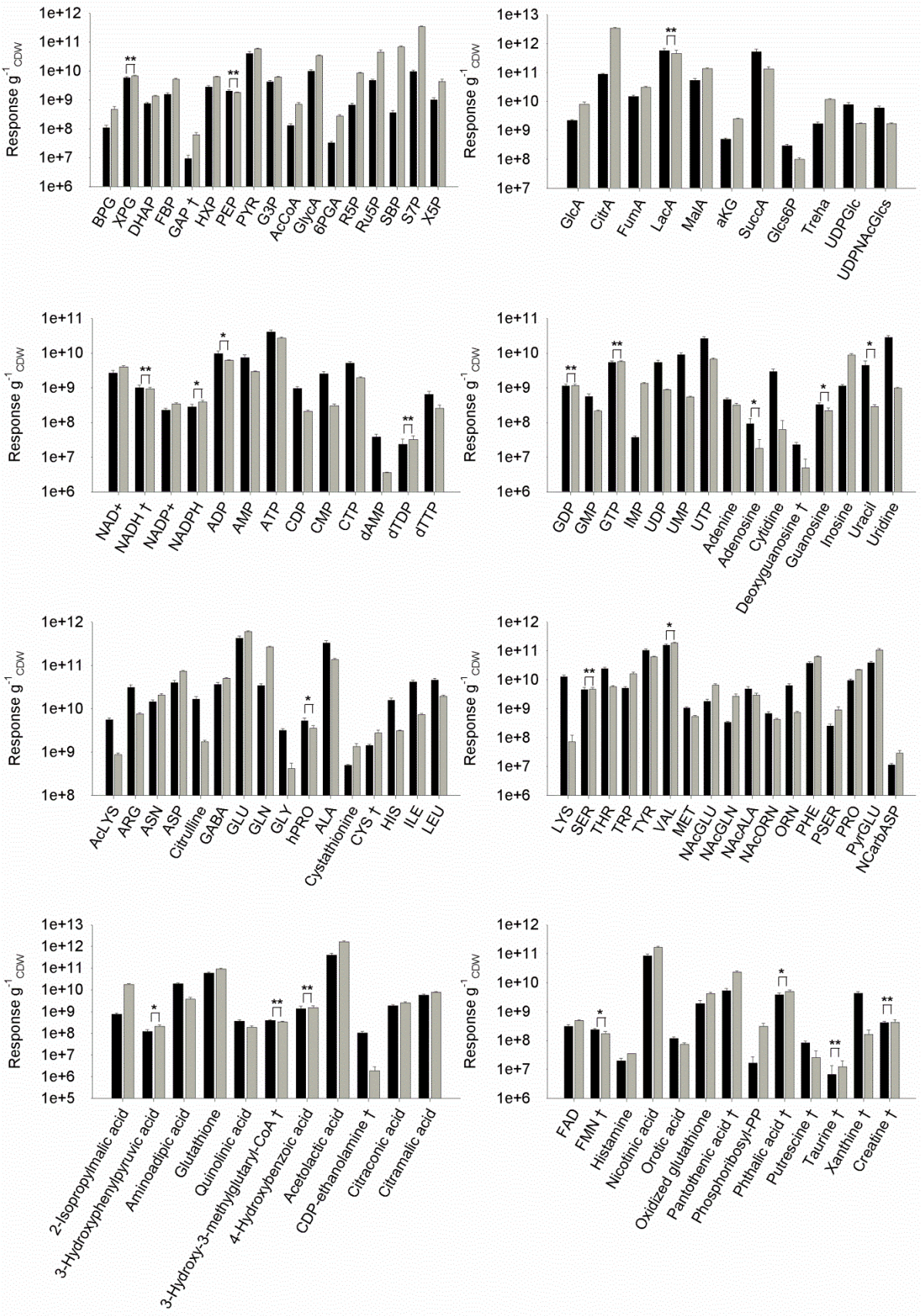

Figure 6-11: Semi-quantitatve comparison of metabolite pools in BP10001 and IBB10B05. Metabolite response per gCDW of BP10001 (black, F6, 24h) and IBB10B05 (grey, F8, phase I), * p value < 0.05 and > 0.01, ** p value > 0.05, unmarked pairs represent significant differences (p value < 0.01); "†" marks metabolite responses based on ^{12}C signals.

7 Discussion

7.1 LC/MS-based quantitative yeast metabolomics

Unbiased determination of intracellular metabolite concentrations using LC/MS as analytical platform necessitates a number of considerations and precautions to be borne in mind with respect to sample preparation and standardization [19], [67]. This work focused on the quantification of intracellular metabolites extracted from natural and recombinant yeasts cultivated under defined physiological and process conditions. Although a sample preparation protocol was available and established at the I.B.B. [14] it was not clear at the beginning of the master thesis whether this procedure would produce metabolite extracts suited for quantitative analysis by the new LC/MS system earmarked for these studies. Important factors such as the sample matrix, media components, the temperature-time profile of the quenching and metabolite extraction steps, as well as the quality of the internal standard and the type of standardization were studied. Results obtained in these studies will be discussed in the following sections.

7.1.1 Sample matrix affecting LC/MS

It is known from the literature that residues of the medium, the quenching and/or extraction solutions present in metabolite samples but also cellular components can affect the elution profile and the MS signals which at the worst can lead to a complete loss of certain m/z signals or even of m/z ranges ([67], Figure 3). These so-called matrix effects are caused by co-eluting compounds. In this work the P_i and S_i (data not shown for S_i) concentration of the cultivation media was identified as strong inhibiting factor for the used LC/MS platform. In particular the MS intensity of HXPs, as they elute close to the P_i peak, were suppressed in dependency of the P_i concentration. Similar observations have been reported by other research groups [68]. ESI performance is very sensitive to high metabolite concentrations [69]. Even for very polar “ESI-appropriate” analytes the rough linearity of the signal response is often lost at high concentrations (> 10 µM). A competition for either charge or space in the ionisation process between the analyte and co-eluting matrix components can lead to saturation, which in turn can result in a complete mask of the analyte (ion suppression) [26]. Further it was clearly observeable that the chroamtographic separation efficiency was reduced in samples including an higher amount of matrix compounds. The reason underlying this

effect, higher P_i concentration (as measured) and/or other matrix compounds, could not be isolated clearly in this work. A accurate clarification requires subsequent experiments.
Definitely an adequate sample preparation is essential to overcome these effects, which begins with the cultivation step. In the following section the adaption of the cultivation media, as a consequence of the observed interferring P_i and S_i concentrations in the LC/MS samples, is described.

7.1.1.1 Adapting yeast cultivation medium for LC/MS metabolomics

Compound-specific chromatograms and mass spectrums of metabolite samples prepared from cells grown on standard mineral medium showed strong deviations from those obtained for purchased "pure" standard compound mixtures. In particular those metabolites co-eluting with P_i were negatively influenced as described in the previous section. Common mineral media for yeast cultivation contain > 100 mM of P_i and ~40 mM of S_i [48], [54] to (i) avoid nutrient limitation and (ii) maintain a constant pH over the time of fermentation. In this work it was demonstraded that P_i had an enormous carry-over throughout the sample workup and interfered strongly in the subsequent LC/MS analysis.
Because P_i and S_i are biomass components a minimum level of either of these compounds must be present in the medium to support biomass formation. Based on the biomass composition reported for *S. cerevisiae* grown aerobically on glucose [70] a minimum concentration of 0.23 mmol L^{-1} for P_i (~0.03 g L^{-1} KH_2PO_4) and 0.04 mmol L^{-1} for S_i (~0.01 g L^{-1} $MgSO_4x7H_2O$) can be calculated which should be sufficient to support cell growth up to a cell density of 3.0 (OD_{600}). In this context different mineral media compositions in which the amount of KH_2PO_4 and $MgSO_4x7H_2O$ / $(NH4)_2SO_4$ were testet. It turned out that concentrations of P_i and S_i can be safely reduced by a factor of 57.6 and 19.7, respectively, without affecting the specific growth rate of *S. cerevisiae* up to a cell density of 3.0 (OD_{600}). The identified concentrations of 0.25 g L^{-1} (= 1.8 mM P_i) for KH_2PO_4 and 0.5 g L^{-1} (= 2 mM S_i) for $MgSO_4x7H_2O$ (avoiding $(NH_4)_2SO_4$ as S_i source) are well below concentration levels strongly affecting LC/MS analytics (> 1 mM).
Despite the successful reduction of two key components interfering with LC/MS analysis, matrix effects still remained an issue in terms of the LC/MS analysis quality of biological samples, in particular when compared to samples containing pure compounds. Further substantial improvements concerning matrix reduction are connected to the subsequent

sample work-up. Based on established work-up protocols [14], [27], [34], the improvements which were carried out in this work are shortly discussed below.

7.1.1.2 Reducing matrix effect by modifying the sample work-up procedure

Beside the media composition the sample work-up, in particular the quenching step represents another potential target to reduce matrix compounds. Along the workflow of the quenching step two events are of relevance in this regard. First the medium is diluted by the quenching solution and second the medium is separated from the cells by decanting. Consequently increasing the dilution factor or adding an additional washing step and decanting as quantitative as possible should be suitable approaches to reduce the content of interfering components. Based on these hypotheses studies were performed to analyse how the volume ratio of SV-to-QS and how additional washing steps affect the content of residual P_i in the LC/MS samples. The study was based on the CM quenching protocol (pure MeOH, -80°C) according to *Canelas et al. (2008)* [27] as this protocol is widely accepted in the scientific community. Cell leakage has been well investigated for *S. cerevisiae* by this group and advantages over other methods in for example handling and the immediate stopping of metabolic activity have been discussed [27], [28]. Hence the goal was to adapt the CM method in order to satisfy sensitivity demands of the LC/MS analytics used.

At the best the immediate stopping of the cell metabolism is accompanied by a proper dilution and a subsequent removal of salt components of the media and other biological matrices. As it was shown in this work unwanted compounds could outlast this step. In case of P_i a significant precipitation of P_i salts was observed right after transferring the biological sample to the quenching solution, resulting in a significant (40-100 %) carry-over of P_i into the LC/MS samples due to different solubility of P_i in the QS (practical insoluble, [64]) and the ES (good solubility). The P_i concentration in the LC/MS sample was affirmed via Saheki assay [63]. Neither variation in the QS-to-SV ratio nor additional washing with QS led to the expected reduction of the P_i level in the LC/MS samples. Even though a washing step proved practically in reduction of P_i (2-fold), it was not adequate to justify the by far longer exposure to the QS which represents a risky stage in terms of metabolite leakage. Significant metabolite leakages were reported for bacteria [23], [29], [71] and more controversially for yeast [8], [27], [32], [35]. On the other hand, the reduction of P_i through the washing step may be explained by the decanting P_i salt precipitate. This was implied by the controversial P_i concentrations determined for the different work-up procedures.

7.1.2 Improving the production of ^{13}C-labeled metabolite extract for internal standardization

The usage of ISTD is indispensable for accurate LC/MS-based quantification in biological matrices [20], [26]. Sample matrices and therefore metabolite-specific signals differ a lot and are not comparable between biological samples and CS. Referring to an ISTD, in contrast, corrects for overloading and matrix effects and hence exclusively enables absolute quantification of intracellular metabolites [67], [69].

In this work the standard protocol for ISTD preparation routinely used at the I.B.B. was improved. The substrate-specific metabolite yield was increased while the amount of residual ^{13}C-glucose in the fermentation broth was minimized without altering the quality of the ISTD by shifting the harvesting time to the late exponential growth phase. LC/MS interfering mineral media salts were reduced (KH_2PO_4) or substituted ($(NH_4)_2SO_4$ by NH_4Cl). Inert gas (N_2) was used to deflate the ethanolic fraction of the ^{13}C-labeled yeast extract and concentrate (factor 10-15) at RT to prevent potential metabolite degradation. Within one and a half day a ready-to-use ^{13}C-labeled yeast extract sufficient for standardization of 600 to 1200 samples could be produced with the new protocol.

Although the preparation protocol of ISTD could be markedly improved the ISTD matrix still affected signal yields in biological samples for HXPs (no clear chromatographic separation) and OxalA (not detectable when ISTD was applied). In the worst case low concentrated metabolites (see following section) were completely masked. To overcome that circumstance it is mandatory to develop preparation methods which particularly address the reduction of biological matrices and salt components. The established protocol should serve as groundwork for further improvements and the upscaling of ISTD production.

7.1.2.1 ISTD matrix impact on the standard calibration

To estimate the applicability of the produced ISTD in terms of matrix impact on the standard calibration an internal and an external approach were compared. While the internal approach, additionally to the calibration standards, included ^{13}C-labeled yeast extract, the external approach should provide MS signals unbiased from the biological matrix.

This was obvious in the comparison of the calibration linearity ranges which showed a lower limit of calibration for the external calibration approach for many metabolites (AMP, ASN, ASP, DHAP, GLN, GLU, αKG, PEP, R5P, Treha) despite of the same upper limits of

calibration. This resulted in higher linearity ranges. There could be some reasons for that. First, lower limits of calibration indicate higher chemical background evoked by the ISTDs matrix which result in lower sensitivity of the MS analysis [67]. Second, low and therefore highly variable ^{13}C- signals of the ISTD could contort the linearity of the internal approach (NADH, NADPH, Treha). Third, the double logarithmic presentation facilitated to reach the linearity criteria [72] (especially at high concentrations of the external approach (ESI saturation [69]), as described for MalA in the results section (see Figure 6-6)). And forth, the calibration standards were measured consecutively from the lowest to the highest concentration which masked possible degradation effects that otherwise were only compensated by internal calibration.

7.1.3 Temperature-time dependencies of critical steps in the workflow of the sample preparation

Turnover rates of intracellular metabolites can be very high in *S. cerevisiae* [73]–[75]. Consequently for recording of representative metabolite profiles it is important to stop cell metabolism immediately during the harvesting process and sustain this metabolic state throughout the further sample work. For yeasts this can be accomplished by quenching of the metabolism at low temperatures. Typically a defined volume (1 mL) of yeast cells (25-30°C depending on the yeasts cultivation temperature) is rapidly transferred by pipetting into 4 mL of a precooled quenching solution (-80°C, 100 % methanol). Further workup involves separation of cells from medium by centrifugation that must be again carried out at low temperatures (a temperature of < -10-20°C is recommended [27], [31], [32]) to preclude changes in the metabolite levels due to cell activity within the still intact cells. Metabolites are then extracted from the cells at high temperatures (80°C using boiling ethanol broadly accepted [34], [35], [76]). Experimentally this is accomplished by transferring a pre-warmed extraction solution to deep-frozen cells (-80°C) and incubation of the resultant suspension for 3 min at 80°C. Although this protocol is widely used for yeasts little is known about the temperature-time dependency of each of these key process steps and whether cells are exposed to critical temperatures where metabolic activity may adulterate the metabolite composition when the cell sample is transferred between extreme temperatures. In this work the focus laid on the sample workup sequence from quenching up to metabolite extraction. The range 10-50°C was defined as critical temperature region in which substantial metabolic activity was assumed. Comparable studies are yet not reported in literature.

While the temperature of the QS could be hold below -20 °C throughout the quenching and centrifugation step (when 50 mL tubes were used) the most critical step in terms of potential enzyme activity occurred during the extraction step. For the standard BE protocol the samples were in a temperature range of potential enzyme activities for 35-45 sec. Straight that time frame must be prevented or at least minimized as the complete cell destruction, metabolite release and the accompanied enzyme inactivation occur at high temperatures (> 60 °C) [35].

As a result of simple handling mistakes (e.g. pouring the BE via the cold tube wall on the pellet) the time between 10 °C and 50 °C could extend up to 45 -35 seconds and the time between 5 °C and 60 °C even up to 60 and 65 seconds for the tested BE volumes of 1.5 mL and 10 mL, respectively. Within these time frames enzymes could adulterate real intracellular metabolite pools of *in-vivo* conditions. Therefore it is of enormous importance to prevent a substantial decrease of BE temperature by wrong handling and ensure a rapid temperature rise of above 60 °C in the cell pellet.

In this work the protocol was adapted by preheating the tube with the frozen cell pellet (on dry ice) in the WB for a split second prior to the BE addition. So the time of potential enzyme activity could be minimized in a range of a few seconds, for BE addition of 1.5 mL with an immediate temperature rise above 50 °C. For 10 mL BE addition an immediate temperature rise in the range of 60 °C to 70 °C could be reached. This resulted in an increase of the real extraction time above 60 °C of 33 % and 57 % for 1.5 mL and 10 mL BE, respectively, within the 3 minutes of incubation in the water bath (~90 °C). The extraction time above 70 °C could even be increased by 87 % and 129 %, respectively.

7.2 Limitations of semi-quantitative metabolite data in biological interpretation

The majority of metabolomics studies are based on untargeted or on semi-quantitative metabolite data originated from peak areas or heights, which enables direct comparison of relative changes of metabolite responses in similar samples. Comprehensive MS and MS/MS metabolite data can be found in respective databases [77], [78] and literature [12], [68], [72], suitable for target identification without applying appropriate standards. This simplifies the applicability of MS-based approaches as the availability of adequate standard compounds is low and the costs are high.

The LC/MS method used in this work covers chemically and structurally diverse metabolites of the central carbon metabolism. Due to the ESI´s ionization mechanism the MS responses are prone to the molecule characteristics, the retention time of the analyte and the associated eluent flow rate and gradient [79], [80]. As a consequence equally concentrated but

chemically diverse metabolites can significantly differ in their MS signals (see Figure 6-9). This effect can be dramatically and could intensify in biological samples as additional matrix effects occur. Hence semi-quantitative data are not suited in the determination of energy charges (ECs), anabolic/catabolic reduction charges and for thermodynamic investigations.
Further, fold changes of metabolite responses must be considered cautiously as they need not correlate with fold changes of metabolite concentrations. As for chemical diverse molecules background signals in the MS differ a lot. For example even blank signals often excess background signals of the biological sample as matrix effects occur rarely. A simple substraction of blank signals leads to incorrect responses.
In conclusion a valid estimation or comparison of normalized MS responses is limited to the same molecule species across biological samples, provided that an accurate internal standard serves as anchor.

7.3 Xylose fermentation by natural and recombinant yeasts

The investigated *C. tenuis* strain CBS4435 can be ranked among the best xylose-to-ethanol fermenting native yeasts [81]. This is demonstrated by the key process parameters obtained in this work which are in good agreement with a former physiological study [54]. Relative to its recombinant opponent BP000 (0.07 g g^{-1}_{CDW} h^{-1} at 30 °C) *C. tenuis* (0.1 g g^{-1}_{CDW} h^{-1} at 25 °C) showed a 1.4-fold higher q_{xylose}. Analysis of specific activities of enzymes constituting the xylose assimilation pathways indicated that *C. tenuis* has a 12 ±6-fold higher specific XR activity (0.66 ±0.04 µmol min^{-1} mg^{-1}; 0.07 ±0.03 µmol min^{-1} mg^{-1} for BP000) while XDH and XK showed comparable specific activities (XDH: 0.39 ±0.04 µmol min^{-1} mg^{-1} for *C. tenuis*; 0.3 ±0.1 µmol min^{-1} mg^{-1} for BP000; XK: 1.2 ±0.1 µmol min^{-1} mg^{-1} for *C. tenuis*; 1.1 ±0.2 µmol min^{-1} mg^{-1} for BP000). The natural xylose assimilating yeast *Scheffersomyces stipitis* showed a similar XR-to-XDH ratio (> 1) [82] as determined for *C. tenuis* (1.7 ±0.3 accompanied by low $Y_{xylitol}$ (~0.1 g g^{-1}) and high $Y_{ethanol}$ (~0.4 g g^{-1} [54]). This is in contrast to former studies [83], [84] where an inverse activity ratio of XR-to-XDH in recombinant yeast strains was suggested to keep $Y_{xylitol}$ low. Reasons for that, controversially to the model conceptions, are not known yet. On the other hand the inverse XR-to-XDH ratio of 0.3 ±0.2 in BP000 led to high $Y_{xylitol}$ (~0.4 g g^{-1}) and low $Y_{ethanol}$ (~0.24 g g^{-1}[43]). This phenotype was associated to the reduced xylose uptake and lower enzyme activity levels in the consecutive pathways of XA [84], and the unbalanced coenzyme usage between XR and XDH in BP000 [51]. Based on the data obtained in the enzyme activity study a reasonable correlation between $Y_{ethanol}$ and enzyme activities cannot be made. Substantial differences which explain

the observed phenotypes should be obvious on the metabolite level. In the following section the results of the metabolite analysis carried out in this work are discussed.

7.3.1 Intracellular metabolite pattern of xylose metabolization

Now, as there is still no explanation for the low $Y_{ethanol}$ in recombinant *S. cerevisiae* strains compared to *C. tenuis*, targeted metabolomics was used to identify factors responsible for that. As both strains express the same xylose assimilation network differences in the metabolite levels should indicate points of different flux control.

The yeast physiology is clearly represented in the adenylate energy charge (AEC) for starving (~0.1 [85]), metabolizing (~0.7 [14]) and growing (~0.8-0,9 [14], [85]) state. Exemplified by an AEC of ~0.7 both strains showed a clear "metabolizing" state after 24 h of xylose fermentation. Actually for *C. tenuis* an AEC of ~0.8 was reached after 48 h of fermentation (attributed to lower AMP and higher ATP levels accompanied by a constant AXP concentration), while no change was observed for BP000. The AEC enhancement in *C. tenuis* was also observed in the guanylate energy charge (GEC) which changed from 0.66 to 0.76. This confirmed that the nucleoside diphosphokinase reactions can be assumed to be equilibrated. Furthermore AEC and GEC suggest a better physiological adaption of *C. tenuis* compared to BP000 to xylose as carbon source. Alternatively an additional consumption of produced ethanol could lead to the observed EC increase.

The more efficient substrate conversion of *C. tenuis* and its adaption to the substrate over time was also reflected in the metabolite pools of the central carbon metabolism. Considering metabolic fluxes (see Figure 7-1 [86]) it was obvious that in *C. tenuis* 88 % of xylose were reduced by NADH usage while in BP000 only 65 % were reduced by NADH usage of XR. This assisted the assumption that a lower $Y_{xylitol}$ and higher $Y_{ethanol}$ is directly linked to the more balanced coenzyme household [14], [87] in *C. tenuis*. Further the more efficient ethanol production came along with a lower flux (2.2-fold relative to q_{xylose}) through the oxidative PPP (oPPP), as it was present in *C. tenuis*. Furthermore the carbon flux towards the oPPP was ~3-fold higher relative to the carbon entering glycolysis at the F6P node in the xylitol producer BP000. This suggests that F6P represents a critical node in xylose metabolism either towards ethanol or xylitol production.

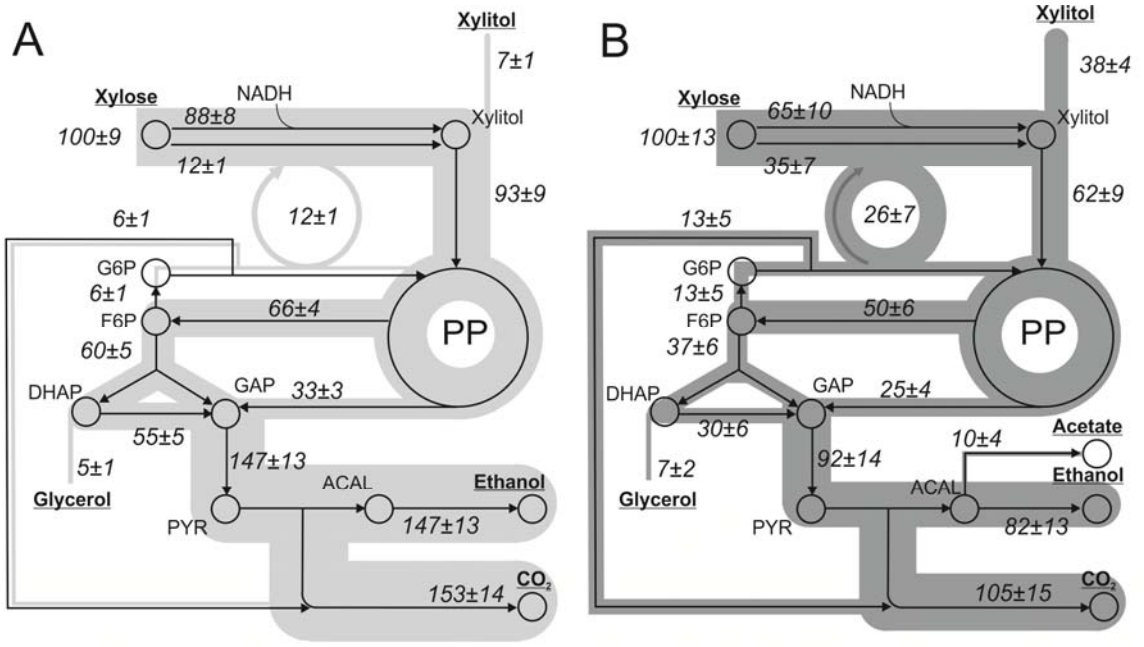

Figure 7-1: Metabolic flux maps of xylose-to-ethanol fermentation for *C. tenuis* (A) and BP000 (B). The figure was prepared for Ref. [86], provided by Mario Klimacek. External metabolites are underlined and relative fluxes normalized to qxylose (0.67 mmol g-1CDW h-1 for C. tenuis and of 0.47 mmol g-1CDW h-1 for BP000) are shown. Averages and respective standard deviations are shown.

FBP, HXP and DHAP were substantially higher in *C. tenuis*, an effect that intensified with fermentation time. These higher metabolite levels fit perfectly to the determined higher flux through the upper (UG) and lower glycolysis (LG) [14]. Higher levels of reactants of phosphofructokinase (PFK) reaction, F6P included in the HXP pool (~5-fold) and FBP (~20-fold), indicated a significantly higher PFK activity which is known as a key regulatory point in glycolysis [88]. These results may indicate that F6P, similar to the PFK from *S. cerevisiae*, regulates the PFK activity allosterically in *C. tenuis* [14]. Additionally high levels of metabolites of the UG, in particular FBP and HXP, play an important role in the activation of enzymes of the LG [89], [90]. One of these important enzymes could be pyruvate kinase (PYK) which was shown to be directly linked to ATP (EC) generation and the production of ethanol in *S. cerevisiae* [89]. G6P and F6P were required for induction and FBP for the enzymes activation. Both reactions could be inhibited by high ATP levels. ATP levels, similar to AMP and ADP, were 2- to 3-fold lower in *C. tenuis*.

Beside the main route of NADH reoxidation via formation of ethanol the metabolite data suggested an enhanced alternative through the reduction of DHAP to G3P by G3PDH, which was shown in > 20-fold higher G3P levels in *C. tenuis*. In this case a decreased glycerol excretion and/or a low activity of glycerol 3-phosphatase (GPP (EC 3.1.3.21)), the enzyme responsible for glycerol generation from G3P, could be possible reasons for that. An absent,

or at least low, activity of GPP could lead to a pathway blocking effect [91] which could shift the carbon flux towards ethanol production. In another attempt blocking the glycerol pathway by deletion of *GPD1* and *GPD2*, the isogenes encoding GPDH, in *S. cerevisiae,* did not lead to an enhanced ethanol yield. Moreover the carbon flux was redirected to xylitol production [92]. Therefore it is conceivable that a main difference between *C. tenuis* and BP000 is due to this route.

Another explanation which could play an important role in balancing the redox cofactors can be linked to the reversibility of the G3PDH reaction and the possible reaction of glycerol to dihydroxyacetone (glycerol DH (EC 1.1.1.156), NADPH usage) and back to DHAP (dihydroxyacetone kinase (EC 2.7.1.29, ATP usage), as entering point into glycolysis [93]. This hypothesis requires a reduced glycerol excretion.

Interestingly, the catabolic reduction charge (CRC) and the anabolic reduction charge (ARC) in *C. tenuis* increased with fermentation time (24 h to 48 h), from 0.29 to 0.36 (CRC) and from 0.37 to 0.43 (ARC). This was attributed to enhanced NADPH (~1.3-fold), NAD^+ (1.3- to 1.5-fold) and NADH (1.5-to 1.6-fold) levels. In contrast CRC (~0.4) and ARC (~0.33) remained constant in BP000 over time. The increase in AcCoA pools together with the observed increase in metabolite levels of the PPP (R5P, Ru5P) can be directly linked to differences in biosynthetic pathways in *C. tenuis* with longer fermentation time. Reasons for that are not known at this point.

Thermodynamic determinations based on the quantified metabolites clearly pointed the reactions of PFK, PYK, G3PDH and G6PDH-lactonase as key regulated in the CCM of both strains, which is in perfect agreement to findings in literature [14], [92], [94]. ΔGG values (kJ mol^{-1}) in the range of -12 to -15 (PFK, PYK), -20 to -25 (G3PDH) and -38 (G6PDH-lactonase) suggested a regulatory function by that enzymes or flux control. In contrast ΔGG values close to zero implied that enzymes operated close to equilibria with a high enzymatic activity compared to the flux through the reaction [14], [95]. Conclusively the thermodynamic analysis led to no substantial differences between the observed strains. This was assumed and confirmed the similarity of xylose metabolization in both strains.

From the semi-quantitative data it was clearly observable that amino acids ILE, LEU, VAL, TYR, THR, PHE and TRP were significantly lower in their MS response in *C. tenuis* compared to BP000 (30- to 7-fold). Reasons for that are not known yet and demand further investigations. Differences in biosynthetic pathways are suggested by higher responses for SBP (PPP), inosine and guanosine (nucleotide synthesis) in *C. tenuis* compared to BP000.

7.4 Comparing metabolizing and growing phenotypes

Effective conversion of lignocellulosic feedstock to ethanol requires anaerobic growth on xylose, as $Y_{ethanol}$ increases with enhanced μ [49]. A prerequisite the evolutionary engineered strain IBB10B05, contrary to its recombinant progenitor BP10001, fulfils. Contrary to BP10001, IBB10B05 showed a biphasic formation of glycerol and xylitol associated to different growth phases. Phase I was glycerol-dominated with a lower μ of 0.015-0.019 h^{-1} and phase II xylitol-dominated with a μ of ~0.027 h^{-1}. An evidence based explanation for the lower μ is not known yet. Product yields and q_{xylose} of BP10001 were in the range of BP000 with the exception of $Y_{xylitol}$ (~0.3 g g^{-1} compared to ~0.4 g g^{-1} in BP000), whereas IBB10B05 showed growth phase dependent 5- to 7-fold higher q_{xylose}, 2- to 6-fold lower $Y_{xylitol}$ and 1- to 4-fold higher $Y_{glycerol}$. $Y_{acetate}$ differed from equal (phase I) to 2-fold lower (phase II) values in IBB10B05. In particular, the higher q_{xylose} correlated perfectly with the specific enzyme activities of the XA-pathway. XR activity was 12- to 19-fold higher in IBB10B05 relative to BP10001, while XDH showed 1.3- to 2.4-fold and XK 1.2- to 1.8-fold higher specific activity.

The biphasic growth of IBB10B05 was known from former studies [49], [56]. The apparent differences in μ (> 50 % lower values for μ were obtained in this study) are most likely due to differences in the cultivation (pH regulation, closed/open reaction conditions). The transition from glycerol to xylitol as characteristic fermentation product was ascribed to CO_2/HCO_3^- accumulation which possibly regulates the xylose metabolism [49]. This hypothesis can be adapted to this study although the bioreactors were permanently sparged with N_2 and hence the produced CO_2 should be discharged. Carefully a possible reason could be the bioreactor setup. Wet gas outlet filters could have produced a backpressure which could have raised the amount of soluble CO_2 in the cell suspension. The glycerol route as NADH regeneration trait could slow down, the redox imbalance could increase and the xylitol production could intensify as a result redox imbalance.

7.4.1 Metabolomic profile of growth on xylose

In agreement with other studies [14], [38] showing a positive correlation between carbon flux through glycolysis and metabolite pools, measured UG intermediates were substantially higher (2- to 4-fold) in the growing strain compared to BP10001, which perfectly fit to the observed higher q_{xylose}. In general differences intensified in growth phase II which can be directly linked to the increase of μ. Biggest effects in the central carbon metabolism were

obvious in the PPP where metabolite levels were 3- to 20-fold higher in IBB10B05. That was in line with the general notion for the growing strain, as PPP is essential for the cells anabolism [88]. Also metabolites of the TCA (CitrA (up to ~150-fold), αKG, MalA, FumA) and amino acids produced from TCA intermediates (GLN, ASP, ASN, GLU) were significantly higher, which is another growth indicator. At the same time the AcCoA pool, an essential precursor in fatty acid synthesis, was ~3-fold larger.

The switch from glycerol to xylitol formation is clearly presented in the glycerol route. G3P, an intermediate in glycerol production, was lowered ~2-fold in phase II. The so induced redox imbalance is presumably reduced by increased NADH usage of XR [49]. The level of PPP metabolites, especially 6PG was factor ~5 higher concentrated in phase II, which suggests an increased flux through this pathway. The amino acid pools clearly accumulated 2.7-fold (GLN) and 1.8-fold (ASP, GLN) in phase II. In summary the determined metabolite pools together with the higher μ point to a higher biosynthetic flux in the xylitol-dominated phase of IBB10B05.

ECs in BP10001 (AEC ~0.83, GEC ~0.84) and IBB10B05 (AEC ~0.86, GEC ~0.86) were high and independent from fermentation time and growth phase, and similar to values found for *S. cerevisiae* strains growing on glucose under anaerobic conditions [14]. This implies good adaption of both strains on the substrate xylose and constant ATP generation. CRCs varied in BP10001 from 0.33 to 0.44 and in IBB10B05 from 0.23 to 0.38. This was attributed to weak and hence strongly varying signals for NADH in the LCMS analysis. In contrast, the ARCs showed high values in the range of 0.54 to 0.67 (BP10001) and 0.58 to 0.62 (IBB10B05). Low CRCs and high ARCs were expected in both strains, as they use the same NADH-preferring XR. Though, it was surprising that BP10001 showed only minor differences to its growing descendent according to the mentioned parameters. Perhaps a circumstance that point out how close BP10001 is away from growing on xylose anaerobically.

Beside the quantitative analysis the semi-quantitative data emphasized the higher flux through the PPP underlying the increased biosynthesis activity. SBP and S7P, intermediates of the PPP, were 186- and 36-fold higher in IBB10B05. PRPP, an activated compound used in nucleotide and histidine synthesis formed from R5P [96], was 18-fold higher in the growing strain. Additionally inosine (7.7-fold), as precursor of RNA nucleotides, was significantly increased.

8 Conclusion

In this study a LC/MS-based targeted metabolomics approach was implemented with which a broad range of chemically diverse intermediates of the CCM, redox, energy and amino acid metabolism of yeast can be determined. Of the 114 metabolites analysed semi-quantitatively 34 were quantified using an internal calibrations approach. This work demonstrates that the composition of the cultivation medium as well as the ratio of SV to QS and the time point of ethanol addition during metabolite extraction are important parameters to be considered before a metabolome experiment is carried out. The preparation of ^{13}C-labeled yeast extract was markedly improved in terms of production time and costs. Anyway, despite considerable improvements, matrix effects still negatively influence the analytical robustness of the LC/MS method used. Separation problems and carry-over effects remain an issue to be focused in following studies.

Targeted metabolomics was applied to xylose-utilizing recombinant *S. cerevisiae* strains and *C. tenuis* and revealed pathways that contribute to (i) efficient xylose-to-ethanol conversion and (ii) anaerobic growth on xylose. F6P was identified as critical regulation node in the central carbon metabolism towards efficient high yield ethanol production of *C. tenuis* compared to BP000. Suggested by the observed G3P pools the glycerol route most likely plays an important role in this context. Further investigations should clarify the underlying mechanisms.

9 References

[1] G. J. Patti, O. Yanes, and G. Siuzdak, “Metabolomics: the apogee of the omics trilogy,” *Nat. Rev.*, vol. 13, no. Molecular Cell Biology, p. 7, 2012.

[2] S. G. Oliver, M. K. Winson, D. B. Kell, and F. Baganz, “Systematic functional analysis of the yeast genome.,” *Trends Biotechnol.*, vol. 16, no. 9, pp. 373–8, Sep. 1998.

[3] H. Tweeddale, L. Notley-McRobb, and T. Ferenci, “Effect of slow growth on metabolism of Escherichia coli, as revealed by global metabolite pool (‘metabolome’) analysis.,” *J. Bacteriol.*, vol. 180, no. 19, pp. 5109–16, Oct. 1998.

[4] M. R. Mashego, K. Rumbold, M. De Mey, E. Vandamme, W. Soetaert, and J. J. Heijnen, “Microbial metabolomics: past, present and future methodologies.,” *Biotechnol. Lett.*, vol. 29, no. 1, pp. 1–16, Jan. 2007.

[5] M. S. Andersen, Å. Rinnan, C. Manach, S. K. Poulsen, E. Pujos-guillot, T. M. Larsen, A. Astrup, and L. O. Dragsted, “Untargeted Metabolomics as a Screening Tool for Estimating Compliance to a Dietary Pattern,” 2013.

[6] O. Fiehn, “Metabolomics--the link between genotypes and phenotypes.,” *Plant Mol. Biol.*, vol. 48, no. 1–2, pp. 155–71, Jan. 2002.

[7] M. Oldiges, S. Lütz, S. Pflug, K. Schroer, N. Stein, and C. Wiendahl, “Metabolomics: current state and evolving methodologies and tools.,” *Appl. Microbiol. Biotechnol.*, vol. 76, no. 3, pp. 495–511, Sep. 2007.

[8] S. G. Villas-Bôas, J. Højer-Pedersen, M. Akesson, J. Smedsgaard, and J. Nielsen, “Global metabolite analysis of yeast: evaluation of sample preparation methods.,” *Yeast*, vol. 22, no. 14, pp. 1155–69, Oct. 2005.

[9] S. G. Villas-Bôas, J. F. Moxley, M. Akesson, G. Stephanopoulos, and J. Nielsen, “High-throughput metabolic state analysis : the missing link in integrated functional genomics of yeasts,” vol. 677, pp. 669–677, 2005.

[10] S. B. Milne, T. P. Mathews, D. S. Myers, P. T. Ivanova, and H. A. Brown, “Sum of the parts: mass spectrometry-based metabolomics.,” *Biochemistry*, vol. 52, no. 22, pp. 3829–40, Jun. 2013.

[11] D. L. Haviland, “Mass Spectrometry for Metabolomics,” *Genet. Eng. Biotechnol. News*, vol. 27, no. 11, Jun. 2007.

[12] W. Lu, E. Kimball, and J. D. Rabinowitz, “A high-performance liquid chromatography-tandem mass spectrometry method for quantitation of nitrogen-containing intracellular metabolites.,” *J. Am. Soc. Mass Spectrom.*, vol. 17, no. 1, pp. 37–50, Jan. 2006.

[13] J. M. Buescher, S. Moco, U. Sauer, and N. Zamboni, “Ultrahigh performance liquid chromatography-tandem mass spectrometry method for fast and robust quantification of anionic and aromatic metabolites.,” *Anal. Chem.*, vol. 82, no. 11, pp. 4403–12, Jun. 2010.

[14] M. Klimacek, S. Krahulec, U. Sauer, and B. Nidetzky, “Limitations in xylose-fermenting Saccharomyces cerevisiae, made evident through comprehensive metabolite profiling and thermodynamic analysis.,” *Appl. Environ. Microbiol.*, vol. 76, no. 22, pp. 7566–74, Nov. 2010.

[15] W. Lu, M. F. Clasquin, E. Melamud, D. Amador-Noguez, A. a Caudy, and J. D. Rabinowitz, “Metabolomic analysis via reversed-phase ion-pairing liquid chromatography coupled to a stand alone orbitrap mass spectrometer.,” *Anal. Chem.*, vol. 82, no. 8, pp. 3212–21, Apr. 2010.

[16] J. M. Büscher, D. Czernik, J. C. Ewald, U. Sauer, and N. Zamboni, “Cross-platform comparison of methods for quantitative metabolomics of primary metabolism.,” *Anal. Chem.*, vol. 81, no. 6, pp. 2135–2143, 2009.

[17] B. Luo, K. Groenke, R. Takors, C. Wandrey, and M. Oldiges, “Simultaneous determination of multiple intracellular metabolites in glycolysis, pentose phosphate pathway and tricarboxylic acid cycle by liquid chromatography-mass spectrometry.,” *J. Chromatogr. A*, vol. 1147, no. 2, pp. 153–64, 2007.

[18] T. M. Annesley, “Ion suppression in mass spectrometry.,” *Clin. Chem.*, vol. 49, no. 7, pp. 1041–4, Jul. 2003.

[19] P. J. Taylor, “Matrix effects: the Achilles heel of quantitative high-performance liquid chromatography-electrospray-tandem mass spectrometry.,” *Clin. Biochem.*, vol. 38, no. 4, pp. 328–34, Apr. 2005.
[20] M. Klimacek, “Quantitative Metabolomics and Its Application in Metabolic Engineering of Microbial Cell Factories Exemplified by the Baker ’ s Yeast,” in *Metabolomics edited by Ute Roessner*, no. Metabolomics, U. Roessner, Ed. Rijeka, Croatia: InTech, 2012, pp. 19–44.
[21] S. Noack and W. Wiechert, “Quantitative metabolomics: a phantom?,” *Trends Biotechnol.*, vol. 32, no. 5, pp. 238–244, Apr. 2014.
[22] W. M. van Gulik, “Fast sampling for quantitative microbial metabolomics.,” *Curr. Opin. Biotechnol.*, vol. 21, no. 1, pp. 27–34, Mar. 2010.
[23] M. Wellerdiek, D. Winterhoff, W. Reule, J. Brandner, and M. Oldiges, “Metabolic quenching of Corynebacterium glutamicum: efficiency of methods and impact of cold shock.,” *Bioprocess Biosyst. Eng.*, vol. 32, no. 5, pp. 581–92, Aug. 2009.
[24] J. Tillack, N. Paczia, K. Nöh, W. Wiechert, and S. Noack, “Error Propagation Analysis for Quantitative Intracellular Metabolomics,” *Metabolites*, vol. 2, no. 4, pp. 1012–1030, Nov. 2012.
[25] M. Yuan, S. B. Breitkopf, X. Yang, and J. M. Asara, “A positive/negative ion-switching, targeted mass spectrometry-based metabolomics platform for bodily fluids, cells, and fresh and fixed tissue.,” *Nat. Protoc.*, vol. 7, no. 5, pp. 872–81, May 2012.
[26] L. L. Jessome and D. A. Volmer, “Ion Suppression : A Major Concern in,” *LCGC*, vol. 24, no. 5, 2006.
[27] A. B. Canelas, C. Ras, A. Pierick, J. C. Dam, J. J. Heijnen, and W. M. Gulik, “Leakage-free rapid quenching technique for yeast metabolomics,” *Metabolomics*, vol. 4, no. 3, pp. 226–239, Jun. 2008.
[28] M. Carnicer, A. B. Canelas, A. Ten Pierick, Z. Zeng, J. van Dam, J. Albiol, P. Ferrer, J. J. Heijnen, and W. van Gulik, “Development of quantitative metabolomics for Pichia pastoris.,” *Metabolomics*, vol. 8, no. 2, pp. 284–298, Apr. 2012.
[29] C. J. Bolten, P. Kiefer, F. Letisse, J.-C. Portais, and C. Wittmann, “Sampling for metabolome analysis of microorganisms.,” *Anal. Chem.*, vol. 79, no. 10, pp. 3843–9, May 2007.
[30] C. J. Bolten and C. Wittmann, “Appropriate sampling for intracellular amino acid analysis in five phylogenetically different yeasts.,” *Biotechnol. Lett.*, vol. 30, no. 11, pp. 1993–2000, Nov. 2008.
[31] W. de Koning and K. van Dam, “A method for the determination of changes of glycolytic metabolites in yeast on a subsecond time scale using extraction at neutral pH.,” *Anal. Biochem.*, vol. 204, no. 1, pp. 118–23, Jul. 1992.
[32] L. P. de Jonge, R. D. Douma, J. J. Heijnen, and W. M. van Gulik, “Optimization of cold methanol quenching for quantitative metabolomics of Penicillium chrysogenum.,” *Metabolomics*, vol. 8, no. 4, pp. 727–735, Aug. 2012.
[33] L. Wu, M. R. Mashego, J. C. van Dam, A. M. Proell, J. L. Vinke, C. Ras, W. a van Winden, W. M. van Gulik, and J. J. Heijnen, “Quantitative analysis of the microbial metabolome by isotope dilution mass spectrometry using uniformly 13C-labeled cell extracts as internal standards.,” *Anal. Biochem.*, vol. 336, no. 2, pp. 164–71, Jan. 2005.
[34] A. B. Canelas, A. Ten Pierick, C. Ras, R. M. Seifar, J. C. van Dam, W. M. Van Gulik, and J. J. Heijnen, “Quantitative evaluation of intracellular metabolite extraction techniques for yeast metabolomics.,” *Anal. Chem.*, vol. 81, no. 17, pp. 7379–7389, Sep. 2009.
[35] B. Gonzalez, J. François, and M. Renaud, “A rapid and reliable method for metabolite extraction in yeast using boiling buffered ethanol.,” *Yeast*, vol. 13, no. 14, pp. 1347–55, Nov. 1997.
[36] R. Prasad Maharjan and T. Ferenci, “Global metabolite analysis: the influence of extraction methodology on metabolome profiles of Escherichia coli,” *Anal. Biochem.*, vol. 313, no. 1, pp. 145–154, Feb. 2003.
[37] J. D. Rabinowitz and E. Kimball, “Acidic acetonitrile for cellular metabolome extraction from Escherichia coli,” *Anal. Chem.*, vol. 79, no. 16, pp. 6167–6173, 2007.
[38] B. Bergdahl, D. Heer, U. Sauer, B. Hahn-Hägerdal, and E. W. van Niel, “Dynamic metabolomics differentiates between carbon and energy starvation in recombinant

Saccharomyces cerevisiae fermenting xylose.," *Biotechnol. Biofuels*, vol. 5, no. 1, p. 34, Jan. 2012.
[39] M. R. Mashego, L. Wu, J. C. Van Dam, C. Ras, J. L. Vinke, W. a Van Winden, W. M. Van Gulik, and J. J. Heijnen, "MIRACLE: mass isotopomer ratio analysis of U-13C-labeled extracts. A new method for accurate quantification of changes in concentrations of intracellular metabolites.," *Biotechnol. Bioeng.*, vol. 85, no. 6, pp. 620–8, Mar. 2004.
[40] G. Sorda, M. Banse, and C. Kemfert, "An overview of biofuel policies across the world," *Energy Policy*, vol. 38, no. 11, pp. 6977–6988, Nov. 2010.
[41] A. Matsushika, H. Inoue, T. Kodaki, and S. Sawayama, "Ethanol production from xylose in engineered Saccharomyces cerevisiae strains: current state and perspectives.," *Appl. Microbiol. Biotechnol.*, vol. 84, no. 1, pp. 37–53, Aug. 2009.
[42] B. Hahn-Hägerdal, K. Karhumaa, C. Fonseca, I. Spencer-Martins, and M. F. Gorwa-Grauslund, "Towards industrial pentose-fermenting yeast strains.," *Appl. Microbiol. Biotechnol.*, vol. 74, no. 5, pp. 937–53, Apr. 2007.
[43] B. Petschacher and B. Nidetzky, "Altering the coenzyme preference of xylose reductase to favor utilization of NADH enhances ethanol yield from xylose in a metabolically engineered strain of Saccharomyces cerevisiae.," *Microb. Cell Fact.*, vol. 7, p. 9, Jan. 2008.
[44] B. C. H. Chu and H. Lee, "Genetic improvement of Saccharomyces cerevisiae for xylose fermentation.," *Biotechnol. Adv.*, vol. 25, no. 5, pp. 425–41, 2007.
[45] K. Karhumaa, R. Garcia Sanchez, B. Hahn-Hägerdal, and M.-F. Gorwa-Grauslund, "Comparison of the xylose reductase-xylitol dehydrogenase and the xylose isomerase pathways for xylose fermentation by recombinant Saccharomyces cerevisiae.," *Microb. Cell Fact.*, vol. 6, p. 5, 2007.
[46] A. A. van Maris, A. Winkler, M. Kuyper, W. A. M. de Laat, J. van Dijken, and J. Pronk, "Development of Efficient Xylose Fermentation in Saccharomyces cerevisiae: Xylose Isomerase as a Key Component," in *Biofuels SE - 57*, vol. 108, L. Olsson, Ed. Springer Berlin Heidelberg, 2007, pp. 179–204.
[47] O. Bengtsson, M. Jeppsson, M. Sonderegger, N. S. Parachin, and U. Sauer, "Identification of common traits in improved xylose-growing Saccharomyces cerevisiae for inverse," pp. 835–847, 2008.
[48] M. Jeppsson, O. Bengtsson, K. Franke, H. Lee, B. Hahn-Hägerdal, and M. F. Gorwa-Grauslund, "The expression of a Pichia stipitis xylose reductase mutant with higher K(M) for NADPH increases ethanol production from xylose in recombinant Saccharomyces cerevisiae.," *Biotechnol. Bioeng.*, vol. 93, no. 4, pp. 665–73, Mar. 2006.
[49] M. Klimacek, E. Kirl, S. Krahulec, K. Longus, V. Novy, and B. Nidetzky, "Stepwise metabolic adaption from pure metabolization to balanced anaerobic growth on xylose explored for recombinant Saccharomyces cerevisiae.," *Microb. Cell Fact.*, vol. 13, no. 1, p. 37, Jan. 2014.
[50] S. Krahulec, B. Petschacher, M. Wallner, K. Longus, M. Klimacek, and B. Nidetzky, "Fermentation of mixed glucose-xylose substrates by engineered strains of Saccharomyces cerevisiae: role of the coenzyme specificity of xylose reductase, and effect of glucose on xylose utilization.," *Microb. Cell Fact.*, vol. 9, p. 16, Jan. 2010.
[51] S. Krahulec, M. Klimacek, and B. Nidetzky, "Analysis and prediction of the physiological effects of altered coenzyme specificity in xylose reductase and xylitol dehydrogenase during xylose fermentation by Saccharomyces cerevisiae.," *J. Biotechnol.*, vol. 158, no. 4, pp. 192–202, Apr. 2012.
[52] J. P. Dijken and W. A. Scheffers, "Redox balances in the metabolism of sugars by yeasts," *FEMS Microbiol. Lett.*, vol. 32, no. 3–4, pp. 199–224, Apr. 1986.
[53] O. Bengtsson, B. Hahn-Hägerdal, and M. F. Gorwa-Grauslund, "Xylose reductase from Pichia stipitis with altered coenzyme preference improves ethanolic xylose fermentation by recombinant Saccharomyces cerevisiae.," *Biotechnol. Biofuels*, vol. 2, p. 9, Jan. 2009.
[54] C. Gruber, "The yeast Candida tenuis : assessment of the organism for xylose fermentation and stereospecific reduction of ketones," *Master thesis*, 2011.
[55] E. Kirl, "Physiological and metabolomic characterisation of recombinant Saccharomyces cerevisiae strain evolved for anaerobic growth on xylose," *Master thesis*, 2011.

[56] V. Novy, S. Krahulec, K. Longus, M. Klimacek, and B. Nidetzky, “Co-fermentation of hexose and pentose sugars in a spent sulfite liquor matrix with genetically modified Saccharomyces cerevisiae.,” *Bioresour. Technol.*, vol. 130, pp. 439–48, Feb. 2013.
[57] B. Petschacher and B. Nidetzky, “Engineering Candida tenuis Xylose Reductase for Improved Utilization of NADH : Antagonistic Effects of Multiple Side Chain Replacements and Performance of Site-Directed Mutants under Simulated In Vivo Conditions,” *Appl. Environ. Microbiol.*, vol. 71, no. 10, 2005.
[58] S. Krahulec, M. Klimacek, and B. Nidetzky, “Engineering of a matched pair of xylose reductase and xylitol dehydrogenase for xylose fermentation by Saccharomyces cerevisiae.,” *Biotechnol. J.*, vol. 4, no. 5, pp. 684–94, May 2009.
[59] van Dijken JP, J. Bauer, L. Brambilla, P. Duboc, J. Francois, C. Gancedo, M. Giuseppin, J. Heijnen, M. Hoare, H. Lange, E. Madden, P. Niederberger, J. Nielsen, J. Parrou, T. Petit, D. Porro, M. Reuss, van Riel N, M. Rizzi, H. Steensma, C. Verrips, J. Vindeløv, and J. Pronk, “An interlaboratory comparison of physiological and genetic properties of four Saccharomyces cerevisiae strains.,” *Enzyme Microb. Technol.*, vol. 26, no. 9–10, pp. 706–714, Jun. 2000.
[60] D. W. Tempest, J. R. Norris, and M. H. Richmond, *Dynamics of Microbial Growth*, no. Bd. 7. John Wiley & Sons Australia, Limited, 1978.
[61] M. M. Bradford, “A rapid and sensitive method for the quantitation of microgram quantities of protein utilizing the principle of protein-dye binding.,” *Anal. Biochem.*, vol. 72, pp. 248–54, May 1976.
[62] E. González, M. R. Fernández, C. Larroy, L. Solà, M. A. Pericàs, X. Parés, and J. A. Biosca, “Characterization of a (2R,3R)-2,3-butanediol dehydrogenase as the Saccharomyces cerevisiae YAL060W gene product. Disruption and induction of the gene.,” *J. Biol. Chem.*, vol. 275, no. 46, pp. 35876–85, Nov. 2000.
[63] S. Saheki, a Takeda, and T. Shimazu, “Assay of inorganic phosphate in the mild pH range, suitable for measurement of glycogen phosphorylase activity.,” *Anal. Biochem.*, vol. 148, no. 2, pp. 277–81, Aug. 1985.
[64] D. R. Lide, Ed., *CRC Handbook of Chemistry and Physics, Internet Version 2005*. Boca Raton, FL: CRC Press, 2005.
[65] P. M. Doran, *Bioprocess Engineering Principles*. Elsevier, 1995.
[66] G. Ditzelmuller, W. Wohrer, C. P. Kubicek, and M. Rohr, “Nucleotide pools of growing, synchronized and stressed cultures of Saccharomyces cerevisiae.,” *Arch. Microbiol.*, vol. 135, no. 1, pp. 63–67, Aug. 1983.
[67] J. Büscher, D. Czernik, J. Ewald, U. Sauer, and N. Zamboni, “Cross-Platform Comparison of Methods for Quantitative Metabolomics of Primary Metabolism.,” *Anal. Chem.*, vol. 81, pp. 2135–2143, 2009.
[68] W. Lu, M. F. Clasquin, E. Melamud, D. Amador-Noguez, A. a Caudy, and J. D. Rabinowitz, “Metabolomic analysis via reversed-phase ion-pairing liquid chromatography coupled to a stand alone orbitrap mass spectrometer.,” *Anal. Chem.*, vol. 82, no. 8, pp. 3212–21, Apr. 2010.
[69] G. Shi, “Application of co-eluting structural analog internal standards for expanded linear dynamic range in liquid chromatography/electrospray mass spectrometry,” *Rapid Commun. Mass Spectrom.*, vol. 17, no. 3, pp. 202–206, 2003.
[70] H. C. Lange and J. J. Heijnen, “Statistical reconciliation of the elemental and molecular biomass composition of Saccharomyces cerevisiae,” *Biotechnol. Bioeng.*, vol. 75, no. 3, pp. 334–344, 2001.
[71] C. Wittmann, J. O. Krömer, P. Kiefer, T. Binz, and E. Heinzle, “Impact of the cold shock phenomenon on quantification of intracellular metabolites in bacteria.,” *Anal. Biochem.*, vol. 327, no. 1, pp. 135–9, May 2004.
[72] J. M. Buescher, S. Moco, U. Sauer, and N. Zamboni, “Ultrahigh performance liquid chromatography-tandem mass spectrometry method for fast and robust quantification of anionic and aromatic metabolites.,” *Anal. Chem.*, vol. 82, no. 11, pp. 4403–4412, Jun. 2010.
[73] U. Theobald, W. Mailinger, M. Reuss, and M. Rizzi, “In Vivo Analysis of Glucose-Induced Fast Changes in Yeast Adenine Nucleotide Pool Applying a Rapid Sampling Technique,” *Anal. Biochem.*, vol. 214, pp. 31–37, 1993.

[74] K. Nöh, A. Wahl, and W. Wiechert, “Computational tools for isotopically instationary 13C labeling experiments under metabolic steady state conditions.,” *Metab. Eng.*, vol. 8, no. 6, pp. 554–77, Nov. 2006.
[75] L. Wu, J. Van Dam, D. Schipper, M. T. a P. Kresnowati, A. M. Proell, C. Ras, W. a. Van Winden, W. M. Van Gulik, and J. J. Heijnen, “Short-term metabolome dynamics and carbon, electron, and ATP balances in chemostat-grown Saccharomyces cerevisiae CEN.PK 113-7D following a glucose pulse,” *Appl. Environ. Microbiol.*, vol. 72, no. 5, pp. 3566–3577, 2006.
[76] S. Kim, D. Y. Lee, G. Wohlgemuth, H. S. Park, O. Fiehn, and K. H. Kim, “Evaluation and Optimization of Metabolome Sample Preparation Methods for Saccharomyces cerevisiae.,” *Anal. Chem.*, Jan. 2013.
[77] C. A. Smith, G. O’Maille, E. J. Want, C. Qin, S. A. Trauger, T. R. Brandon, D. E. Custodio, R. Abagyan, and G. Siuzdak, “METLIN: a metabolite mass spectral database.,” *Ther. Drug Monit.*, vol. 27, no. 6, pp. 747–751, Dec. 2005.
[78] D. S. Wishart, T. Jewison, A. C. Guo, M. Wilson, C. Knox, Y. Liu, Y. Djoumbou, R. Mandal, F. Aziat, E. Dong, S. Bouatra, I. Sinelnikov, D. Arndt, J. Xia, P. Liu, F. Yallou, T. Bjorndahl, R. Perez-Pineiro, R. Eisner, F. Allen, V. Neveu, R. Greiner, and A. Scalbert, “HMDB 3.0--The Human Metabolome Database in 2013.,” *Nucleic Acids Res.*, vol. 41, no. Database issue, pp. D801–7, Jan. 2013.
[79] R. King, R. Bonfiglio, C. Fernandez-Metzler, C. Miller-Stein, and T. Olah, “Mechanistic investigation of ionization suppression in electrospray ionization,” *J. Am. Soc. Mass Spectrom.*, vol. 11, no. 11, pp. 942–950, 2000.
[80] C. S. Ho, C. W. K. Lam, M. H. M. Chan, R. C. K. Cheung, L. K. Law, L. C. W. Lit, K. F. Ng, M. W. M. Suen, and H. L. Tai, “Electrospray ionisation mass spectrometry: principles and clinical applications.,” *Clin. Biochem. Rev.*, vol. 24, no. 1, pp. 3–12, 2003.
[81] a. Toivola, D. Yarrow, and E. Van Den Bosch, “Alcoholic fermentation of D-xylose by yeasts,” *Appl. Environ. Microbiol.*, vol. 47, no. 6, pp. 1221–1223, 1984.
[82] C. F. Wahlbom, W. H. Van Zyl, L. J. Jönsson, B. Hahn-Hägerdal, and R. R. Cordero Otero, “Generation of the improved recombinant xylose-utilizing Saccharomyces cerevisiae TMB 3400 by random mutagenesis and physiological comparison with Pichia stipitis CBS 6054,” *FEMS Yeast Res.*, vol. 3, no. 3, pp. 319–326, 2003.
[83] A. Eliasson, J. H. S. Hofmeyr, S. Pedler, and B. Hahn-Hägerdal, “The xylose reductase/xylitol dehydrogenase/xylulokinase ratio affects product formation in recombinant xylose-utilising Saccharomyces cerevisiae,” *Enzyme Microb. Technol.*, vol. 29, no. 4–5, pp. 288–297, 2001.
[84] A. Matsushika and S. Sawayama, “Efficient bioethanol production from xylose by recombinant saccharomyces cerevisiae requires high activity of xylose reductase and moderate xylulokinase activity.,” *J. Biosci. Bioeng.*, vol. 106, no. 3, pp. 306–309, 2008.
[85] W. J. Ball and D. E. Atkinson, “Adenylate energy charge in Saccharomyces cerevisiae during starvation.,” *J. Bacteriol.*, vol. 121, no. 3, pp. 975–82, Mar. 1975.
[86] G. Trausinger, C. Gruber, S. Krahulec, C. Magnes, B. Nidetzky, and M. Klimacek, “Kinetic and metabolic control of xylose fermentation explored for the yeast-type xylose assimilation pathway,” *Biotechnol. Biofuels / Revis.*, 2015.
[87] S. Krahulec, R. Kratzer, K. Longus, and B. Nidetzky, “Comparison of Scheffersomyces stipitis strains CBS 5773 and CBS 6054 with regard to their xylose metabolism: Implications for xylose fermentation,” *Microbiologyopen*, vol. 1, no. 1, pp. 64–70, 2012.
[88] S. Vaseghi, A. Baumeister, M. Rizzi, and M. Reuss, “In vivo dynamics of the pentose phosphate pathway in Saccharomyces cerevisiae.,” *Metab. Eng.*, vol. 1, no. 2, pp. 128–40, 1999.
[89] E. Boles, J. Heinisch, and F. K. Zimmermann, “Different signals control the activation of glycolysis in the yeast Saccharomyces cerevisiae.,” *Yeast*, vol. 9, no. 7, pp. 761–770, 1993.
[90] S. Muller, E. Boles, M. May, and F. K. Zimmermann, “Different internal metabolites trigger the induction of glycolytic gene expression in Saccharomyces cerevisiae,” *J. Bacteriol.*, vol. 177, no. 15, pp. 4517–4519, 1995.
[91] A. K. Påhlman, K. Granath, R. Ansell, S. Hohmann, and L. Adler, “The Yeast Glycerol 3-Phosphatases Gpp1p and Gpp2p Are Required for Glycerol Biosynthesis and Differentially

Involved in the Cellular Responses to Osmotic, Anaerobic, and Oxidative Stress," *J. Biol. Chem.*, vol. 276, no. 5, pp. 3555–3563, 2001.
[92] G. Hubmann, S. Guillouet, and E. Nevoigt, "Gpd1 and Gpd2 fine-tuning for sustainable reduction of glycerol formation in Saccharomyces cerevisiae," *Appl. Environ. Microbiol.*, vol. 77, no. 17, pp. 5857–5867, 2011.
[93] D. J. Wohlbach, A. Kuo, T. K. Sato, K. M. Potts, A. a Salamov, K. M. Labutti, H. Sun, A. Clum, J. L. Pangilinan, E. a Lindquist, S. Lucas, A. Lapidus, M. Jin, C. Gunawan, V. Balan, B. E. Dale, T. W. Jeffries, R. Zinkel, K. W. Barry, I. V Grigoriev, and A. P. Gasch, "Comparative genomics of xylose-fermenting fungi for enhanced biofuel production.," *Proc. Natl. Acad. Sci. U. S. A.*, vol. 108, no. 32, pp. 13212–13217, 2011.
[94] A. Stincone, A. Prigione, T. Cramer, M. M. C. Wamelink, K. Campbell, E. Cheung, V. Olin-Sandoval, N.-M. Gruening, A. Krueger, M. Tauqeer Alam, M. a Keller, M. Breitenbach, K. M. Brindle, J. D. Rabinowitz, and M. Ralser, "The return of metabolism: biochemistry and physiology of the pentose phosphate pathway.," *Biol. Rev. Camb. Philos. Soc.*, Sep. 2014.
[95] A. Kümmel, S. Panke, and M. Heinemann, "Putative regulatory sites unraveled by network-embedded thermodynamic analysis of metabolome data.," *Mol. Syst. Biol.*, vol. 2, p. 2006.0034, 2006.
[96] M. Kanehisa and S. Goto, "KEGG: kyoto encyclopedia of genes and genomes.," *Nucleic Acids Res.*, vol. 28, no. 1, pp. 27–30, Jan. 2000.